

PRECISE TEMPORAL PROCESSING IN THE GERBIL AUDITORY BRAINSTEM

Dissertation
zur Erlangung des Grades eines Doktors
der Naturwissenschaften

an der Fakultät für Biologie
der Ludwig-Maximilians-Universität München

vorgelegt von
Antje Brand

München, im Januar 2003

1. Gutachter: PD Dr. Benedikt Grothe
2. Gutachter: Prof. Dr. Gerhard Neuweiler

eingereicht am 20. Januar 2003

Tag der mündlichen Prüfung: 14. März 2003

Nothing shocks me. I'm a scientist.
Harrison Ford, as Indiana Jones

Success is the ability to go from one
failure to another with no loss of
enthusiasm.
Sir Winston Churchill



Table of Contents

1. Summary / Zusammenfassung	1
2. Introduction	5
2.1 <i>The Medial Superior Olive</i>	5
2.1.1 <i>Temporal processing in a spatial context.....</i>	5
2.1.2 <i>The role of the MSO in sound recognition</i>	12
2.2 <i>The Superior Paraolivary Nucleus.....</i>	14
2.3 <i>The gerbil as an animal model.....</i>	16
2.4 <i>The scope of this study</i>	17
3. Methods	19
3.1 <i>Stereotaxia and Surgery</i>	19
3.2 <i>Neuronal Recordings</i>	21
3.3 <i>Acoustic stimulation</i>	22
3.4 <i>Recording Procedure</i>	22
3.5 <i>Pharmacology</i>	23
3.6 <i>Data Analysis</i>	24
3.7 <i>Histology</i>	25
3.7.1 <i>Histology of HRP Injections.....</i>	26
3.7.2 <i>Histology of bead injections</i>	27
3.8 <i>MSO - Reconstruction.....</i>	27
4. Results	29
4.1 <i>The Medial Superior Olive.....</i>	29
4.1.1 <i>Reconstruction of recording sites.....</i>	29
4.1.2 <i>Spontaneous activity.....</i>	33
4.1.3 <i>Tuning characteristics</i>	34
4.1.4 <i>Tonotopic Representation.....</i>	35
4.1.5 <i>Response pattern</i>	38
4.1.6 <i>Response latency</i>	41
4.1.7 <i>Binaural response characteristics.....</i>	42
4.1.8 <i>ITD sensitivity to low frequency pure tones</i>	43
4.1.9 <i>Effects of glycinergic inhibition in the MSO</i>	47
4.1.9.1 <i>General effects</i>	47
4.1.9.2 <i>Glycinergic inhibition in ITD coding</i>	48
4.1.10 <i>ITD sensitivity to high frequencies</i>	52
4.1.11 <i>Responses to SAM</i>	53
4.1.11.1 <i>Rate-based modulation transfer functions.....</i>	54
4.1.11.2 <i>Vector-strength based modulation transfer functions</i>	55
4.1.11.3 <i>Monaural stimulation with SAM.....</i>	56
4.1.12 <i>Glycinergic inhibition and high frequency temporal processing....</i>	57
4.2 <i>The Superior Paraolivary Nucleus.....</i>	59
4.2.1 <i>Reconstruction of recording sites.....</i>	59
4.2.2 <i>Spontaneous activity.....</i>	60
4.2.3 <i>Tuning characteristics</i>	60

4.2.4	<i>Response pattern</i>	61
4.2.5	<i>Response latency</i>	63
4.2.6	<i>Binaural response characteristics</i>	64
4.2.7	<i>Responses to SAM</i>	67
4.2.8	<i>Pharmacology</i>	70
4.3	<i>Comparison of neuronal properties in MSO and SPN</i>	73
5.	Discussion	75
5.1	<i>The Medial Superior Olive</i>	75
5.1.1	<i>Localization of low frequency sounds</i>	75
5.1.1.1	<i>Representation of auditory space</i>	75
5.1.1.2	<i>Comparison to other ITD studies</i>	76
5.1.1.3	<i>Models of the representation of auditory space</i>	77
5.1.1.4	<i>Encoding of ITDs in the avian system</i>	78
5.1.2.	<i>The role of inhibition in ITD coding</i>	80
5.1.2.1	<i>The mammalian system</i>	80
5.1.2.2	<i>The avian system</i>	84
5.1.3	<i>High frequency temporal processing</i>	85
5.1.3.1	<i>Temporal processing in non-spatial context</i>	85
5.1.3.2	<i>Spatial Processing of high frequency cues</i>	87
5.1.4	<i>General response characteristics</i>	88
5.1.5	<i>Reconstruction of recording sites</i>	91
5.1.6	<i>Technical challenges of recording from single MSO neurons</i>	92
5.2	<i>The Superior Paraolivary Nucleus</i>	94
5.2.1	<i>Temporal processing</i>	94
5.2.2	<i>Binaural processing</i>	97
5.2.3	<i>Tonotopy and cell subsets</i>	98
6.	References	99
	List of Abbreviations	116
	Acknowledgements	117
	Curriculum Vitae	118

Sound localization and recognition are two important tasks of the auditory system. Both require accurate processing of temporal cues.

Microsecond differences in the arrival time of a sound at the two ears (interaural time differences, ITDs) are the main cue for localizing low frequency sound sources in space. Traditionally, ITDs are thought to be encoded by an array of coincidence-detector neurons, receiving excitatory inputs from the two ears via axons of variable length (“delay lines”), aligned in a topographic map of azimuthal auditory space. Convincing evidence for the existence of such a map in the mammalian ITD detector, the medial superior olive (MSO) is, however, lacking. Equally undetermined is the role of a temporally glycinergic inhibitory input to MSO neurons. Using *in vivo* recordings from the MSO of the Mongolian gerbil, the present study showed that the responses of ITD-sensitive neurons are inconsistent with the idea of a topographic map of auditory space. Moreover, whereas the maxima of ITD functions were found to be outside, the steepest slope was positioned in the physiologically encountered range of ITDs. Local iontophoretic application of glycine and its antagonist strychnine revealed that precisely-timed glycinergic inhibition plays a critical role in determining the mechanism of ITD tuning, by shifting the slope into the physiological range of ITDs.

Natural sounds are modulated in frequency and amplitude and their recognition depends on the analysis of, amongst others, temporal cues. The bat MSO has been shown to be involved in filtering of sinusoidally amplitude modulated (SAM) sounds. This observation led to the assumption that the MSO serves different functions in high and low frequency hearing mammals, namely filtering of temporal cues in high and sound localization in low frequency hearing animals. However, the response to temporally structured sounds has only rarely been investigated in low frequency hearing animals. This study showed that MSO neurons in the gerbil (a rodent that uses ITDs for sound localization) exhibit filter properties in response to the temporal structure of SAM sounds. These results provide evidence for the fact that the MSO in low frequency hearing animals cannot only be linked to temporal processing of spatial cues, but has additional temporal functions.

Auditory information is processed in a number of parallel paths in the ascending auditory pathway. At the brainstem level, several structures are involved, which are known to serve different well-defined functions. However, the function of one

prominent brainstem nucleus, the rodent superior paraolivary nucleus (SPN) is unknown. Two hypotheses have been tested using extracellular single cell physiology in the gerbil.

The existence of binaural inputs indicates that the SPN might be involved in sound localization. Although almost half of the neurons exhibited binaural interactions (most of them excited from both ears), effects of ITDs and interaural intensity differences were weak and ambiguous. Thus, a straightforward function of SPN in sound localization appears to be unlikely.

Inputs from octopus and multipolar/stellate cells of the cochlear nucleus, and from principal cells of the medial nucleus of the trapezoid body, could relate to precise temporal processing in the SPN. Based on discharge types, two subpopulations of SPN cells were observed: sustained discharges and phasic ON or OFF responses. The temporal precision of ON responders in response to pure tones and SAM was significantly higher than that in sustained responders. The existence of at least two subpopulations of neurons (ON and sustained responders) is in line with different subsets of SPN cells that can be distinguished morphologically and may point to them having different roles in the processing of temporal sound features.

Parts of the data from chapter 4.1.8 and 4.1.9 are published in
Brand, A., Behrend, O., Marquardt, T., McAlpine, D., and Grothe, B. Precise inhibition is essential for microsecond interaural time difference coding. *Nature* 417: 543-547, 2002.

Data from chapter 4.2 are published in
Behrend O, Brand A, Kapfer C and Grothe B, Auditory response properties in the superior paraolivary nucleus of the gerbil. *J Neurophysiol* 87: 2915-2929, 2002.

Schall-Lokalisation und Schallerkennung sind zwei wichtige Aufgaben des Hörsystems. Für beide ist die präzise Verarbeitung zeitlicher Parameter von entscheidender Bedeutung.

Die Lokalisation von tief-frequenten Schallquellen im Raum wird durch den Vergleich der Ankunftszeiten des Schalls an den beiden Ohren erreicht. Es wird angenommen, daß diese sogenannten interauralen Zeitdifferenzen (ITDs) von einer Gruppe von Neuronen verarbeitet werden, die erregende Eingänge von beiden Ohren erhalten. Diese Neurone antworten besonders stark, wenn der Eingang von beiden Ohren gleichzeitig am Neuron eintrifft. Jedes Neuron ist auf eine andere ITD (also eine andere Position im horizontalen Raum) abgestimmt, da die Erregung über Axone unterschiedlicher Länge („Verzögerungsketten“) weitergeleitet wird. Dadurch kann die Horizontale topographisch abgebildet werden. Allerdings fehlen bisher überzeugende Beweise für eine solche Raumkarte in der mittleren oberen Olive (MSO), dem Kerngebiet, in dem Zeitdifferenzen bei Säugetieren verarbeitet werden. Zudem ist auch nicht geklärt, welche Rolle die zeitlich sehr genaue, glyzinerge Hemmung auf MSO Neurone bei der ITD Verarbeitung spielt. Mit Hilfe von *in vivo* Ableitungen in der MSO der mongolischen Wüstenrennmaus, konnte in der vorliegenden Studie gezeigt werden, daß die Antwort ITD empfindlicher Neurone nicht mit der Idee einer Raumkarte in Einklang gebracht werden kann. Die stärkste Antwort der ITD empfindlichen Neurone ist außerhalb des Bereichs von ITDs, die die Wüstenrennmaus detektieren kann. Allerdings ist die größte Steigung der ITD Funktionen genau im physiologischen Bereich plaziert. Durch iontophoretische Blockade der glyzinerger Hemmungen konnte zudem gezeigt werden, daß eine zeitlich präzise Hemmung dafür sorgt, daß die Steigung der ITD Funktionen im physiologisch relevanten Bereich plaziert wird.

Natürlich vorkommende Laute sind in Frequenz und Amplitude moduliert und bei der Erkennung solcher Laute spielt die Zeitverarbeitung eine wichtige Rolle. Bei Fledermäusen konnte gezeigt werden, daß MSO Neurone an der Filterung von sinusförmigen Amplitudenmodulationen (SAM) beteiligt sind. Aufgrund dieser Beobachtung nahm man an, daß das Kerngebiet MSO verschiedene Aufgaben in Tieren hat, die verschiedene Frequenzbereiche hören. Filterung von Amplitudenmodulationen wurde als Aufgabe der MSO in hoch-frequenten Hörern angenommen, während die MSO bei tief-frequenten Hörern der Schall-Lokalisation mit ITDs dienen soll. Allerdings

wurde die Antwort von MSO Neuronen auf SAM in Tieren, die gut tief-frequent hören bisher nur wenig untersucht. In der vorliegenden Arbeit wurde gezeigt, daß in der MSO der Wüstenrennmaus hochfrequente Neurone existieren, die Filtereigenschaften in der Antwort auf SAM aufzeigen. Diese Ergebnisse deuten darauf hin, daß MSO Neurone bei tief-frequenten Hörern nicht nur ITD verarbeiten, sondern auch bei der Verarbeitung anderer zeitlicher Parameter beteiligt sind.

Es ist bekannt, daß auf Ebene des Stammhirns unterschiedliche Kerngebiete verschiedene Funktionen erfüllen. Allerdings ist über ein auffälliges Kerngebiets, den „superior paraolivary nucleus (SPN)“ nur wenig bekannt.

Das Vorhandensein von Eingängen von beiden Ohren deutet darauf hin, daß der SPN zum einen an der Schall-Lokalisation beteiligt sein könnte. Obwohl allerdings die Hälfte der Neurone Eingänge von beiden Ohren erhält (meist erregend), sind die Antworten auf Zeit- und Intensitätsdifferenzen schwach ausgeprägt und nicht eindeutig. Die Neurone des SPN scheinen also nicht bei der Bestimmung der Schallrichtung beteiligt zu sein.

Eingänge von Octopus- und multipolaren (Stern-) Zellen des Nucleus cochlearis und von Zellen des medialen Nucleus des Trapezkörpers könnten allerdings ein Hinweis auf präzise zeitliche Verarbeitung im SPN sein. Zwei Untergruppen von Zellen, eingeteilt aufgrund ihres Antwortmusters auf Reintöne, wurden im SPN gefunden: tonische Antworten und phasische ON und OFF Antworten. Die zeitliche Genauigkeit der Zellen die phasisch (ON) auf Reintöne oder SAM antworten war signifikant besser als die von tonisch antwortenden Zellen. Die Existenz von diesen zwei Untergruppen von Neuronen, steht im Einklang mit verschiedenen Gruppen von SPN Zellen, die man aufgrund ihrer Morphologie unterscheiden kann und deutet darauf hin, daß die verschiedenen Populationen an Neuronen unterschiedliche Rollen bei der Zeitverarbeitung auditorischer Parameter spielen.

Auszüge der Ergebnisse von Kapitel 4.1.8 und 4.1.9 sind veröffentlicht in
Brand, A., Behrend, O., Marquardt, T., McAlpine, D., and Grothe, B. Precise inhibition is essential for microsecond interaural time difference coding. *Nature* 417: 543-547, 2002.

Die Ergebnisse aus Kapitel 4.2 sind veröffentlicht in
Behrend O, Brand A, Kapfer C and Grothe B, Auditory response properties in the superior paraolivary nucleus of the gerbil *J Neurophysiol* 87: 2915-2929, 2002.

All mammals rely on processing of acoustic information for survival. The tasks performed by the auditory system are detection, identification and localization of sounds. After detecting a sound, its physical features (amplitude, frequency and timing) are used to identify the sound and to localize its source. The processing of temporal cues is crucial for both tasks, identification and localization.

2.1 *The Medial Superior Olive*

2.1.1 *Temporal processing in a spatial context*

The localization of a sound source is behaviorally relevant in a variety of situations, like escaping from a predator based on the direction of a sound the predator makes. Likewise, sound localization can be critical for accurately orienting towards the sounds of prey or mates, particularly in dark or other visually impairing environments.

Theories on how sounds are localized in the horizontal plane were already postulated in the 19th century (Thompson 1882). Sir John William Strutt (Rayleigh 1877) observed that if a sound source is positioned to the side of a listener, the amplitude of that sound is lower at one ear (the one farther away from the source) than at the other ear. That is because the head can physically block sound energy, thereby producing a sound shadow (see Fig. 2.1 A), resulting in an interaural intensity difference (IID). Sound sources

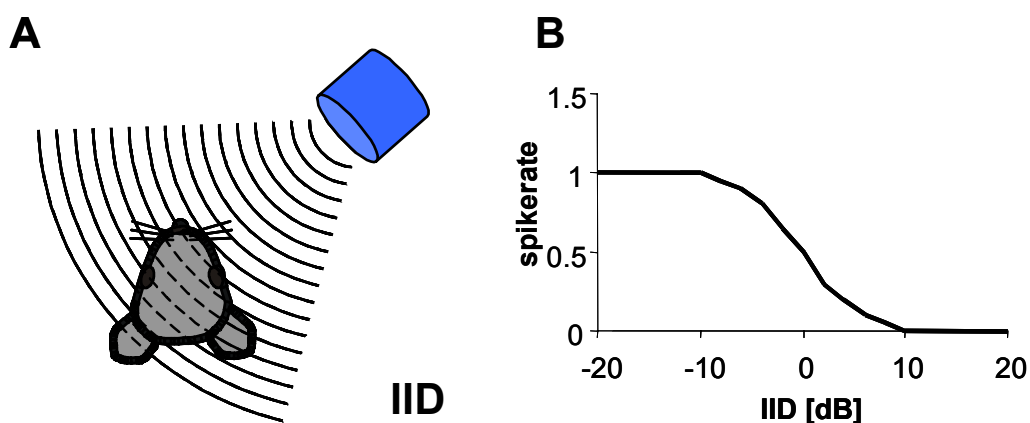


Figure 2.1

Sound localization with interaural intensity differences (IIDs). **A** The sound is louder at the right ear compared to the left ear (sound shadow of the head). This difference in amplitude is computed to localize high frequency sound sources. **B** Response function of an IID detection neuron.

located laterally generate large IIDs, while sound sources near the midline generate small IIDs. Thus, the IID magnitude can be used as a cue to determine the position of a sound source in the azimuth. Today, we know that IIDs are encoded by neurons in the lateral superior olive (LSO), a nucleus of the superior olivary complex (SOC), located in the auditory brainstem. The underlying neuronal mechanism is a subtraction based on ipsilateral excitation and contralateral inhibition (Fig. 2.1 B).

However, detectable IIDs are only generated for relatively high frequencies, e.g. for sound waves with wavelengths longer than the diameter of the head (or the inter-ear distance, respectively). It was relatively unclear how lower frequency sounds were localized, until Lord Rayleigh revealed that a different cue, interaural time differences (ITDs), in addition to IIDs, were used to localize low frequency sounds in the azimuth (“duplex-theory of sound localization”, Rayleigh 1907). The difference in arrival time at the two ears (see Fig. 2.2 A) is the only available cue to localize pure tones of low

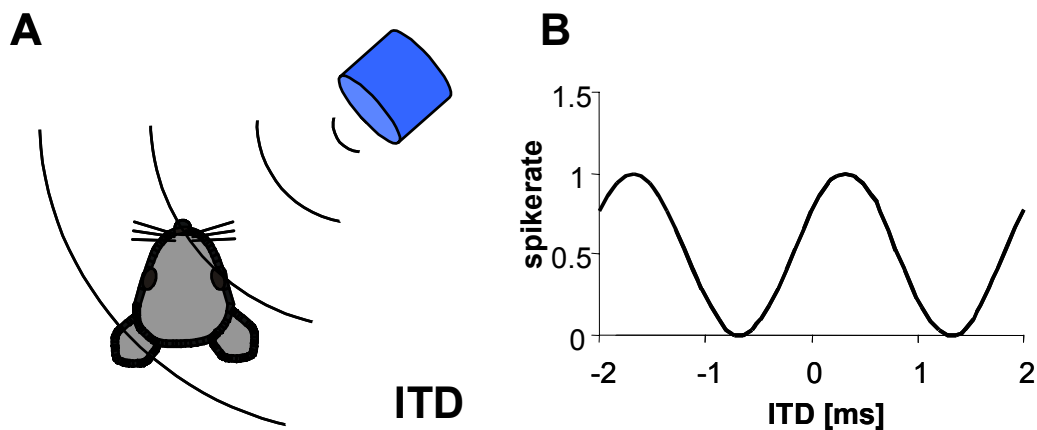


Figure 2.2

Sound localization with interaural time differences (ITDs). **A** The sound is earlier at the right ear than at the left ear. This difference in travel time is computed to localize low frequency sound sources. **B** ITD function of a coincidence detector neuron as proposed by Jeffress.

frequencies. The magnitude of ITDs is dependent on the inter-ear distance of a listener, e.g. the maximum ITD generated in humans is about $650 \mu\text{s}$ (Fedderson et al. 1957). Maximum ITDs generated in animals with smaller heads are accordingly smaller: $400 \mu\text{s}$ for cats, $120 \mu\text{s}$ for gerbils (Calford et al. 1986, Heffner and Heffner 1988, Heffner and Heffner 1992, Yin and Chan 1990). Although these temporal disparities are extremely small, behavioral studies have shown that ITD cues are used for sound localization (Heffner et al. 1994b, Heffner and Heffner 1988, Rayleigh 1907). Psychophysical studies have revealed that mammals, including humans, can resolve ITDs in the range of tens of

μs (humans: 7-30 μs , cats: 25 μs , for review see Blauert 1983). This degree of temporal resolution is in noticeable contrast to other tasks. For example, human listeners, and other mammals are not able to detect gaps in broadband noise if the gaps are shorter than 1 to 2 ms, orders of magnitude greater than the observed resolution in ITD coding (Blauert 1983, Mills 1958, Rayleigh 1907, Wakeford and Robinson 1974). Hence, processing of ITDs must involve specially adapted structures with high temporal acuity.

In 1948, Lloyd Jeffress proposed a model of how the brain might encode ITDs. Three general assumptions are crucial for his model to work. The first assumption is that the inputs to single neurons, that are sensitive to ITDs, encode the temporal structure of a sound. This is achieved by correlating the neuronal response to a certain phase within the cyclic pattern of sound pressure waves, e.g. of a pure tone sine wave (referred to as phase-locking). Secondly, the ITD encoding neurons fire maximally when excitatory phase-locked input from the ipsi- and contralateral ears arrives coincidentally. Third, there must be what Jeffress called “delay lines” (Fig. 2.3) in the processing pathway to compensate for the differences in travel time outside the head. If the conduction time of

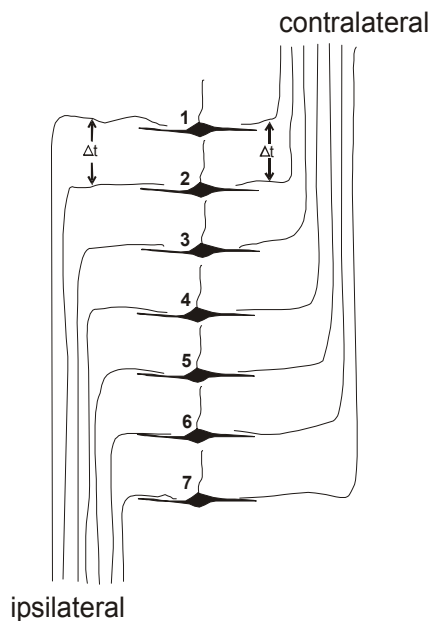


Figure 2.3

The Jeffress model of delay lines, modified by Goldberg and Brown (1969). Coincidence detector neurons fire maximally if the inputs from the contralateral and ipsilateral side arrive at the same time, e.g. when a sound travels exactly the same time from ipsi- and contralateral, neuron #4 is the only one excited, whereas a sound conveyed by the ipsilateral ear that leads the contralateral ear by six times Δt then neuron #1 will be activated.

the input were equal to all neurons, all cells would only respond to the same ITD (thus to one position in space). To get coincident input at a given neuron, the conduction delay in the brain must be longer for the ipsilateral side (same side as the sound source) than at the contralateral (opposite) side. A systematic arrangement of ipsi- and contralateral inputs onto an array of coincidence detector neurons would allow each neuron to

respond maximally to a different ITD in the horizontal plane. The position of a neuron in the array would thus systematically relate to a certain horizontal location, thereby creating a place-code of azimuthal position.

The medial superior olive (MSO), which is a part of the SOC in mammals, is the first station where excitatory binaural inputs converge, and hence, the neurons in the MSO are the first ones to be able to encode ITDs. Several findings support MSO neurons as ITD encoding structures. Somata of MSO neurons are systematically arranged in the parasagittal plane (Kapfer et al. 2002, Nordeen et al. 1983, Perkins 1973, Ramon y Cajal 1907). MSO neurons are bipolar and get excitatory input from both the ipsilateral and contralateral spherical bushy cells of the anteroventral cochlear nucleus (AVCN, Osen 1969, Raymon y Cajal 1907, Stotler 1953, Warr 1966, for review see Schwartz 1992, Thompson and Schofield 2000, see Fig. 2.4). Low frequency spherical bushy cells in the

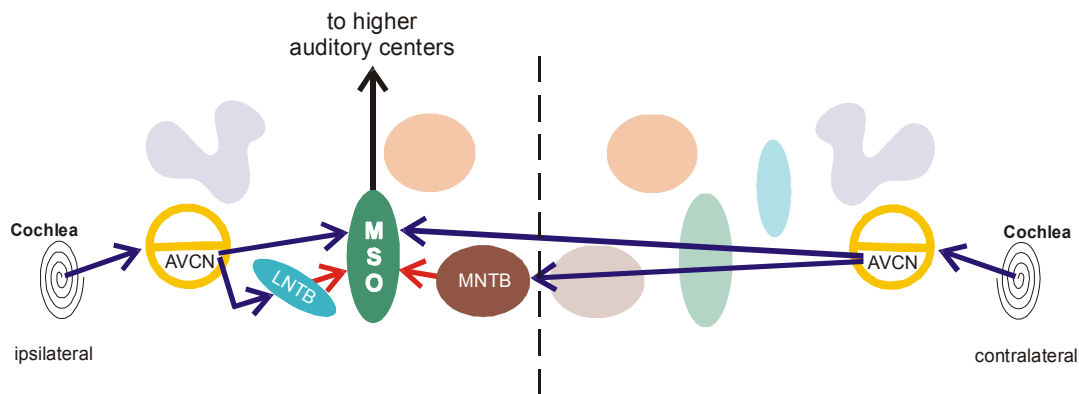


Figure 2.4

Schematic drawing of the connections to the medial superior olive, MSO.

AVCN, anteroventral cochlear nucleus; LNTB, lateral nucleus of the trapezoid body; MNTB, medial nucleus of the trapezoid body

excitatory projections in blue, inhibitory projections in red

AVCN correlate their discharge to a certain phase of a pure tone sine wave (phase-locking), thereby encoding the temporal structure of the sound (Joris et al. 1994ab). MSO neurons also discharge with phase-locked responses to low frequency pure tones (Batra et al. 1997a, Crow et al. 1978, Galambos et al. 1959, Goldberg and Brown 1969, Spitzer and Semple 1995, Yin and Chan 1990). Studies with ongoing pure tones, in various low frequency hearing animals (see Table 2.1) showed that MSO neurons discharge maximally at a certain “best ITD” (see Fig. 2.2). When a neuron is tested with different frequencies this best ITD remains stable. This means that an individual neuron codes for one ITD, independent of stimulus frequency (so called “peak-type” response to ITDs).

Author	Animal	N	Electrodes	Verification of recording sites	Frequency distribution	ITD sensitive neurons
Caird and Klinke 1983	cat	~ 5	glass pipettes (18-30 M Ω)	alcian blue fast green	0.25 to 1.25 kHz	5
Clark and Dunlop 1968	cat	73 (field potentials)	metal microelectrodes glass pipettes	electrolytic lesions	?	-
Crow et al. 1978	kangaroo rat	~28	tungsten microelectrodes	electrode tracks	“low frequency”	28
Galambos et al. 1959	cat	~ 12	metal microelectrodes	electrode tracks	-	-
Goldberg and Brown 1968/1969 ²	dog whole SOC	105 (mainly field potentials) /22	metal microelectrodes	electrode tracks	1.5 to 11.8 kHz	6 ¹
Guinan et al 1972ab	cat	19	metal microelectrodes glass pipettes	electrode tracks electrolytic lesions	?	-
Batra et al. 1997ab ²	rabbit whole SOC	124	metal microelectrodes	electrolytic lesions	?	38 ³
Langford 1984	chinchilla	136	glass pipettes (low impedance)	30% of recordings marked with alcian blue	0.2 to 1.1 kHz	30
Moushegian et al. 1964	cat	10	metal microelectrodes	electrode tracks	0.6 kHz	1
Moushegian et al. 1967	cat	~ 53	metal microelectrodes	electrode tracks	?	
Moushegian et al. 1975	kangaroo rat	31	metal microelectrodes	electrode tracks	“low frequency”	6
Spitzer and Semple 1995	gerbil	~ 19 in MSO	tungsten microelectrodes (2-5 M Ω)	electrolytic lesions	?	19
Yin and Chan 1990	cat	34	tungsten microelectrodes glass pipettes (5-20 M Ω)	electrolytic lesions fast Green	Below 3 kHz (biased sample)	32

Table 2.1

Electrophysiological studies in the MSO of low frequency hearing animals.

¹ number of neurons tested at low frequencies below 0.6 kHz

² the studies are addressing response pattern and ITD sensitivity in the whole SOC, it is unclear which recordings stem from which nucleus

³ number of neurons displaying “peak-type” response to ITDs

The binaural excitatory inputs to MSO neurons and the systematical arrangement of somata, as well as their neuronal properties in response to ITDs, namely the periodic shape of ITD functions and stability of the maximal discharge independent of stimulus frequency, are indicative for the proposed coincidence detection mechanism. These findings led to the assumption that a Jeffress-type mechanism for the processing of ITDs is realized in mammals.

However, there are two major aspects that are not in line with the idea that the mammalian MSO acts as a Jeffress-type coincidence encoding structure. One of the most striking aspects in the model of Jeffress is the idea of axonal arrangements to compensate for differences of travel times outside the head. So far, no convincing evidence has been found for the existence of such delay lines in mammals. Two studies in cats (Beckius et al. 1999, Smith et al. 1993) attempted to estimate the length and patterning of single axons from the AVCN to the MSO. Filling of axons turned out to be difficult and the length of only a small number of axons could be evaluated. Moreover, only some neurons from the contralateral cochlear nucleus followed an arrangement proposed by Jeffress, whereas others showed restricted projections patterns not consistent with the idea of delay lines. The ipsilateral inputs to the MSO showed multiple collaterals, but reconstruction of those inputs also did not conform to the Jeffress model.

The only study physiologically addressing the question of a topographic representation of ITDs presents only weak evidence for a space-map (Yin and Chan 1990). The most likely place for a space-map is the rostrocaudal extension of the MSO. The mediolateral extension consists of only one or few rows of cells (Kapfer et al. 2002, Nordeen et al. 1983, Perkins 1973, Ramon y Cajal 1907) and in the dorsoventral axis the best frequency (BF) of neurons is mapped from low to high frequencies. Indeed, Yin and Chan (1990) revealed a weak linear relationship between recording position and maxima of ITD functions in the rostrocaudal dimension in the brain. However, there is a fundamental problem, concerning the interpretation of this set of data. Yin and Chan penetrated the MSO from ventral to dorsal in reverse direction (thus going from high BF to low BF). Any dependency of best ITD on BF (as indicated by McAlpine et al. 2001 for the guinea pig midbrain) would cause a systematic shift of ITD as found by Yin and Chan (1990) and could lead to the assumption that an apparent space map is present.

Furthermore, no topographic representation of ITDs is found at higher level of the ascending auditory pathway such as the inferior colliculus, the superior colliculus or the

auditory cortex (Fitzpatrick et al. 2002, McAlpine et al. 2001, Skottun 1998, Skottun et al. 2001).

A second problem with applying the Jeffress model to the mammalian MSO concerns the role of inhibitory input. The Jeffress model does not address inhibition, even though there is anatomical evidence of massive glycinergic inhibitory input from the lateral nucleus of the trapezoid body (LNTB, driven by globular bushy cells of the ipsilateral AVCN) and the more prominent input from the medial nucleus of the trapezoid body (MNTB, driven by globular bushy cells of the contralateral AVCN; Cant 1991, Cant and Hyson 1992, Grothe and Sanes 1993, Helfert et al. 1989, Kuwabara and Zook 1992, Peyret et al. 1986, Saint-Marie et al. 1989, Smith 1995, for review see Thompson and Schofield 2000, see Fig. 2.4). The input to the MNTB is conducted via the calyces of Held, synapses that have an extremely low variability in their timing and produce only very short synaptic delays (for review see von Gersdorff and Borst 2002), which are therefore well suited for precise temporal transmission. In fact, MNTB neurons faithfully phase-lock to the waveform of a pure tone up to at least 1 kHz (Kopp-Scheinflug et al. 2002, Paolini et al. 2001, Smith et al. 1991, Smith et al. 1998, Wu and Kelly 1993).

Physiological evidence on the role of inhibition only comes from *in vitro* studies in the MSO. Grothe and Sanes (1993) were the first to show that stimulus evoked glycinergic inhibition is involved in stimulus coding in the MSO. In a subsequent study the authors could show (Grothe and Sanes 1994), that the exact timing of inhibition is important for processing of temporal cues.

Goldberg and Brown (1969) and Yin and Chan (1990) speculated about the role of inhibition in ITD coding because of the observation that the response of MSO neurons drops below the spontaneous rate at “unfavourable” ITDs. A model by Colburn et al. (1990), however, could explain the observed effects without implementing any inhibition. The authors concluded that there is no prominent role of inhibition, but that ITD coding relies only on the coincidence detection of excitatory inputs. It remains unclear if and how inhibition is involved in the processing of ITDs.

In contrast to mammals, ITD coding in birds seems to be in accordance with the Jeffress model. The nucleus laminaris (NL) in the auditory brainstem represents the avian ITD encoding structure. It is the first station of binaural excitatory interaction (Carr and Konishi 1990, Sullivan and Konishi 1984). The input to the NL is conducted bilaterally from neurons of both nuclei magnocellulares (NM) that phase-lock to pure tones (up to

8 kHz in barn owls, Koppl 1997, Sullivan and Konishi 1984). Anatomical studies in chicken reveal a monolayer of bipolar cells with spatially segregated input from ipsi- and contralateral NM (Ramon y Cajal 1907, Rubel and Parks 1975). Axons from the contralateral NM branch into the NL along the mediolateral extension and act as delay lines as proposed by Jeffress (Parks and Rubel 1978, Rubel and Parks 1975, Young and Rubel 1983, Young and Rubel 1986). Physiological properties are in line with the proposed coincidence detection mechanism - neurons in the NL fire maximally at a certain ITD by coincidence detection of excitatory inputs (Overholt et al. 1992).

The NL in the barn owl, however, is expanded and contains a three dimensional array of neurons (Carr and Boudreau 1993). The arrangement of delay lines is realized several times in the dorsoventral axis (Carr and Konishi 1988, Carr and Konishi 1990, Carr and Boudreau 1993). This evolutionary development of many parallel maps is discussed in the context of an improved sensitivity to ITDs (Carr and Code 2000), useful for an animal that relies on sound localization for catching prey.

Neurophysiological studies in the barn owl revealed that NL neurons are sensitive to ITDs and that their response shows the characteristic cyclic shape indicating coincidence detection mechanisms (Carr and Konishi 1988, Carr and Konishi 1990, Sullivan and Konishi 1984, Sullivan and Konishi 1986, Viète et al. 1997). Therefore, in both the chicken and the barn owl coincidence detection mechanism and representation of ITDS in the brain are in line with the assumption of the Jeffress model.

At first sight, the mammalian and the avian coincidence detector share common characteristics, namely binaural excitatory inputs and coincidence detection of those inputs. However, one crucial assumption of the Jeffress model, the existence of delay lines has not been detected in the mammalian system. It seems that at level of the brainstem ITDs are not represented in form of a space-map as in birds, but in a different way, as already indicated by findings in the midbrain, McAlpine et al. 2001 (see discussion).

2.1.2 The role of the MSO in sound recognition

As discussed in the previous chapter, the major role of the MSO in mammals seems to be sound localization. This implies that an ITD encoder such as the MSO is only necessary in animals that are able to use ITDs for sound localization. For animals that hear only high frequencies, IIDs are the main cue for sound localization. However, it has

been shown that the MSO is not only present in high frequency hearing animals such as bats and rats (for review see Covey and Casseday 1995, Grothe 2000) but that it is also well developed. Electrophysiological studies have shown that bat MSO neurons are sensitive to ITDs in envelopes of high frequency carriers (e.g. sinusoidal amplitude modulations, SAM, Grothe and Park 1998), and that those ITD functions display the typical sinusoidal shape. Moreover, these neurons responded maximally at one particular ITD independent of SAM modulation frequency. However, only a small range of ITDs is of behavioral relevance for bats due to their small inter-ear distance. The observed ITD functions did not exhibit any significant changes in response rate in the physiologically relevant range. Therefore, a role of the bat MSO in ITD coding is very unlikely (as it is probably in all other small high frequency hearing animals). It is in fact the existing connectivity in the MSO (binaural excitatory and inhibitory input) that is capable of creating epiphenomenal ITD sensitivity when tested with unphysiological ITDs. The underlying circuits are therefore most likely involved in the processing of other temporal stimulus features.

Almost all structures in the auditory brainstem (with exception of the dorsal nucleus of the lateral lemniscus, DNLL and the MSO) follow the temporal structure of SAM up to high modulation frequencies (tested up to 100 Hz). Auditory nerve fibers synchronize their response to the envelope frequency, i.e. they phase-lock to a certain phase of the modulation envelope up to 1000 Hz. Neurons in the ventral cochlear nucleus show a similar response as observed in the auditory nerve, i.e. they also phase-lock up to high modulation frequencies > 800 Hz (Moller 1972, Moller 1976, Vater 1982, for review see: Rhode and Greenberg 1991). At the next stations of the ascending pathway (SOC, lateral lemniscus) some neurons encode the temporal structure up to high modulation frequencies like their cochlear nucleus inputs (LSO: Joris and Yin 1995, lateral lemniscus: Huffman et al. 1998, MNTB: Grothe et al. 1997, SOC: Kuwada and Batra 1999). However, it has been shown that MSO and DNLL neurons in the auditory brainstem of bats exhibit low-pass filter characteristics for the temporal structure of SAM; they do not respond to modulation frequencies above 400 Hz. (DNLL: Yang and Pollak 1997, MSO: Grothe et al. 1992, Grothe 1994, Grothe et al. 1997, Grothe et al. 2001).

Amplitude modulations create a temporal pattern in sound that contains essential information for sound recognition. For example a sound deprived of frequency information still enables a listener to understand the meaning because of the temporal pattern (Shannon et al. 1995). The observed temporal filters in mammals were discussed

in the context of echo suppression in terms of the precedence effect (the suppression of information from a sound source that is later in time compared to a sound source earlier in time, Litovsky and Yin 1998). By suppressing of reverberations and echoes from the acoustic background, spatial- temporal fields could be established by MSO neurons (Grothe and Neuweiler 2000).

2.2 *The Superior Paraolivary Nucleus*

Sound localization involves three of the major nuclei in the superior olivary complex. The LSO encodes amplitude information and, in a parallel pathway, the MSO encodes timing information. The MNTB provides inhibitory inputs to both nuclei that are participating in the processing of localization cues. Other nuclei in the brainstem seem to be involved in temporal processing of monaural inputs, like the ventral nucleus of the lateral lemniscus (Covey and Casseday 1991), or in monaural spectral integration that may be necessary for sound elevation coding, such as the dorsal cochlear nucleus (May 2000).

There is another prominent auditory brainstem structure whose function is not known: the superior paraolivary nucleus (SPN) in rodents or its putative homologue, the dorsomedial periolivary nucleus (DMPO) described in carnivores (Harrison and Feldman 1970, Houtgast and Aoki 1994, Irving and Harrison 1967, Moore 1988, Osen et al. 1984, Smith et al. 1991) and bats (Grothe et al. 1994, Zook and Casseday 1982, Zook and DiCaprio 1988). The SPN is a prominent structure located medially or mediodorsally to the MSO and dorsolaterally to the MNTB (Harrison and Warr 1962, Kudo et al. 1990, Kuwabara and Zook 1992, Nordeen et al. 1983, Ollo and Schwartz 1979, Saint Marie and Baker 1990, Schofield and Cant 1991, Schofield 1991, Willard and Martin 1983). SPN neurons are driven by direct excitatory inputs from both cochlear nuclei (CN, see Fig. 2.5) and project directly to the auditory midbrain, making it a potentially fast and important part of the ascending auditory system (for review: Thompson and Schofield 2000). Based on the connection pattern and the immunohistochemistry of SPN neurons, the nucleus could be involved in sound localization, or more generally in processing of temporal aspects of sound. The SPN receives bilateral inputs from the ventral cochlear nucleus (VCN) and unilateral input from the ipsilateral MNTB (driven by the contralateral ear and inhibitory, see above). Because these inputs are comparable to those of the MSO or the LSO (see above) one might expect ITD sensitivity based on binaural excitation (E/E) and/or IID sensitivity based on the interaction of ipsilateral excitation

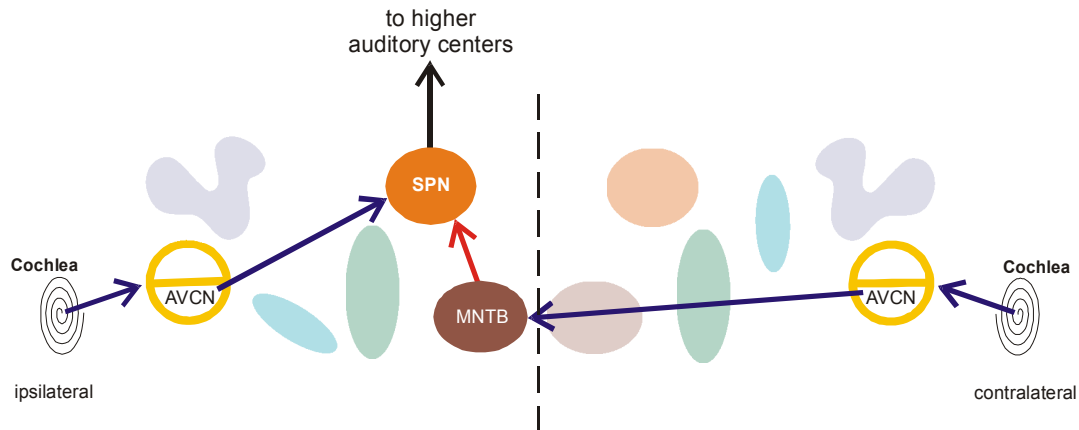


Figure 2.5

Schematic drawing of the connection to the superior periolivary complex, SPN, AVCN, anteroventral cochlear nucleus; MNTB, medial nucleus of the trapezoid body, excitatory connections in blue, inhibitory connections in red

and contralateral inhibition (E/I). In fact, Spitzer and Semple (1995) and Batra et al. (1997ab) found several ITD-sensitive neurons in a non-defined mediodorsal area of the SOC, partly exhibiting patterns different to the “peak-type” ITD responses observed in MSO neurons.

The cell types providing excitatory and inhibitory input to the SPN could indicate a role of SPN neurons in general temporal processing. Excitatory inputs derive from neurons in the posteroventral cochlear nucleus (PVCN) octopus and multipolar/stellate cells (Friauf and Ostwald 1988, Schofield 1995, Thompson and Thompson 1991). *In vivo* and *in vitro* studies have shown that these cells are well suited to transmit precise temporal information (Ferragamo et al. 1998, Gardner et al. 1999, Rhode et al. 1983b, Rhode and Greenberg 1994, Smith and Rhode 1989). Moreover, the inhibitory input derives from MNTB principal cells (Banks and Smith 1992, Kuwabara et al. 1991, Sommer et al. 1993) and is supposedly glycinergic (Wenthold et al. 1987). The MNTB gets its input from globular bushy cells of the AVCN via the calyces of held which stand for accurate signal transmission (see above). Hence, the SPN is a target of precisely timed excitatory and inhibitory inputs. Taken together, based on the knowledge of input patterns, the SPN could support either complex filtering properties due to the interaction of excitatory and inhibitory inputs (compare: Grothe 1994, Kuwada and Batra 1999) or very precise transmission of temporal information to the auditory midbrain.

2.3 *The gerbil as an animal model*

An ideal animal to investigate questions on general temporal processing (in the context of sound localization and recognition) is the Mongolian gerbil, *Meriones unguiculatus*. The gerbil, a small rodent, lives in burrow systems in the big deserts of Mongolia and northern China. In addition to having well developed low frequency hearing, gerbils also hear well in the high frequency range up to 60 kHz (Ryan 1976).

Communication over long distances (as necessary in desert planes) and through soil requires low frequency signals. Even though some of the gerbil's communication signals are in the frequency range above 2 kHz ("high frequencies" at which sufficient ITDs are produced by the head and can be used for sound localization), a characteristic behavior of the gerbil is to alert its conspecifics when a predator is approaching, by "drumming" (rhythmic beating on the ground with the hind limbs), a low frequency signal. This elicits escaping behavior of other gerbils in the area (Yapa 1994). Therefore low frequency hearing is vital for gerbils e.g. to escape attacking predators, like the little owl (Lay 1974).

The gerbil's hearing system displays several adaptations to low frequency hearing useful for carrying information over long distances. A comparative study by Webster and Plassman (1992), about evolution of low frequency hearing, showed that gerbils possess big bullae and big tympani, in addition to freely moving ossicles and comparatively long basilar membranes. These are all morphological characteristics required for low frequency hearing (Rosowski 1992, Webster and Webster 1975).

Behavioral studies confirmed that gerbils have good low frequency hearing down to 20 Hz and that they are able to lateralize low frequency pure tones (Heffner and Heffner 1988, Ryan 1976), hence that they use ITDs for sound localization. The mammalian ITD detector, the MSO, is well developed in these animals (Kapfer et al. 2002, Nordeen et al. 1983).

Moreover, there is already evidence from gerbil MSO studies that inhibition is important for processing of binaural cues. As already mentioned, an *in vitro* study showed that inhibitory input on gerbil MSO neurons has a profound impact on encoding various stimulus parameters, including ITDs (Grothe and Sanes 1994). Further evidence of the importance of inhibition comes from a developmental study in the gerbil MSO comparing distribution of glycinergic synapses in animals before hearing onset to those of adult animals (Kapfer et al. 2002). The authors showed a developmental refinement of

glycinergic synapses and, moreover, that this refinement is activity dependent and requires binaural cues.

Given the animal's broad hearing range, the gerbil is suitable for studies on ITD encoding and its representation in the brain and, furthermore, for investigations on temporal processing in auditory brainstem structures in general.

2.4 The scope of this study

The general role of the MSO in mammals is still not clear. The accomplished studies may suggest that there are different functions of the nucleus in different animals depending on their audiogram. These functions are consequently ITD-based sound localization in low frequency and pattern recognition in high frequency hearing animals – both tasks involving temporal processing. However, it is also known that there are neurons in the MSO of low frequency hearing animals that show tuning to high frequencies, a finding in line with the ability of those animals to hear well in the high frequency range (Batra et al 1997a, Goldberg and Brown 1968, Guinan et al. 1972a, Yin and Chan 1990). It is therefore possible that the MSO in low frequency hearing animals serves both, sound localization and pattern recognition.

Even though the MSO is accepted to be the ITD encoding structure – the mechanism of how ITDs are encoded in mammals is unclear. The elegant Jeffress model could predict ITD coding in birds and has been assumed to be an adequate description for mammals as well, even though final evidence for delay lines is missing and the role of MNTB inputs is unclear. Only recently, the idea of a “Jeffress-like” space map has been challenged by studies in the rabbit (Fitzpatrick et al. 2000, 2002) and the guinea pig (McAlpine et al. 2001).

As shown above, the gerbil is a convenient model for studying low and high frequency temporal processing in the MSO. It can be assumed that low frequency MSO neurons are involved in the processing of ITDs and, moreover, that a significant proportion in the gerbil MSO is tuned to higher frequency. The gerbil is suitable to contribute to the understanding how ITDs are encoded and represented in the MSO and, moreover, what the general of MSO and SPN in temporal processing might be. The following questions were addressed using electrophysiological and neuropharmacological methods.

- I. Is there a topographical representation of space at the level of the brainstem?
- II. What is the role of glycinergic inhibition in processing of ITDs in the MSO?
- III. Are there high frequency neurons in the gerbil MSO and if so are these neurons involved in spatial and/or non-spatial temporal processing?
- IV. Is the SPN involved in ITD/IID processing and/or precise temporal processing?

Electrophysiological recordings have been performed extracellularly on single cells in MSO and SPN of 59 male and female Mongolian gerbils (*Meriones unguiculatus*) from an in-house breeding colony.

3.1 Stereotaxia and Surgery

Initially the animals were anesthetized with an intraperitoneal injection of Ketamine (10 mg / 100 g) and Rompun (2%). During surgery and recording sessions, the same mixture was applied continuously by intramuscular injection (0.15 – 0.25 ml/h).

Skin and tissue covering the upper part of the skull were dissected and carefully pushed aside laterally (no muscles cover this part of the skull). Three prominent sutures become visible (see Fig. 3.1). The saggital suture divides the bilateral skull, intersected by

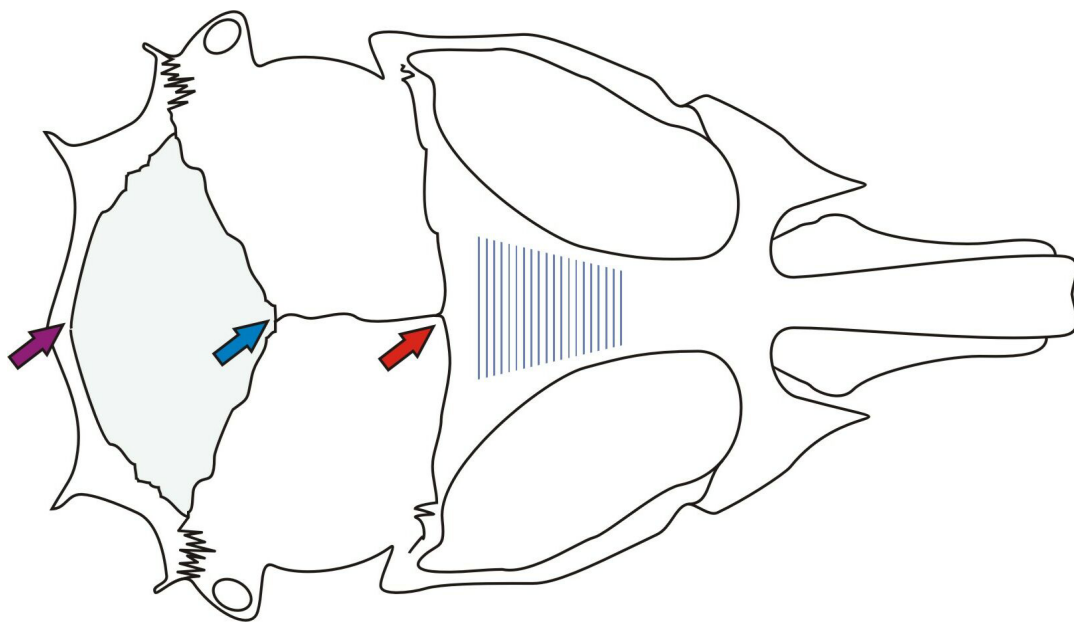


Figure 3.1

Schematic drawing of gerbil skull, dorsal view. The red/blue arrow marks the bregma/lambda point. The purple arrow marks the point, on the most caudal suture, that was also used for stereotactic measurements. For details see text.

the more rostral bregmoid suture and the more caudal lambdoid suture. Intersections are established at the Bregma point and the Lambda point, respectively. These intersections are very similar from animal to animal and could be used as reference points in stereotaxic measurements.

To get a standardized measure for positioning the electrode to penetrate the gerbil's brain a stereotactic device was used. The animal's head was reproducibly secured in the stereotactic device with a metal rod that was mounted onto the skull rostral to the bregmoid suture (hatched area in Fig. 3.1) with UV-sensitive dental restorative material (Charisma, Heraeus Kulzer, Dormagen, Germany). This allows leveling the animal's skull in a normalized position independent of size differences between animals. The caudal part of the skull (green shaded area in Fig.3.1) was leveled parallel to the horizontal plane by bringing the Lambda point (blue arrow in Fig. 3.1 and 3.2) and a corresponding point

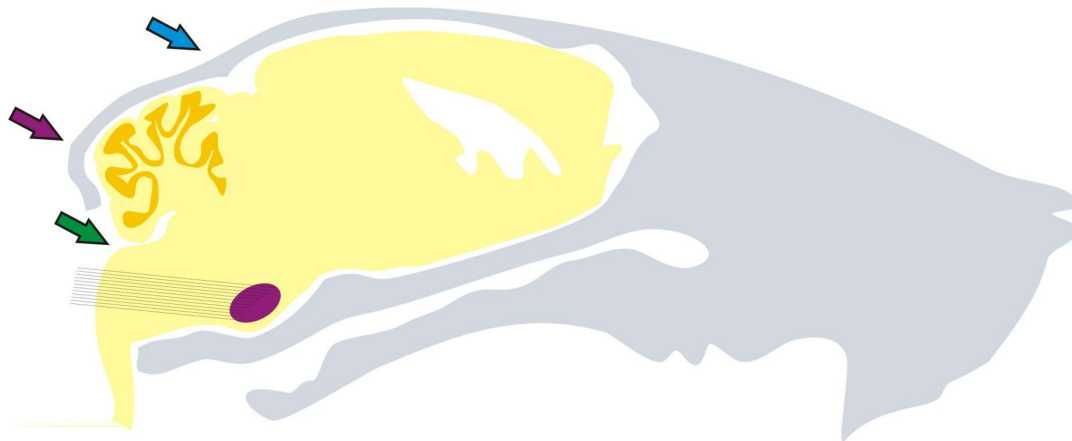


Figure 3.2

Schematic drawing of gerbil skull, saggital plane, about 800 μm laterally to the midline. The green arrow indicates the intercept of cerebellum and the brainstem. The blue arrow marks the Lambda point, the purple area the caudal suture (see Fig. 3.2). The purple area in the brain indicates the SOC, dotted lines resemble electrode penetrations (modified from Loskota et al. 1974).

at the most caudal suture (indicated by purple arrow in Fig. 3.1 and 3.2) into the same plane. Two points, each 2000 μm lateral from the Bregma point, (red arrow in Fig. 3.1) on or near (depending on the suture's course) the bregmoid suture were used to level the head in the lateral direction. To penetrate the electrode into the MSO or the SPN through the *Foramen magnum* at the caudal end of the skull, the animal was rotated 60 degrees rostrally (see gerbil brain atlas; Loskota et al. 1974, Spitzer and Semple 1995, compare Fig. 3.2).

After positioning the head, muscles and connective tissue overlaying the foramen magnum and, subsequently, the dura the brain were removed carefully. Parts of the cerebellum and both hemispheres of the brainstem were visible and allowed positioning of the electrode. Electrode positions were oriented on the intercept of the cerebellum and the midbrain hemispheres (green arrow in Fig. 3.2) and controlled with micromanipulator gages ("Digimatic", Mitutoyo, Neuss, Germany) in all three

dimensions (mediolateral, dorsoventral and rostrocaudal). Electrodes were advanced under remote control, using a motorized micromanipulator (DC3314, World Precision Instruments, Germany) and a piezodriven (PM-10-1, World Precision Instruments, Germany).

During recording sessions the animal was placed on a heating cushion (36° C) in a sound attenuated chamber fixed with the metal rod. Saline (0.9 %) was applied frequently to the opening to avoid dehydration of the brain. Typical recording periods lasted 10 – 14 hours.

3.2 *Neuronal Recordings*

As a first approach, to estimate the recording position in the SOC, low impedance tungsten electrodes (1 or 5 M Ω , World Precision Instruments, Germany) were lowered into the brainstem to monitor overall auditory activity (evoked potentials or multi units). The signal was amplified by a microelectrode extracellular amplifier (EXT-01, npi electronics, Germany) and displayed on an oscilloscope (Yokogawa, DL 708E, Japan). After the location of auditory activity, the metal electrode was removed and a high impedance glass electrode was penetrated into the same region. Single unit responses were recorded extracellularly with those glass pipettes, filled with 2 M sodium acetate (impedance 10 – 30 M Ω). Recorded signals were fed via an electrometer (Electro 705, World Precision Instruments, Germany) and an amplifier (Toellner 7601, Germany) into a 50 / 60 Hz noise eliminator (Humbug, Quest Scientific, Canada), a 0.7 to 3 kHz band-pass filter (spike conditioner PC1, System II, Tucker Davis Technologies, USA) and a spike discriminator (SD1, System II, Tucker Davis Technologies, USA). Only action potentials from single neurons with a signal to noise ratio of >5 were recorded. Action potentials were registered using an event timer (ET1, System II, Tucker Davis Technologies, USA; temporal accuracy 2.5 μ s) and a DSP-Board in a PC (System II, Tucker Davis Technologies, USA) before storage for offline analysis. The recording of action potentials and stimulus generation was controlled by custom-made software (“spike”, D. Molter, Zoologisches Institut der LMU, München and B. Warren, University of Washington, Seattle).

3.3 *Acoustic stimulation*

Acoustic stimuli were delivered using a Tucker Davis Technologies System II (USA), consisting of a 16-bit digital-analog converter (DA3-2; sampling rate 250 Hz), anti-aliasing filters (FT-6; cut-off 100 kHz), and two digital attenuators per channel (PA4). Stimuli were presented via an electrostatic speaker driver (ED1, System 3, Tucker Davis Technologies, USA) and two electrostatic speakers (System 3, Tucker Davis Technologies, USA) or a headphone buffer HB6 (System II, Tucker Davis Technologies, USA) and two Beyer Dynamics speakers (model TD 990, Germany). Both systems were fitted to the ear via 5 mm diameter probe tubes. Both sets of earphones, including the tubes, were calibrated using a ¼ inch microphone (Reinstorp VtS, Germany), a measuring amplifier (MV 302, Microtech, Germany) and a waveform analyzer (Stanford Research Systems, SR770 FFT network analyzer, USA).

3.4 *Recording Procedure*

To search for acoustic responses, pure tones, sinusoidally amplitude modulated pure tones (SAM; modulation frequency 10 – 1000 Hz, modulation depth 100%), upward frequency modulated sounds (500 Hz – 50 kHz), or noise stimuli were delivered binaurally with varying amplitude. The stimulus duration was 100 ms; the rise-fall time was 5 ms to cover at least approximately 3 times the period of the lowest stimulus frequency used (unless otherwise stated). After encountering and isolation of a neuron, a tuning curve was measured, using 40 or 100 ms pure tones. Subsequently, frequency was set to BF and attenuation to 20 dB above threshold (a.T.) if not otherwise stated. Then binaural properties were examined by presenting pure tones, SAM or noise stimuli at various ITDs or IIDs. Sensitivity to IIDs was measured with the stimulus intensity kept constant at one ear and systematically varied at the other ear (over a range of at least 40 dB). Sensitivity to static ITDs was tested with pure tones (low frequency neurons; BF < 2 kHz), trains of tone pulses (5 pulses, 5 ms pulse duration, rise-fall time 0.5 ms, variable inter-stimulus interval of 1 – 20 ms), short upwards frequency modulated sweeps (5 pulses, 5 ms duration, rise-fall time 0.5 ms, variable inter-stimulus intervals) or SAM stimuli. All stimuli were presented at each neuron's BF. Pure tone ITDs were additionally measured at some other frequencies near BF. The stimulus delay was constant at one ear and varied at the other ear in 50 to 200 μ s steps covering a range of up to \pm 5 ms.

Binaural or monaural SAM stimuli were presented at different modulation frequencies. The carrier frequency was set to each neuron's BF. The modulation frequency of the SAM stimuli covered a range from 20-1000 Hz in 11 logarithmic steps, and the modulation depth was 100%.

For all stimulus paradigms, at least 10 repetitions per modulation frequency were presented in a random order with an inter-stimulus interval of 250 ms or more, to avoid adaptation effects.

3.5 Pharmacology

To evaluate the effect of glycinergic inhibition, data was also collected during application of glycine or the glycine antagonist strychnine. "Piggy back" multibarrel electrodes (Harvey and Caspary 1980) were used for iontophoretic application of glycine and the glycine receptor antagonist strychnine. A blank of a 5-barrel glass electrode (World Precision Instruments, Berlin, Germany, outer diameter of a single barrel 1.2 mm with filament) was pulled (Narishige, Puller PE-02, Japan) and the tip was cut with a scalpel blade under microscopic control to a total diameter of approximately 20 – 30 μm . A common single-barrel electrode (Harvard Apparatus Inc., USA, outer diameter 1.5 mm, inner diameter 0.86 mm, with filament) was bent approximately 10 mm from the tip to fit into the kerf built by the arrangement of the five barrels. The recording electrode was glued to the multibarrel with the help of a piece of plastic as base and clay for fixation (see Fig. 3.3 for electrode arrangement). The tip of the recording electrode protruded about 5 to 15 μm beyond the tip of the multibarrel electrode.

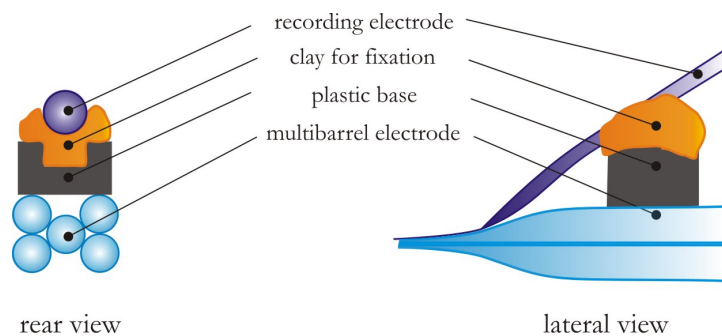


Figure 3.3
Arrangement of the „piggy back“ electrode for the iontophoretic application of drugs.

Typically, three barrels were filled either with glycine (0.5 M, pH 4) or strychnine (10 mM, pH 3.5). One barrel was filled with horseradish peroxidase (HRP, Sigma, Germany) to mark recording sites. The remaining barrel was filled with 1 M sodium acetate to serve

as a balancing channel. The recording electrode was filled with 2 M sodium acetate as in the non-pharmacological experiments (impedance around 10 - 20 M Ω). The drug and the balancing electrodes were connected via Teflon coated silver wires to a micro-iontophoresis system (Neurophore MVCS, npi electronics, Germany or Neurophore BH-2 System, Medical Systems, Harvard Apparatus, Inc., USA) that was used to generate and monitor ejection (glycine 10 – 40 nA; strychnine \leq 240 nA) and retention currents (-24 nA). The sum channel that was connected to the balancing electrode was used to offset current effects. The recording electrode was controlled via an electrometer, as described above.

3.6 Data Analysis

Data were analyzed offline using individual spike times, Peri-Stimulus-Time histograms (PSTHs, bin width 1 ms), and inter spike intervals (bin width 0.5 ms). As a measure for sharpness of frequency tuning, Q_{10dB} values were calculated using the formula

$$Q_{10dB} = \frac{\text{BF}}{\text{tuning width 10 dB above threshold}}.$$

To assess ITD-sensitivity, the measured interaural delays were plotted against normalized spikerate for each tested frequency (either pure tone frequency or modulation frequencies for ITDs in high frequency envelopes).

For the analysis of best ITDs and for the vector strength (VS) of phase-locking to pure tones and SAM, circular statistics (Batschelet 1991) were used. Each value in a distribution of values (either the ITD functions or the raster plots of the response for phase-locking) defines a vector with the angle ϕ . The sum of those vectors forms the so-called mean vector. By calculation of the best interaural phase difference (the direction of the calculated vector for the ITD function) the best ITD of the neuron was evaluated for each test frequency if the neurons showed ITD sensitivity.

The direction of the mean vector is defined as

$$r = \arctan\left(\frac{\sum \cos \phi_i}{\sum \sin \phi_i}\right) + k.$$

The length of the mean vector (vector strength VS) allows evaluating the degree to which neuronal responses are correlated with the phase of the pure tone frequency or the modulation frequency respectively

$$VS = \sqrt{\frac{\left(\sum_{i=1}^n \cos \phi_i\right)^2 + \left(\sum_{i=1}^n \sin \phi_i\right)^2}{n}}.$$

The VS can be between 0 and 1, a VS of one equals optimal synchronization whereas a calculated VS of zero would indicate that there is no correlation between stimulus frequency and neuronal response. Only statistically significant VS values that fulfilled the $p < 0.005$ criterion in the Rayleigh test (Batschelet 1991) were used. To quantify neuronal discharges evoked by SAM, modulation transfer functions (MTFs) based on spikerate and vector strength (VS) were plotted. For calculating MTFs, the response to the first cycle was excluded from the analysis. If the first cycle was shorter than 10 ms, the first 10 ms (hence for frequencies above 100 Hz) of the response were excluded. As a criterion for filter cut-offs, a 50% drop in spikerate based MTFs was used. Accordingly, for VS based MTFs the modulation rate at which the VS dropped below 0.3 or became insignificant was regarded as a cut-off.

3.7 Histology

To assure recordings were obtained from either MSO or SPN, defined positions in the brain were marked at the end of a recording session. For labeling recording sites two different dyes were used. When recording with multibarrel electrodes, HRP was applied iontophoretically (Neurophore MVCS, npi electronics, Germany or Neurophore BH-2 System, Medical Systems, Harvard Apparatus, Inc., USA) with 720 nA for 8 minutes out

of one of the pipettes of the multibarrel. Alternatively, when recording with single barrels, either HRP or latex particles coupled with either the red-fluorescent dye Rhodamine or the green-fluorescent dye Fluorescein (“fluorescent beads”, Fluorescent Latex Microspheres, Lumafluor Inc., USA) were used. These were injected through a cut glass pipette (tip size: 20 μm diameter), positioned at the site of recording, with a pressure injector (PDES – L, npi electronics, Germany, three times 2 psi for 50 ms). This was necessary because neither HRP nor fluorescent beads could be injected through high impedance electrodes.

At the end of the experiment the animals were injected with the same volume of anesthesia (Ketamin/Rompun) as for the initial narcosis. They were perfused intracardially with heparinized 0.9% saline for 5 minutes followed by 4% paraformaldehyde and 25% glutaraldehyde for 40 minutes (for perfusing the bead injected brains no glutaraldehyde was added to reduce fluorescent background). The brain was then removed from the skull and stored in sucrose for cryoprotection (10%, 20%, 30% solutions were applied successively, and the brain remained in each solution until it sank). Finally, the brain was embedded in egg yolk (fixated with 1 ml of 25% glutaraldehyde) in an embedding chamber. The brain was positioned in the chamber under optical control and with reference to the gerbil brain atlas (Loskota et al. 1974), such that the brain orientation was comparable to the one after stereotactic measures (recall that the caudal part of the skull was leveled into the horizontal plane). The brain was then mounted on a cryostat (Leica Microsystems CM 3050S, Nussloch, Germany) to obtain frontal sections ($\sim 48 \mu\text{m}$) of the superior olivary complex (SOC). To compare injection sites and brain morphology, sections were collected in two alternating rows. One series was stained with cresyl-violet (following standard protocols to stain nerve cells) for orientation purposes. The other series was stained depending on the type of injection (see below).

3.7.1 Histology of HRP Injections

To visualize HRP injections, the sections were stained with diaminobenzidine, intensified by cytochrome (following procedures originally described by Adams 1977). After dehydration in alcohols (isopropanol, butanol) of different concentrations and xylol, HRP stained sections were dried, embedded in Krystallon (Merck, Germany) and

covered with a cover slip. Recording sites were located by light microscopy (Axiophot, Zeiss, Germany) and digitized with a digital camera (Axiocam, Zeiss, Germany) for offline analysis.

3.7.2 *Histology of bead injections*

To evaluate recording sites marked with fluorescent beads brains were only quickly dehydrated in alcohol, because the fluorescence of the beads is alcohol sensitive. To shorten the “normal” dehydration protocol, sections were dehydrated in 100 % Ethanol for 10 s followed by two times 10 seconds in Xylol. Dried slices have been embedded in Entellan (Merck, Germany) and covered with a cover slip. To verify recording sites, sections were analyzed with an epifluorescent microscope (Axiophot, Zeiss, Germany) using appropriate filter sets for Rhodamin- and Fluorescein-beads respectively. SOC-sections with marked areas were digitized and stored for offline analysis.

3.8 *MSO - Reconstruction*

Only few positions were directly stained by either HRP or fluorescent beads, therefore the position of other recordings in the same session had to be reconstructed. The brains were embedded in the same position, as they were oriented before rotation of the animal. In acute experiments the skull covering the cerebellum (see above and Fig. 3.2) was leveled horizontally. To assure that the fixated brains are embedded in the same stereotactic position, the reference points on the skull were superimposed onto the cerebellum and these points were accordingly used to level the dorsal part of the cerebellum into the horizontal plane in the embedding chamber. Following this procedure, penetration coordinates (in the mediolateral, dorsoventral and rostrocaudal axis) relatively to the injection and the penetration angle allowed to calculate position of further recordings.

To compare data between animals, the MSOs of all successfully recorded animals were measured in all three dimensions (mediolateral, dorsoventral, rostrocaudal, see Fig. 3.4 A, B). The averages of those measures were taken to calculate dimensions of a “model” MSO to compensate for size differences of the nucleus in single animals. Furthermore, because there are considerable size differences of the MSO from rostral to

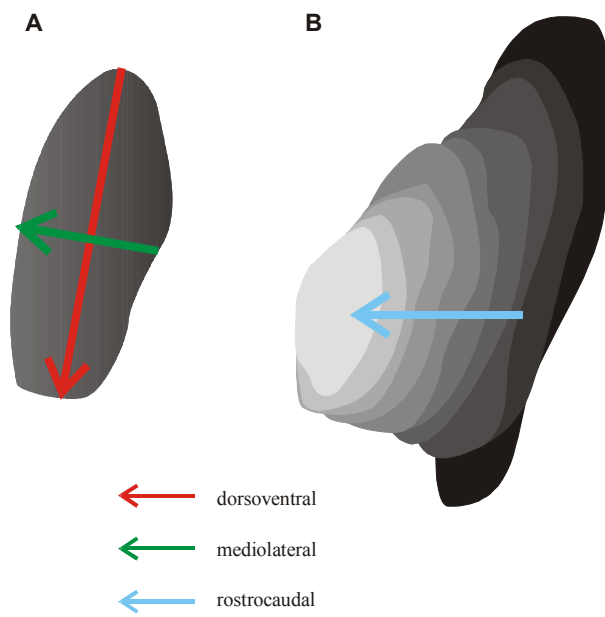


Figure 3.4
Schematical horizontal MSO sections depicting mediolateral and dorsoventral measurements (A) and the rostrocaudal dimension (B).

caudal (compare Fig. 3.4 B), the dorsoventral and mediolateral MSO measures were normalized to the respective greatest value (referred to as normalized MSO).

4.1 *The Medial Superior Olive*

Extracellular activity was recorded from single neurons in the MSO. Because of the important role of the MSO in low frequency processing, neurons were tested with ITDs in low frequency pure tones, presented binaurally via earphones. Furthermore, evidence for the role of high frequency neurons in temporal processing was obtained. Thus, neurons were analyzed in two groups, depending on frequency. Two kHz was defined as a broader frequency, because no ITD sensitivity was observed in neurons with BFs above that frequency and furthermore, phase-locking to pure tones got weaker as shown below. Additionally, general response characteristics were analyzed.

4.1.1 *Reconstruction of recording sites*

Neuronal recording sites were reconstructed using positions marked at the end of an recording session. Figure 4.1 (left upper panel) shows an HRP injection at the medial border of the MSO, about 200 μm caudally to the position at which the MSO first appeared on a section. The nucleus was measured in the dorsoventral and mediolateral extension (blue and red arrows, respectively, middle upper panel in Fig. 4.1). Then the position of the injection was measured relatively to the center of the dimension of the MSO in that section (right panel in Fig. 4.1). This injection point was used to reconstruct other recording positions in the same animal (penetration coordinates were controlled digitally). Recording positions were transferred into a coordinate system (see Fig. 4.1 lower panels).

Because only in rare cases more than two units were recorded in a single session, statements about overall neuronal organization in single animals are impossible. Therefore, recording sites were transferred into a “model” MSO, determined by the circumferences of all MSOs in which neurons were recorded. This “model MSO” allowed a correlation of recording positions with neuronal properties (e.g. BF to reveal tonotopic representation). Furthermore, normalizing the mediolateral and dorsoventral axes of the MSOs evened out size differences of the nucleus in the rostrocaudal dimension. Figure 4.2 displays all recording sites in “model” and normalized MSO.

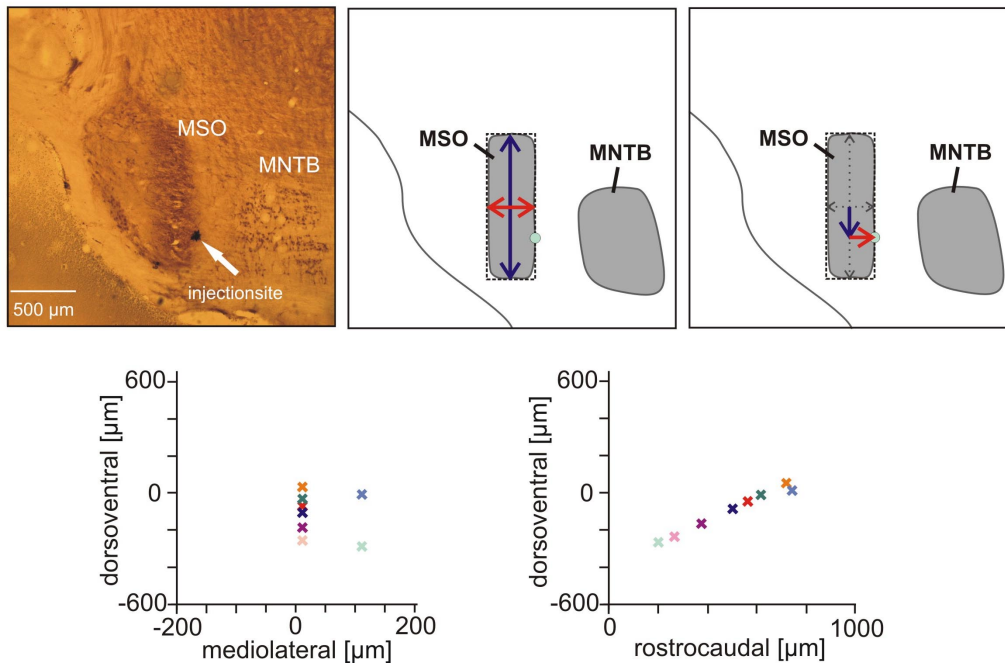


Figure 4.1

Reconstruction of recording sites in one of the gerbils used in this study. **A** Coronal section of the MSO showing an HRP injection at the border of the MSO. **B, C** Exemplification of measures taken in the MSO, for details see text. **D, E** Transfer of coordinates of reconstructed recording sites, displayed for the mediolateral axis (**D**) and the rostrocaudal axis (**E**).

In a subset of experiments ($N=29$) two fluorescent dyes were injected at different sites, with two electrodes at the same penetration coordinates to confirm the accuracy of the penetrations. In the mediolateral extension the same injections site was hit with an accuracy of $\pm 80 \mu\text{m}$ and with an accuracy of $\pm 100 \mu\text{m}$ in the dorsoventral axis. For the rostrocaudal extension an accuracy of $\pm 100 \mu\text{m}$ was assumed because marked brain sections, that were processed to reveal HRP or bead injections, were collected approximately each $100 \mu\text{m}$. Given the errors in each of the three dimensions the reconstructed MSO neurons were divided into three subpopulations. 1. Neurons that have proven to be in the MSO, because they were directly verified with marker injections at the recording site or were recorded in the same penetration in which a position was labeled (referred to as “MSO”). 2. Neurons that were calculated to be in the MSO given the confirmed accuracy (“most likely MSO”). 3. Neurons that were calculated to be in the MSO, but which could as well lie outside the MSO given the margin of error (“potentially MSO”). Using this classification, 12 neurons were MSO neurons, 32 neurons were most likely and 28 neurons were potentially located in the MSO.

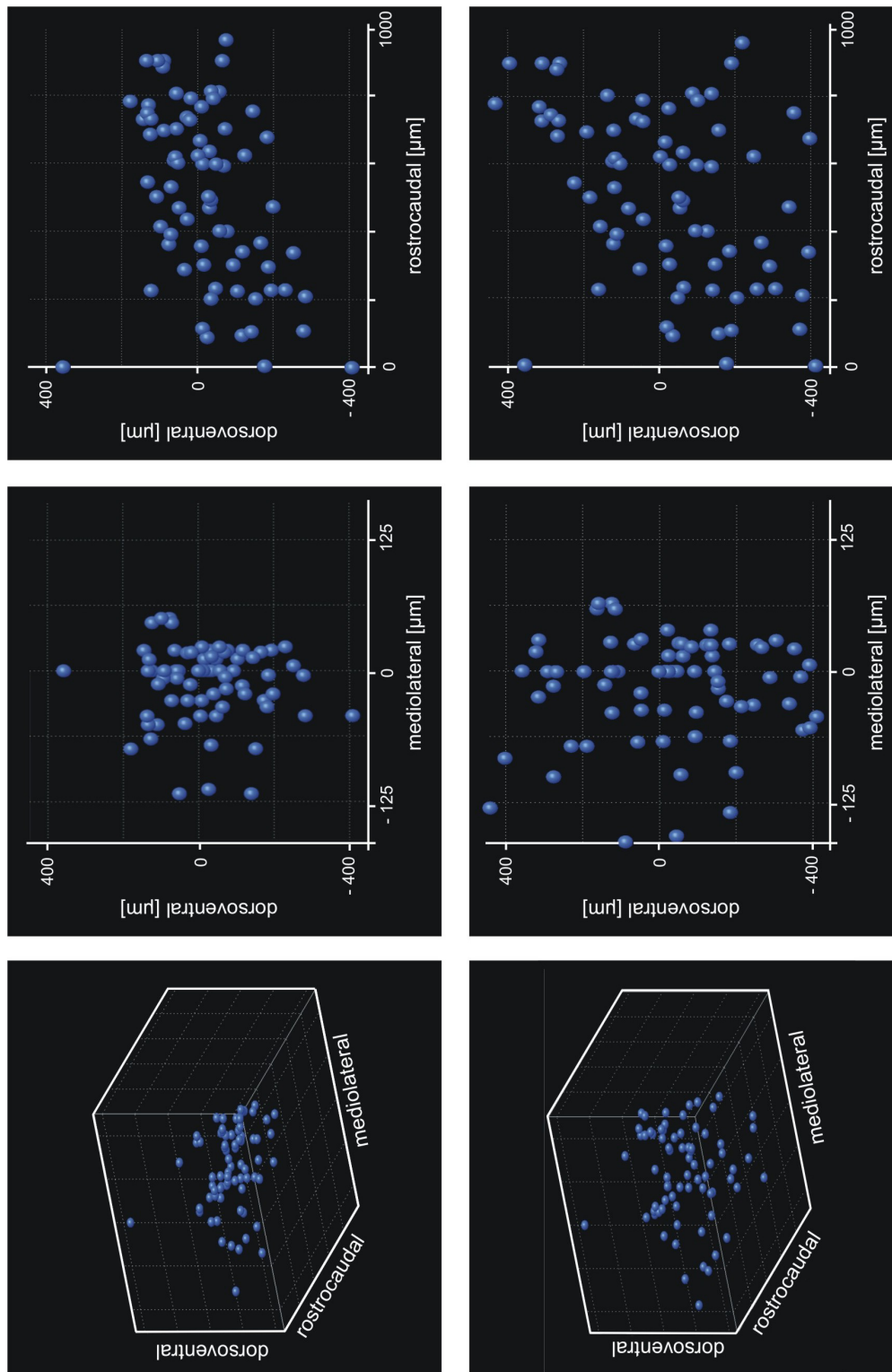


Figure 4.2

Sites of all neurons recorded in “model” (*upper row*) and normalized (*lower row*) MSO. *Left column* Distribution of recorded MSO neurons in a 3D plot. To clarify alignment of the neurons in the mediolateral and dorsoventral axis, *middle* and *right columns* show 2D plots for the respective axes. Note that neuronal recordings are concentrated at the somatic region (approximately $\pm 25 \mu\text{m}$), but that some recordings are far outside in the dendritic region. In the *right columns* it is noticeable that recording sites follow clearly the electrodes tracks arising from the penetration through the foramen magnum.

		MSO	most likely MSO	potentially MSO	all neurons
spontaneous rate	low	2/13 (15 %)	9/31 (29 %)	6/28 (21 %)	17/72 (24 %)
	moderate	8/13 (62 %)	16/31 (52 %)	14/28 (50 %)	38/72 (52 %)
	high	3/13 (23 %)	6/31 (19 %)	8/28 (29 %)	17/72 (24 %)
BF	< 2 kHz	8/12 (67 %)	20/32 (63%)	9/26 (35 %)	37/70 (53 %)
	≥ 2 kHz	4/12 (33 %)	12/32 (37%)	17/26 (65 %)	33/70 (47 %)
Q _{10dB}	< 2 kHz	1/4 (25%)	6/14 (43 %)	5/10 (50%)	12/28 (43 %)
	≥ 2 kHz	3/4 (75%)	8/14 (57%)	5/10 (50%)	16/28 (57 %)
RLF	monotonic	5/5 (100 %)	13/16 (81%)	12/14 (86 %)	30/35 (86 %)
	non-monot.	0/5 (0%)	3/16 (19 %)	2/14 (14 %)	5/35 (14%)
response pattern to pure tone	ON	2/12 (17 %)	7/30 (23%)	5/26 (19 %)	14/68 (21 %)
	OFF	0/12 (0 %)	1/30 (3 %)	0/26 (0 %)	1/68 (2 %)
	tonic	2/12 (17 %)	7/30 (23 %)	10/26 (39 %)	19/68 (28 %)
	phase-locking	6/12 (50 %)	11/30 (37%)	10/26 (39 %)	27/68 (40 %)
	chopper	0/12 (0 %)	3/30 (10 %)	0/26 (0 %)	3/68 (4 %)
	primary like	2/12 (17%)	1/30 (3 %)	1/26 (4 %)	4/68 (6 %)
latency [ms]	< 2 kHz	7.8 ± 5.4 (N=5)	5.9 ± 5.4 (N=16)	5.9 ± 3.6 (N=9)	6.2 ± 4.8 (N=30)
	≥ 2 kHz	2.7 ± 0.7 (N=3)	4.8 ± 3.3 (N=10)	4.9 ± 5.4 (N=14)	4.6 ± 4.3 (N=27)
jitter [μs]	< 2 kHz	1200 ± 1002 (N=5)	807 ± 1171 (N=16)	456 ± 292 (N=9)	764 ± 950 (N=30)
	≥ 2 kHz	400 ± 173 (N=3)	370 ± 216 (N=10)	607 ± 956 (N=9)	496 ± 699 (N=27)
binaural properties	E/E	7/12 (58 %)	16/26 (62 %)	10/20 (50 %)	33/58 (57 %)
	0/E	3/12 (25 %)	6/26 (23 %)	6/20 (30 %)	15/58 (26 %)
	E/0	2/12 (17 %)	4/26 (15 %)	4/20 (20 %)	10/58 (17 %)

Table 4.1

Distribution of general response properties in the MSO for the three subpopulations of neurons (directly reconstructed to be in the MSO, most likely in the MSO and potentially in the MSO, see text) and for all neurons. First letter in the category binaural properties indicates ipsilateral input, the second letter contralateral input

BF, best frequency

RLF, rate level function

E, excitatory

0, no overall input

Data was analyzed for the whole population of neurons and as well divided into the three subpopulations. The analysis of all neurons is described in the text, whereas data for the three subpopulations (MSO, most likely MSO and potentially MSO) is shown in Table 4.1. Figures for single response properties combine information about all neurons and the three subpopulations.

4.1.2 Spontaneous activity

Spontaneous activity in MSO neurons ranged from 0 up to 72.4 action potentials (referred to as “spikes” in the following) per second. Combining all neurons, 17 neurons (24%) showed low spontaneous rates, below 1 spike per second, 38 neurons (52%) showed moderate rates, between 1 and 10 spikes per second, whereas the remaining 17 neurons (24%) fired more than 10 spikes per second spontaneously. The averaged spontaneous activity was 9.2 ± 14.7 spikes / s. Figure 4.3 shows the distribution of spontaneous activity for the three subpopulation of neurons (MSO, most likely MSO and potentially MSO neurons, for data of the three populations see Table 4.1).

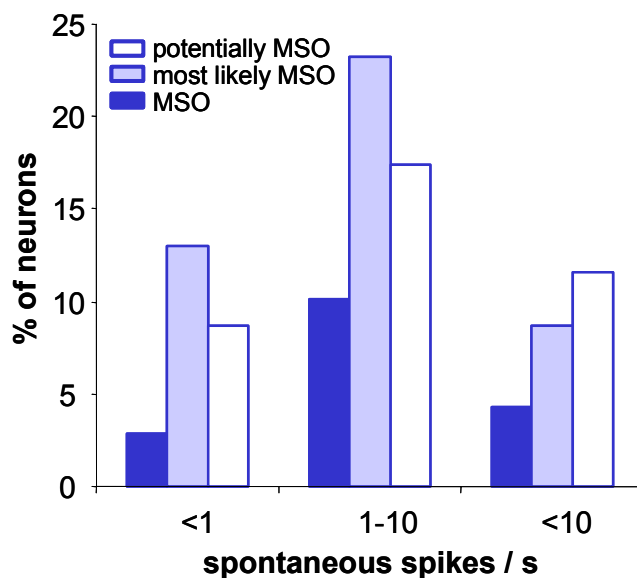


Figure 4.3
Distribution of spontaneous activity for the three subpopulations of MSO neurons.

4.1.3 Tuning characteristics

Within the sample of recorded neurons, 97 % (70/72) responded to stimulation with pure tones. Of the remaining 3% (2/72), one neuron responded only to noise and one could only be driven by brief upward frequency-modulated pulses.

Best frequencies (BFs) of the 70 neurons that were responsive to pure tones ranged from 500 Hz to 30 kHz, reflecting most of the gerbil audiogram (Ryan 1976). MSO neurons showed a bias towards low frequencies. More than half of the neurons (37/70, 53%) had best frequencies below 2 kHz. The threshold of the response varied from -10 to 73 dB SPL. BF and threshold of all neurons (and divided into the three subpopulations) is depicted in figure 4.4.

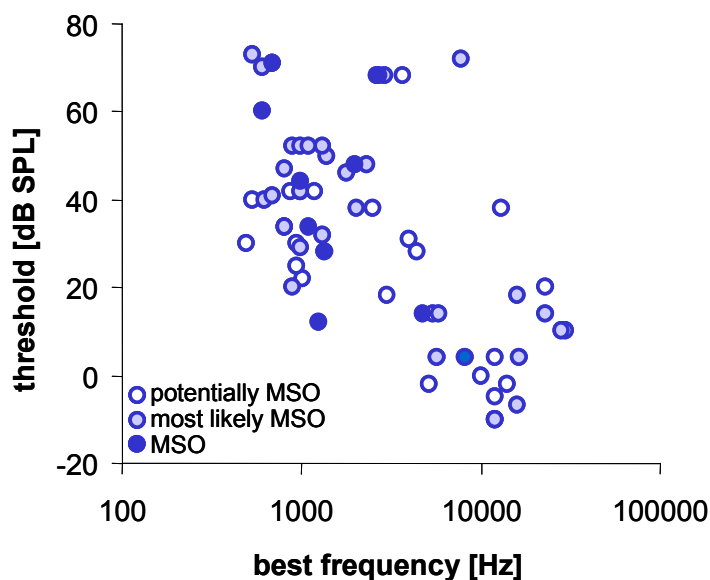


Figure 4.4
Distribution of best frequencies and threshold in dB SPL in response to pure tones in the gerbil MSO.

All of the tuning curves showed a typical v-shaped form with a single minimum. To analyze the broadness of tuning of MSO neurons, in 27 neurons Q_{10dB} values have been calculated (low Q_{10dB} values indicate broad tuning). The values ranged from 0.4 to 10.1 with an average of $2.9 (\pm 2.1)$. Comparison of Q_{10dB} values of tuning for low frequency (3.7 ± 2.4) and high frequency neurons (1.9 ± 1.0) revealed that neurons with $BF > 2$ kHz have greater values (t-test, $p < 0.018$) indicating sharper tuning at high frequencies. Moreover, only high frequency neurons showed narrow tuning with Q_{10dB} values > 4 . In figure 4.5, Q_{10dB} values are plotted against BF for all three subpopulations of neurons.

Rate-level functions (RLFs) at BF of 34 neurons were tested over a range of ≥ 40 dB using binaural stimulation (IID=0), irrespective of the binaural properties of the cell. In 86% of the neurons (30/35) raising sound pressure level caused monotonic increases in

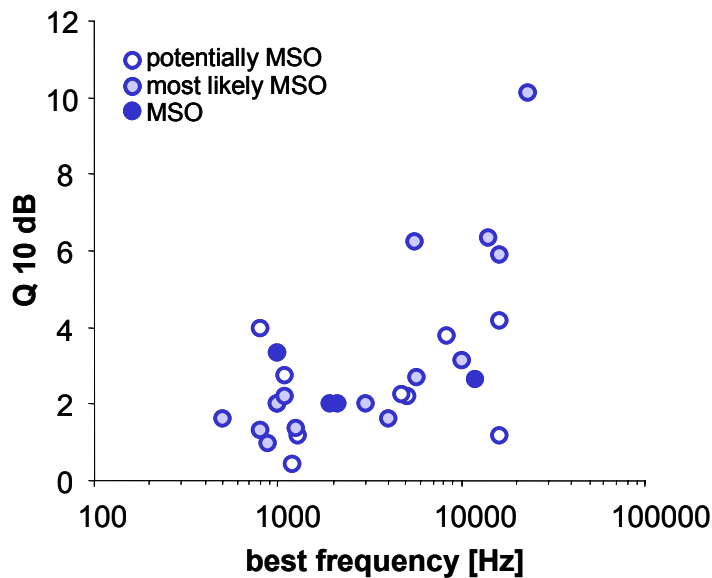


Figure 4.5
Distribution of Q_{10dB} values
in dependency of BF.

discharge rate. Only 14% (5/35) of the neurons (displaying BFs from 1200 Hz to 2300 Hz) exhibited non-monotonic RLFs. Figure 4.6 shows monotonic (Fig. 4.6 A) and non-monotonic (Fig. 4.6 B) RLFs for the three subpopulations of neurons.

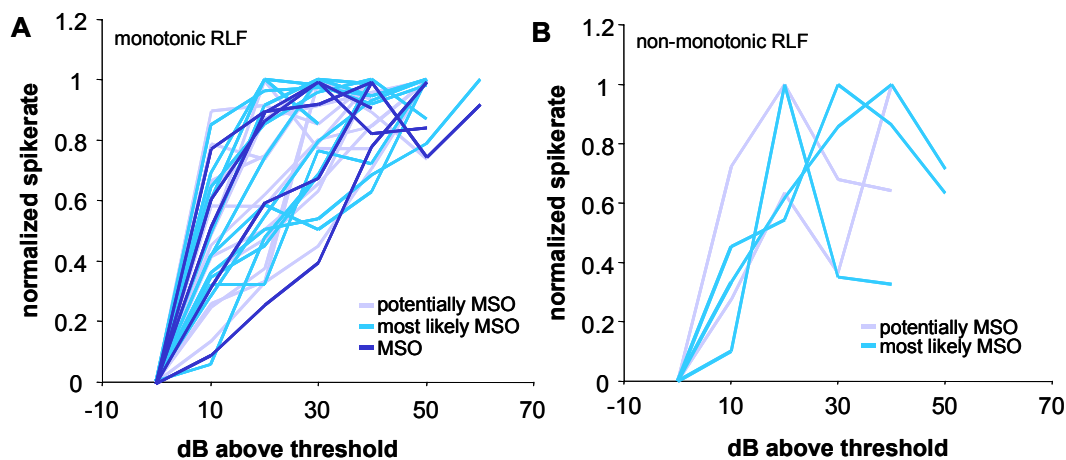


Figure 4.6
Rate Level Functions (RLF) in the gerbil MSO. **A** monotonic RLF, **B** non-monotonic RLF

4.1.4 Tonotopic Representation

To address the question of a topographic representation of frequency in the gerbil MSO, BFs were correlated to recording sites. The tonotopic map is likely to follow the dorsoventral axis (as in the MSO of other mammals (Covey et al. 1991, Goldberg and Brown 1968, Guinan et al. 1972b, Harnischfeger et al. 1985)). Data of all neurons responding to pure tones (70/72) are pooled in Figure 4.7 for “model” MSO and

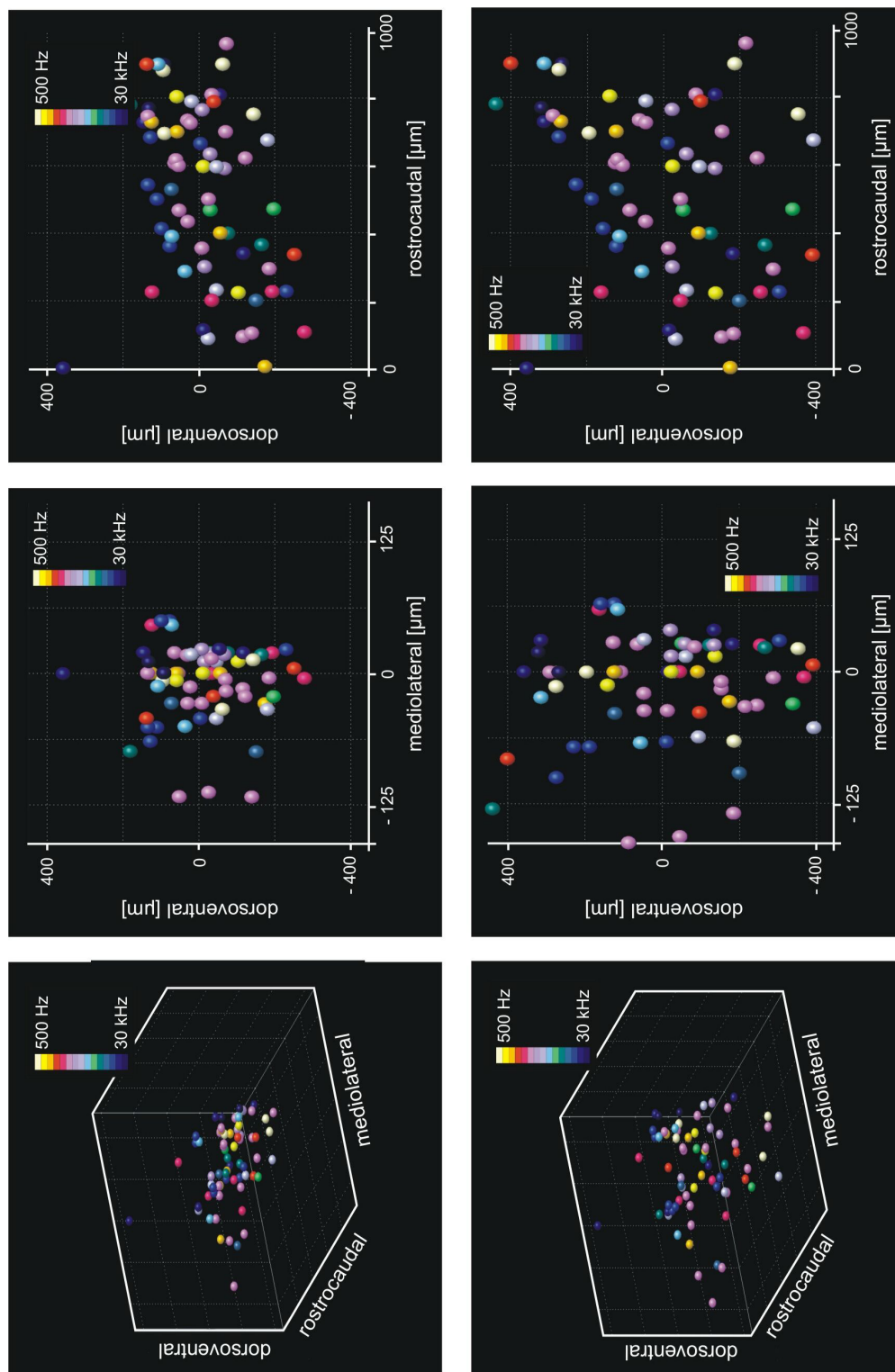
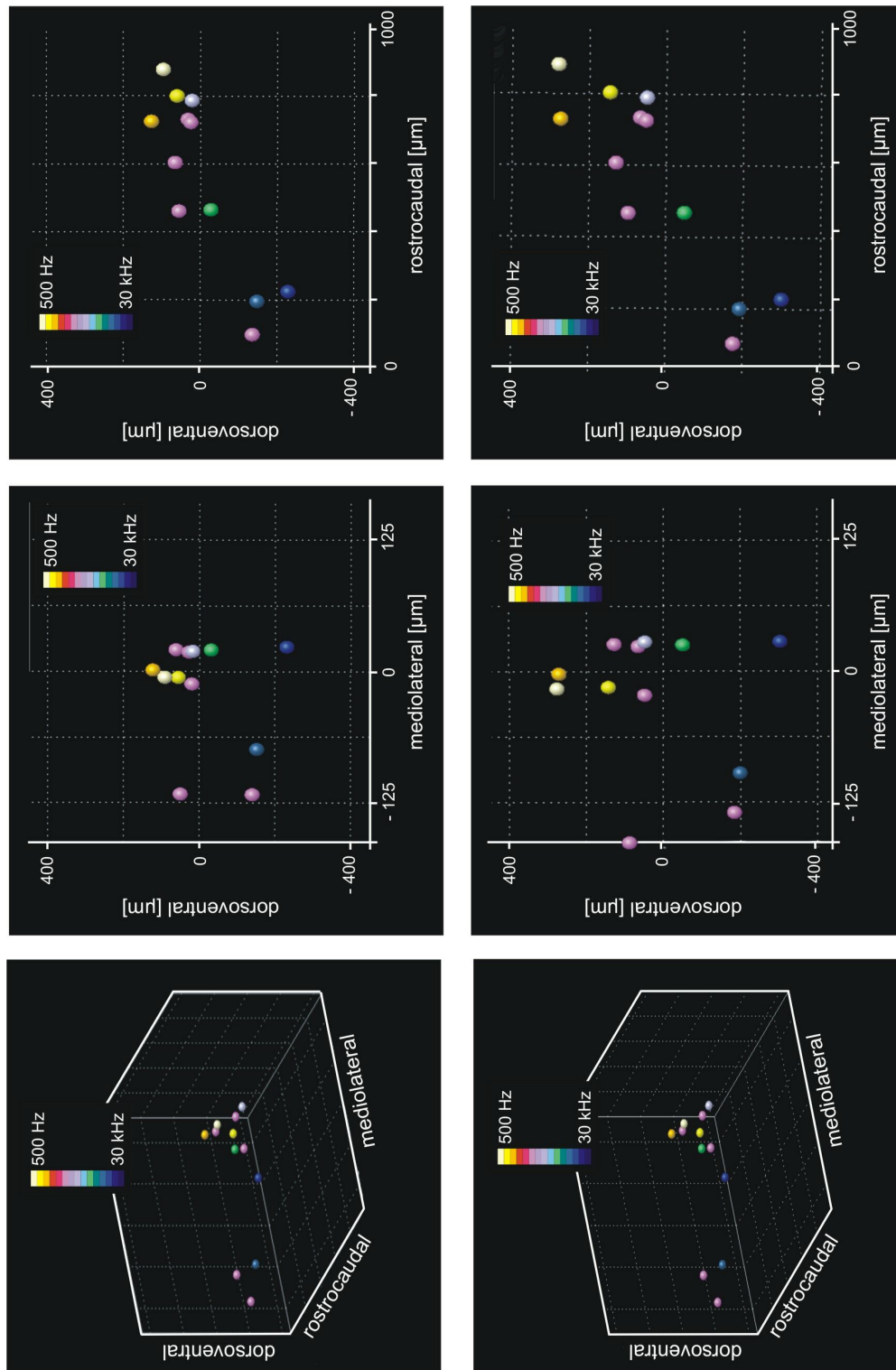


Figure 4.7

Correlation of recording site and BF in “model” (*upper row*) and normalized MSO (*lower row*). *Left column* 3D plots of all neurons, *middle column* mediolateral alignment of BFs, *right column* alignment in the rostrocaudal axis, BFs are color coded from yellow for low frequencies and blue for high frequencies, see insets (frequency in logarithmic steps).

**Figure 4.8**

Correlation of recording sites and BF for those neurons that were directly reconstructed to be in the MSO. Arrangement of panels as in figure 4.7.

normalized MSO.

Additionally, correlation values are given for BF and position in the mediolateral axis and the rostrocaudal axis, respectively, and for all three subpopulations of neurons (see table 4.1). No significant correlation was found.

However, reconstruction of only those recording sites directly marked by either HRP or fluorescent beads, revealed a trend of tonotopic organization along the dorsoventral axis from low to high frequencies (correlation highly significant, $r = 0.82$ for “model” MSO and $r = 0.78$ for normalized MSO, see Fig. 4.8). Table 4.2 combines correlation values for all investigated subpopulations.

		“model” MSO all MSO; most likely; potentially	normalized MSO all MSO; most likely; potentially
all neurons	mediolateral	0.139 0.154; 0.262; 0.155	0.142 0.154; 0.285; 0.164
	rostraucaudal	0.322 0.823; 0.278; 0.597	0.322 0.783; 0.334; 0.527
binaural neurons	mediolateral	0.266 0.712; 0.577; 0.325	0.281 0.754; 0.596; 0.351
	rostrocaudal	0.281 0.646; 0.069; 0.553	0.252 0.712; 0.577; 0.325
binaural and manipulated neurons	mediolateral	0.230 0.814; 0.451; 0.363	0.255 0.753; 0.480; 0.383
	rostrocaudal	0.313 0.939; 0.335; 0.539	0.137 0.874; 0.336; 0.541
directly marked neurons	mediolateral	0.154	0.154
	rostrocaudal	0.823	0.784

Table 4.2

Correlation coefficient r of BF and recording sites for “model” MSO and normalized MSO neurons. Note that there are some high correlation values for the mediolateral axis. Given the small numbers of neurons in those cases and the low probability of a tonotopic representation along the mediolateral axis (one row of somata) those values were not taken as an indication for a topographic representation of frequency.

4.1.5 Response pattern

Out of the population of neurons responding to pure tones, 78% (53/68) showed sustained discharge patterns when tested at their BF, 20 dB a. T.. Peri-Stimulus-Time histograms (PSTHs) of 19 of these neurons showed sustained firing without strong onset effects or pauses (for an example see Fig. 4.9 A), whereas four neurons responded with primary-like discharge patterns. Three neurons exhibited some regularity in their firing

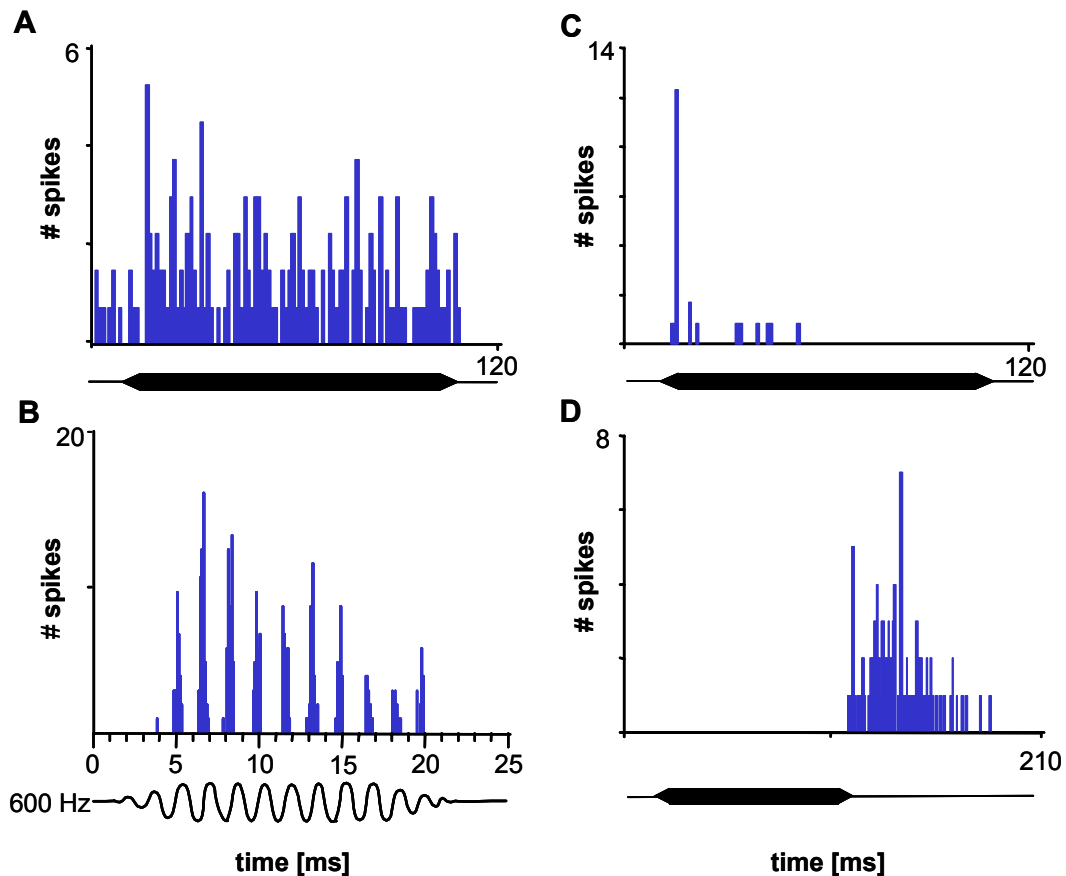


Figure 4.9

Peristimulus time histograms (PSTH) of MSO neurons. **A** Neuron with sustained response displaying a smooth PSTH. **B** Neuron with a phase-locking response to BF. **C, D** PSTH of a neuron with a phasic ON, OFF discharge respectively (stimulus duration is indicated by the horizontal black bars (A, B, D) and by the 600 Hz sinewave in C; bin width 1 ms in A, C; 0.5 ms in D, 0.1 ms in B, Histograms are derived from 10 repetitions).

pattern that was not correlated to the stimulus frequency (“chopping”). The remaining 27 cells synchronized their response to the stimulus cycle, hence, their response was phase-locked to the best frequency (ranging from 500 Hz to 3 kHz, see Fig. 4.9B) with synchronization values ranging from 0.31 to 0.92 (average 0.68 ± 0.21). The strength of phase-locking is dependent on BF, neurons with lower BFs display higher vector strength (VS) values than neurons with higher BF (Fig. 4.10, correlation highly significant, $r = 0.86$). Moreover, neurons that do not phase-lock to the stimulus frequency at BF showed a synchronized response to pure tones in the low frequency tail of their tuning curve. Interestingly, out of 26 sustained neurons with low BFs (< 2 kHz), 22 phase-locked to the stimulus.

Phasic discharge patterns in response to pure tones were found in 15 neurons (22% of the neurons that responded to pure tones), 14 showing a discharge to the stimulus onset

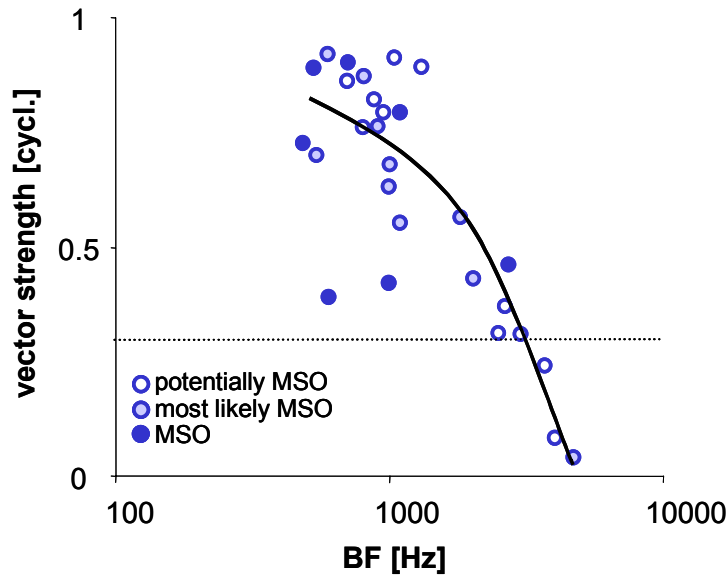


Figure 4.10
Correlation of best frequency and vector strength of the response to pure tones in the gerbil MSO.

(ON response) and one neuron showing a discharge to the stimulus offset (OFF response, Fig. 4.9 C, D). Figure 4.11 displays the distribution of response patterns for all neurons and the different subpopulations (see also Table 4.1).

Two out of the population of neurons responding to pure tones showed low spike counts and unreliable discharge when stimulated with pure tones, which made analysis difficult. One was driven best by SAM (modulation frequency 200 Hz) stimulation, the other one by frequency-modulated pulses. Therefore, these neurons were excluded from the analysis of response patterns.

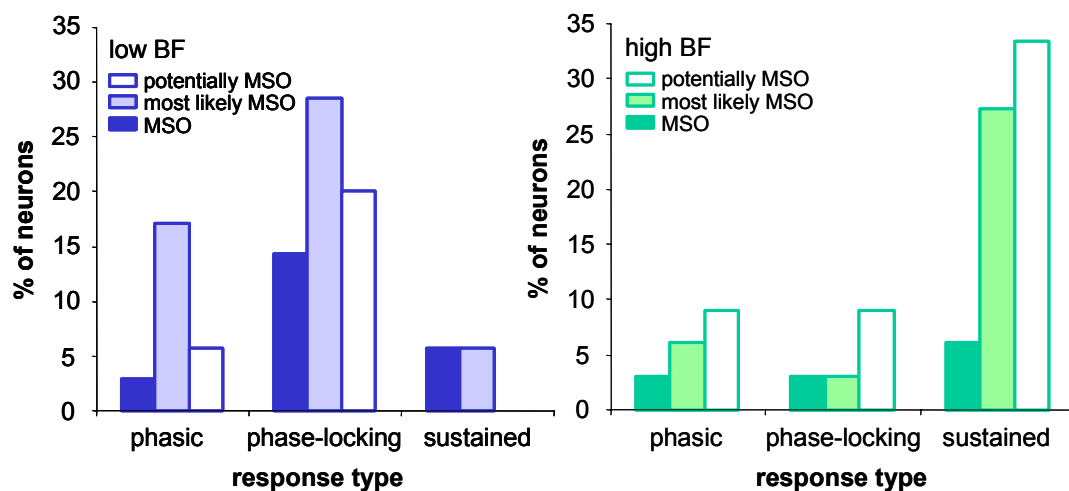


Figure 4.11
Distribution of discharge types in response to pure tones in the MSO. **A** for low BF, **B** for high BF.

4.1.6 Response latency

The latency of the first spike in response to a pure tone was evaluated at BF, 20 dB a. T. at half-rise time of the stimulus (equals 2.5 ms). In 13 (out of 70) neurons responding to pure tones, first spike latency was difficult to determine because of low spikerates and/or high spontaneous activity. For the 57 remaining neurons the mean value was 5.5 ± 4.8 ms. Low frequency neurons (BF below 2 kHz) showed a longer average latency (6.6 ± 4.5 ms, ranging from 2.1 to 24.2 ms) compared to high frequency neurons (4.2 ± 4.5 ms in the range from 1.7 to 23.3 ms) with a weak statistical significance ($p < 0.017$, t-test). The latency of one high frequency neurons (out of the population of neurons that are only potentially in the MSO) displayed an atypical latency of more than 10 ms longer than the remaining neurons. Exclusion of this neuron from the analysis led to an averaged latency of the high frequency neurons of 3.5 ± 2.4 ms, which is statistically different to the latency of low frequency neurons ($p < 0.002$, t-test). Figure 4.12 shows

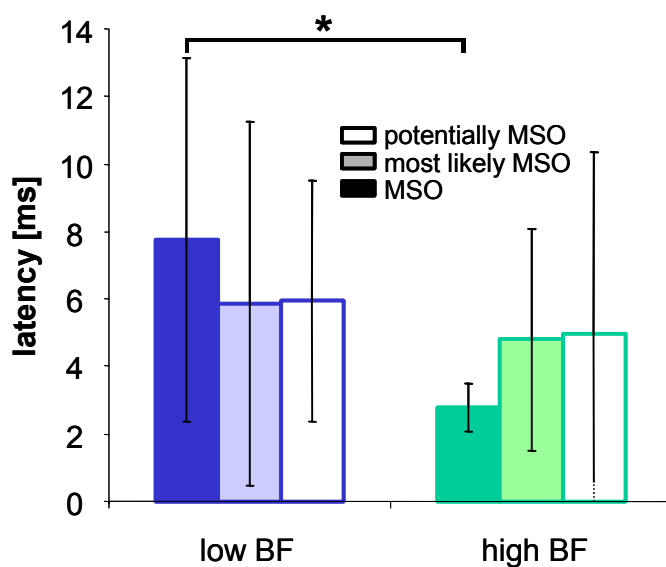


Figure 4.12

Distribution of latency in low and high BF neurons. The latency in high frequency neurons is significantly shorter than in low frequency neurons (*).

the latency values for the different subpopulations (see also table 4.1). In 85 % of the neurons tested over a range of at least 30 dB ($N=39$), the first spike latency decreased as a function of intensity with an average ratio of 0.2 ms/dB. Phase-locking low frequency neurons ($N=3$) were excluded from the analysis because the latency shift due to changes in sound amplitude is depending on stimulus phase in these neurons and is not comparable to the time-intensity trading ratio of non phase-locking neurons. The

remaining six neurons showed no systematic change in latency, when the intensity level exceeded their threshold > 10 dB.

The temporal precision of the first spike of the neurons (jitter) was $633 \pm 840 \mu\text{s}$, with no significant difference in accuracy in the population of low (jitter: $746 \pm 950 \mu\text{s}$) and high frequency (jitter: $496 \pm 699 \mu\text{s}$) neurons for all three subpopulations (see Fig. 4.13). Overall values for the accuracy of the first spike were widely distributed ranging from less than $100 \mu\text{s}$ to more than 3 ms for both populations. For values of the subpopulations see Table 4.1.

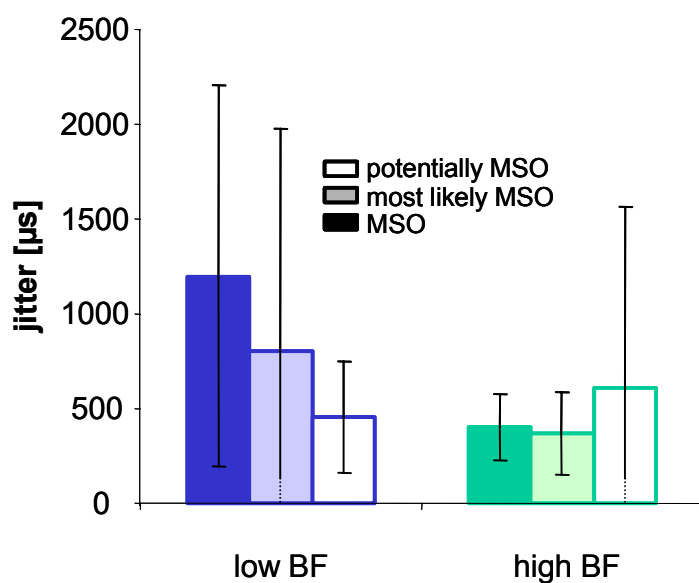


Figure 4.13

Distribution of jitter in low and high BF neurons in gerbil MSO neurons.

4.1.7 Binaural response characteristics

The binaural properties of 58 neurons were evaluated. It has been shown that stimulation with different paradigms influences the predication about overall binaural inputs (Grothe et al. 1997). Therefore neurons have been tested not only with pure tones, but also with a variety of different stimuli (SAM, noise, SFM, FM-sweeps etc.). Neurons have been characterized by their overall input from each ear (unilateral combinations of excitation and inhibition are not addressed) as either excitatory (E) or no input (0). No overall inhibitory influence could be allocated to one side throughout the entire population of cells investigated.

More than half of the neurons in the sample (33/58; 57%) showed clear binaural excitatory or facilitatory (E) interactions. The remaining 43% of the neurons were excited only by either the ipsilateral ear (E/0; 10/58; 17%) or the contralateral ear alone (0/E;

15/58; 26%). More low frequency neurons (22/33, 67%) were binaurally innervated than high frequency neurons (11/25, 44%). Hence more high frequency neurons were monaural (in particular there were more 0/E neurons: 9/25; 36% then E/0 neurons: 5/25; 20%) compared to neurons with low BF (0/E: 6/33, 18%; E/0: 5/33, 15%). Figure 4.14 summarizes overall binaural input patterns for all neurons for all three subpopulations depending on BF (see also table 4.1).

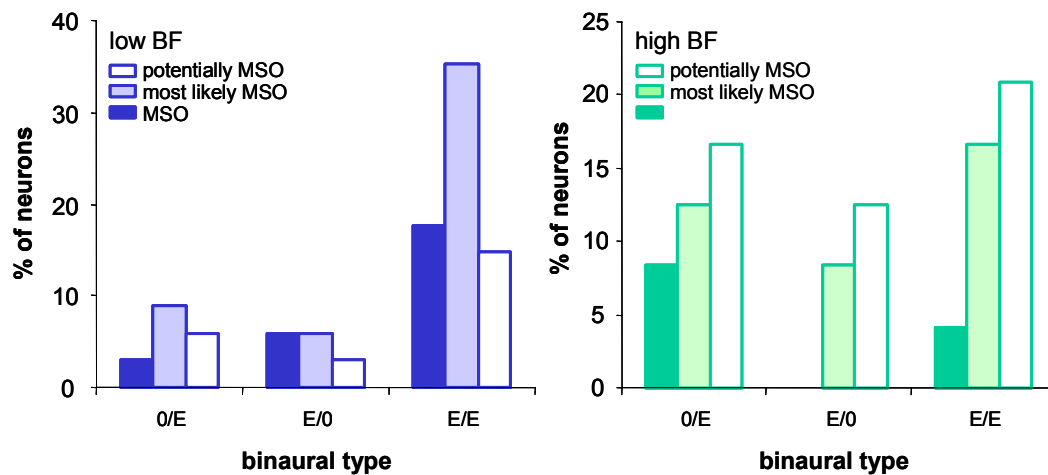


Figure 4.14

Distribution of overall binaural properties (E, excitatory; 0, no effects) in the MSO for low (A) and high (B) frequency neurons. The first letter indicates ipsilateral, the second letter contralateral effects.

4.1.8 ITD sensitivity to low frequency pure tones

Low frequency E/E neurons (N=22) were tested with static ITDs via earphones. Five of those neurons were directly reconstructed to be in the MSO, 13 neurons were most likely located in the MSO and four neurons were potentially in the MSO (the only errors are in the rostrocaudal dimension and are small). All neurons were located in or near the soma region of the MSO. Thus, all binaural low frequency neurons (with BF's from 500 Hz to 1300 Hz) were sensitive to interaural time differences with 30 to 85 % of the function's dynamic range (see Fig. 4.15 for exemplification of taken measures) within the behaviorally relevant range for the gerbil (roughly $\pm 120 \mu\text{s}$).

18 cells were sensitive to ITDs of pure tones. The remaining 4 neurons showed ITD sensitivity to broadband stimuli only. The maximal discharge of all these ITD sensitive neurons occurred, when the contralateral stimulus was leading in time (thus at a positive ITD, per definition). Figure 4.16 A shows an example of an ITD sensitive neuron tested

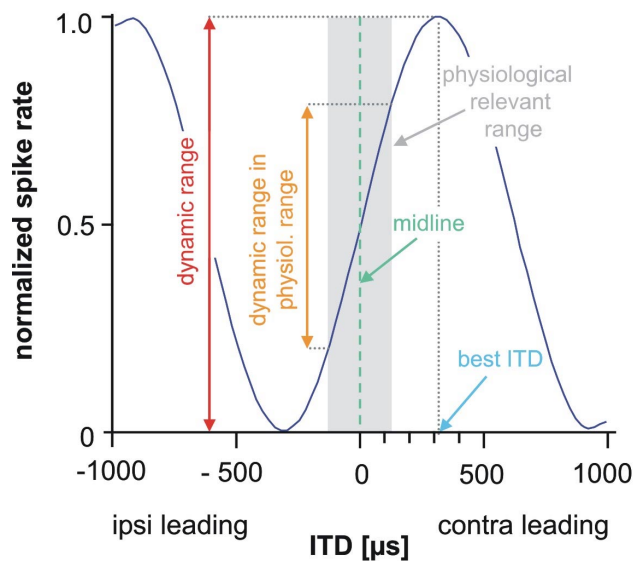


Figure 4.15
Exemplification of the measures taken to analyze ITD functions.

for low frequency pure tones. The ITD functions show a cyclic pattern related to the test frequency.

For a single neuron, the best ITD is largely independent of the used stimulation frequency, an indirect evidence for coincidence detection of binaural excitatory inputs (Rose et al. 1966). The stability of the best ITD can be evaluated by an analysis of the mean vectors of those ITD functions. Plotting mean vectors against test frequency and a linear regression of those values (following methods described by Yin and Kuwada 1983) resulted in an intersection point with the y-axis (at a so called characteristic phase, CP)

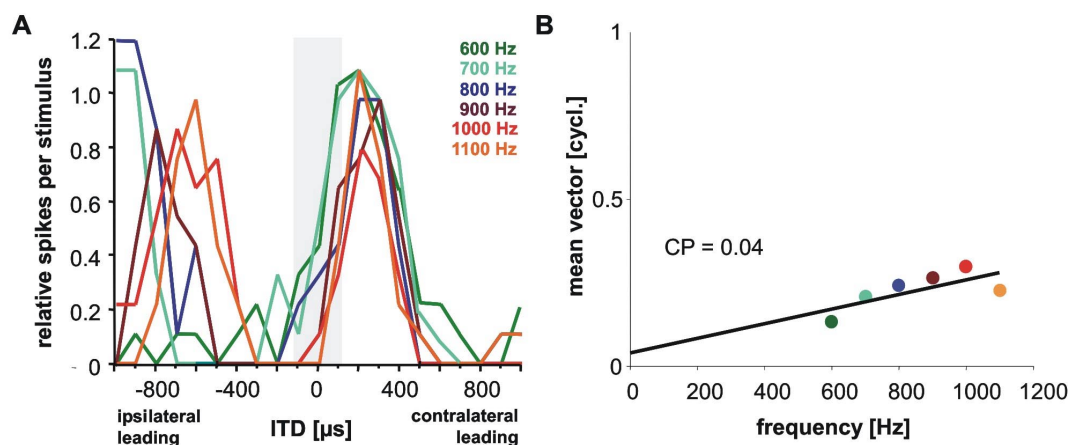


Figure 4.16

A ITD function of a MSO neuron, tested with pure tones at different frequencies. The peak ITD is independent of stimulus frequency, as verified with mean vector calculation and CP calculation (see text) **(B)**. The intercept with the y-axis near 0 indicates the “peak-type” sensitivity. The blue area in A indicates the physiological relevant range for gerbils ($\pm 120 \mu\text{s}$).

around 0 (or 1) cycles, indicating an underlying mechanism of coincidence of binaural excitation¹. For the neuron in figure 4.16 A the characteristic phase is at 0.04 cycles (see Fig. 4.16 B) confirming that the maximum of the ITD functions is independent of frequency in this neuron. 8 neurons were tested with at least three different frequencies (including the BF of the neuron) to evaluate independency of the ITD sensitivity of frequency. All of them discharged maximally at the same ITD independent of stimulus frequency, thus displayed CP values around 0 or 1.

Maxima of ITD functions in all 22 neurons were outside or at the positive border of the physiological range ($\pm 120\mu\text{s}$, see Fig. 4.17). However, the slope of the ITD functions

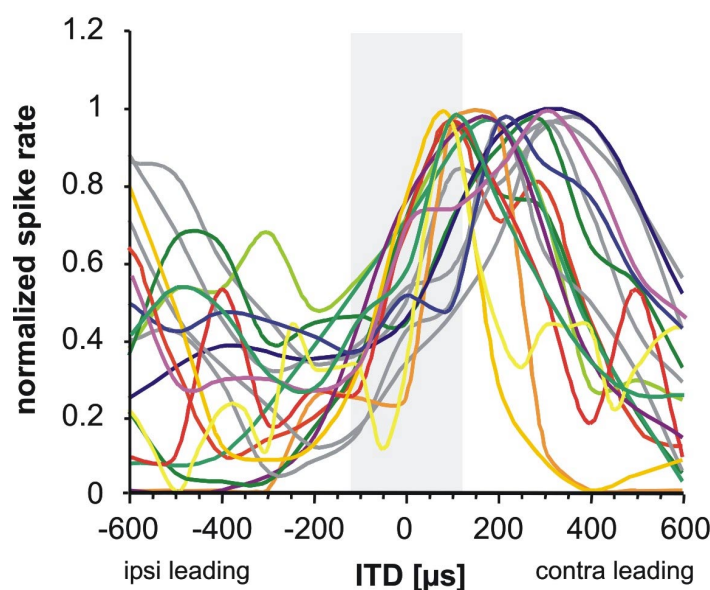


Figure 4.17
ITD functions of gerbil MSO neurons each tested at its BF, 20 dB above threshold. Note that the peaks are outside the physiological range (blue area). The steepest slopes of the ITD functions are within the relevant range.

was maximally within the physiological range. Therefore, rate information got unambiguous and little changes in ITD would therefore lead to a great change in response rate.

The cyclic shape of the ITD function is dependent on the best frequency of a neuron - ITD tuning in neurons with lower BF is broader than the tuning in neurons with higher BF. To adjust the maximal slope into the relevant range, maxima of ITD functions must be positioned at larger ITDs for neurons with low BF, than for neurons with high BF. Hence, to always tune the slope into the physiological range the position of the ITD function's maximum should be systematically dependent on the BF of the neuron.

As shown in figure 4.18, in the population of neurons tested, the ITD that evoked maximal response in a neuron was dependent on neuronal tuning for sound frequency.

¹ Consequently, if the trough of the ITD functions is stable at a given ITD independent of stimulation frequency) the intercept with the y-axis is at a value of 0.5, indicating an E/I or I/E mechanism.

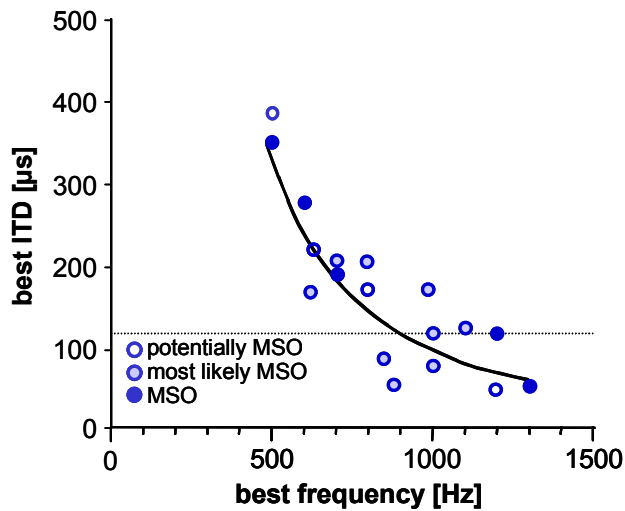


Figure 4.18

Distribution of best ITDs as a function of BF of the neurons in figure 4.17.

Only ITDs below the dotted line are within the physiologically relevant range of ITDs. Solid line, third order polynomial fit. Dotted line, upper limit of the gerbil's physiological range of ITDs.

Neurons with relatively low BF responded best at larger ITDs, whereas neurons with higher BF responded to relatively small ITDs. This correlation between best frequency and best ITD is highly significant ($r=0.82$, see Fig. 4.18). Neurons with similar BFs were therefore always tuned to similar ITDs. To compare the interaural time delays at which maximal response occurred, independent of BF, all ITD functions were normalized for each neuron's best frequency by calculating the corresponding interaural phase differences (IPDs). The ITD functions of the investigated neurons always displayed maxima at an IPD of $+0.12$ cycles (± 0.046 , $N=18$). This, again, confirms the systematic relationship of BF and ITD seen in figure 4.18.

A crucial assumption of the Jeffress model is coincidence detection of binaural excitatory inputs. Monaural period histograms indicate the relative timing of inputs to the MSO from each ear by calculating the phase angle. If the observed response is in line with coincidence detection, the discharge of a neuron should be maximal when the phases of the two monaural responses get equal by introducing an appropriate ITD. Then it is assured that the two monaural inputs arrive at a MSO neuron simultaneously (compare Yin and Chan 1990). Due to difficulties holding neurons for long time periods only few cells were tested with monaural stimulation. For three ITD sensitive neurons monaural responses were obtained at 20 dB a.T.. In all tested neurons only pure tone stimulation from one side elicited a response, even though this response was much weaker compared to binaural stimulation. Out of three monaurally tested neurons two responded to stimulation of the contralateral side only, one neuron discharged only when stimulated ipsilaterally. Thus, no prediction of best ITDs by comparing monaural responses was possible.

4.1.9 Effects of glycinergic inhibition in the MSO

4.1.9.1 General effects

MSO neurons show prominent glycinergic inhibition on their somata (Kapfer et al. 2002). Therefore, low and high frequency neurons were tested with glycine and/or its antagonist strychnine by iontophoretical application of either drug. Application of drugs turned out to be difficult and was only successful in few cases.

A critical point in neuropharmacological experiments is getting the drug to the receptor. In pre-experiments and in tests during actual recording sessions the dependence of the current strength on drug effect was tested. The amperage is a measure for the amount of glycine applied through the drug electrode via iontophoresis. Figure 4.19 shows the response of one neuron (most likely in the MSO) to pure tone

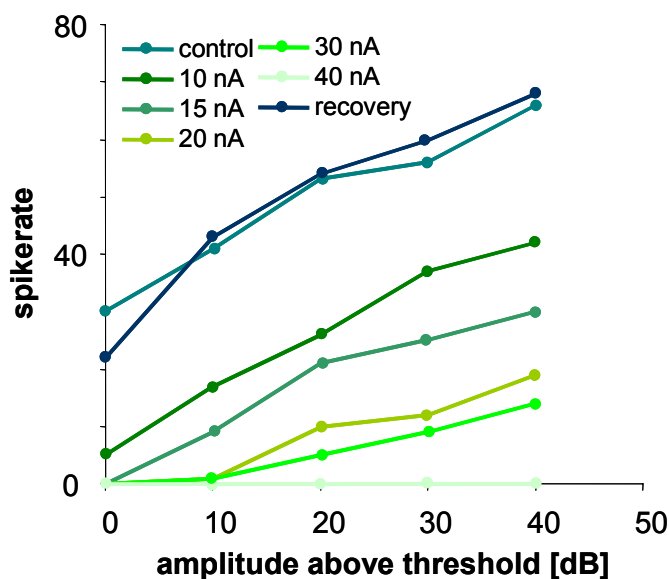


Figure 4.19

Glycine application in a MSO neuron. Increasing amperages (as a measure for increasing doses of glycine) led to gradual decrease of the response of the neuron. After termination of application the neuronal response recovers to control situation values.

stimulation, while using different amperages to apply the neurotransmitter glycine. The response gets gradually weaker with higher amperages (thus higher concentrations of glycine). Switching off the current and thereby stopping drug application reversed the effect of glycine (compare “control” and “recovery” in Fig. 4.19). These observations allowed the conclusion that the drug was applied successfully and acts on the glycine receptor. Because glycine is a comparatively small drug the time course of effect and recovery is short (few ms). For strychnine application time and duration until an effect occurs is much longer (and additionally higher injection currents are needed).

18 neurons have been tested with either glycine (N=5), strychnine (N=10) or both (N=3). Interestingly, no changes in discharge pattern were observed, but the discharge rates of neurons were influenced by pharmacological manipulations (all but one were directly reconstructed to be in the MSO or were most likely in the MSO). In all tested cells glycine significantly inhibited stimulus evoked response, in four neurons glycine application blocked the response completely. In figure 4.20 the response of a MSO

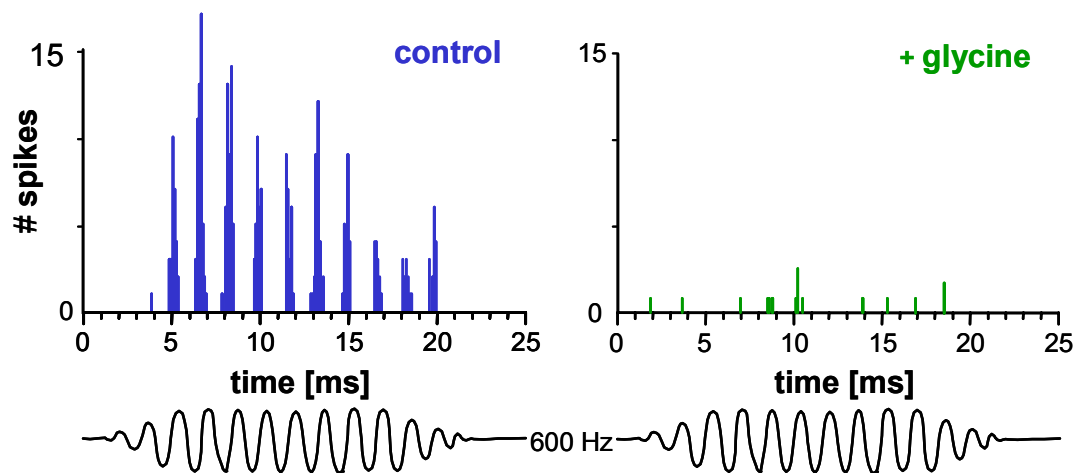


Figure 4.20

PSTH showing precise phase-locking of a MSO neuron in response to a 600 Hz pure tone (same neuron as in figure 4.9 B). Iontophoretic application of glycine for a few seconds completely inhibits the tone evoked response.

neuron (same neuron as in Fig. 4.9 B) to pure tone stimulation is shown before and during the application of glycine. Application of glycine inhibited the phase-locked response to a 600 Hz pure tone.

The glycine antagonist strychnine affected the response in 13 neurons. In all cells strychnine caused an increase in stimulus driven responses (up to 5.5 times more spikerate as in control situations). Spontaneous activity was also influenced by application of strychnine (up to 2.6 times control).

4.1.9.2 *Glycinergic inhibition in ITD coding*

To assess the role of the massive glycinergic input in ITD encoding, glycine and strychnine were applied to low BF neurons while presenting static ITD. Note that MSO recordings are known to be demanding (see discussion) – applying drugs while recording makes the technique even more challenging. Application of strychnine was successful in five ITD sensitive neurons. In all of those neurons the discharge rate increased by 50 –

86% of the maximal discharge at binaural stimulation (with an ITD of 0). Figure 4.21 shows the response of an example neuron before and during strychnine application. The

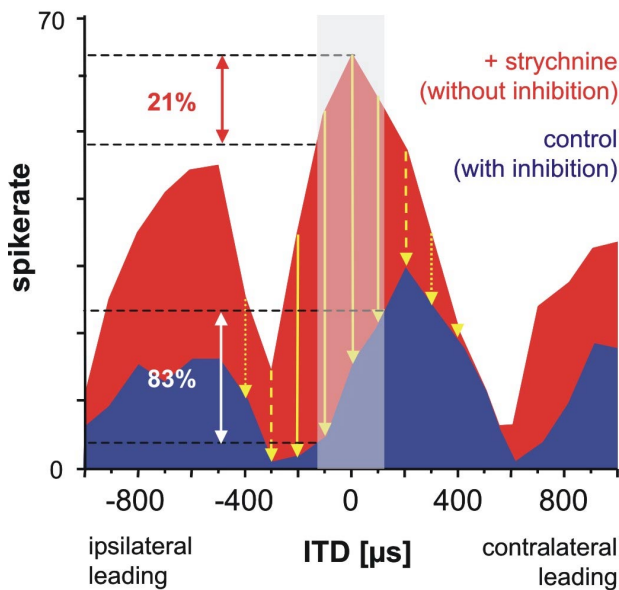


Figure 4.21

ITD function of a neuron during control condition and strychnine application. Dynamic range of the ITD response under control conditions is 83 % (blue); the best ITD is outside the physiological relevant range (light blue bar). During blockade of glycinergic inhibition from application of strychnine (red), the best ITD is at zero ITD, and the dynamic range of the response is reduced to 21%. Hence glycinergic inhibition reduces spike counts and shifts the left slope into the relevant range of ITDs.

blue curve shows the ITD function under control recording conditions, in the absence of strychnine. The ITD function has the typical cyclic shape with maximal discharge at positive ITDs (+170 μ s, equals 0.16 IPD), outside the physiologically relevant range. A maximal proportion of the dynamic part of the ITD function is in the physiologically relevant range (about 83%). During iontophoretic application of strychnine the maximum of the ITD function shifted to the midline to +50 μ s, some 120 μ s from its initial maximum, corresponding to a shift in best IPD of 0.127 cycles. As a consequence of the best ITD shifting to midline, the steepest slope of the function fell outside the physiologically relevant range of ITDs. Additionally, the function became non-monotonic within the physiological range and, hence, ambiguous for ITD. Note also that the dynamic range within the physiological range (see Fig. 4.15) was reduced from 83% to 21%. The effect that maxima of ITD functions shifted to the midline, thereby minimizing the dynamic part inside the physiological range, was seen in all five neurons tested. When expressed in terms of the equivalent best IPD, the maximal response of these five neurons before application of strychnine was at an average IPD of 0.148 (\pm 0.054) cycles. During application of strychnine the best IPD shifted to 0.021 (\pm 0.53) cycles. Hence, strychnine caused an average shift of -0.127 cycles (\pm 0.064) near to 0 IPD (= 0 ITD). The shifts observed in all five neurons were statistically significant (t-test, $p < 0.014$). Figure 4.22 shows the averaged IPD functions for the five neurons after first

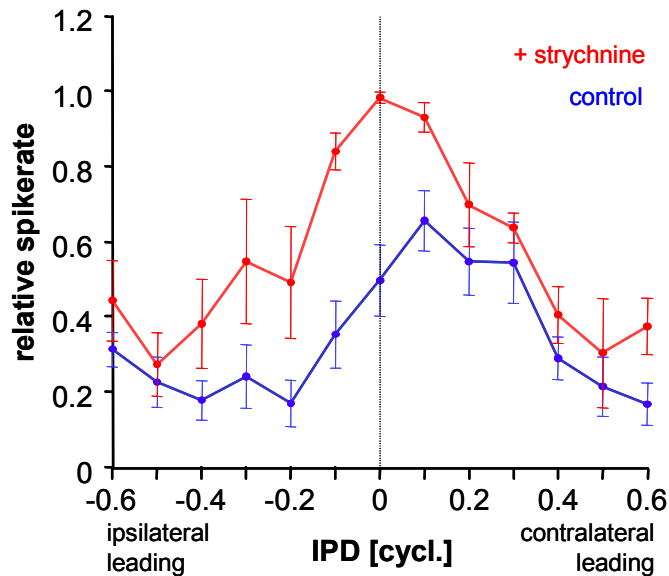


Figure 4.22

Averaged interaural delay functions (ITDs converted to IPDs thereby normalizing for BF) for all five ITD sensitive neurons tested under control conditions (blue) and during application of strychnine (red). Before averaging, each neuron's IPD function was normalized to the maximal response during strychnine application. Error bars: standard error of the mean.

normalizing each function to the strychnine-evoked maximum discharge rate. On average, iontophoresis of strychnine produced a 67% ($\pm 9.8\%$) reduction of the dynamic range of the response across the physiologically relevant range of ITDs.

The yellow arrows in Figure 4.21 indicate the apparent effect of the glycinergic inhibition, which differed for different ITDs, being stronger when the ipsilateral stimulus was leading in time than when the contralateral stimulus was leading.

Different combinations of excitation and inhibition could explain the observed effect of the glycinergic inhibition. One could assume ipsilateral inhibition lagging the ipsilateral excitation, contralateral inhibition leading contralateral excitation or a combination of both (see discussion).

Evidence for contralateral leading inhibition preceding contralateral excitation came from one experiment with short frequency modulated sweeps (duration 5 ms, rise/fall time 0.5 ms) presented at different ITDs. The neuron responded with only one single spike to a single presentation to the stimulus, hence the interaction of both inputs can be directly evaluated. Figure 4.23 A shows that the neuron responded to ipsilateral (light green) and contralateral (orange) stimulation independently, when the stimuli were far apart and not overlapping. When the two stimuli were presented closer to each other (thus at shorter delays) the response to the ipsilateral stimulus got weaker (even though the ipsilateral stimulus eliciting the response it was still leading in time, Fig 4.23 A, second and third panel) and almost disappeared (Fig 4.23 A, fourth panel). This observation can only be explained by a contralateral inhibitory potential, which is preceding the excitatory potential, which causes the response to the contralateral

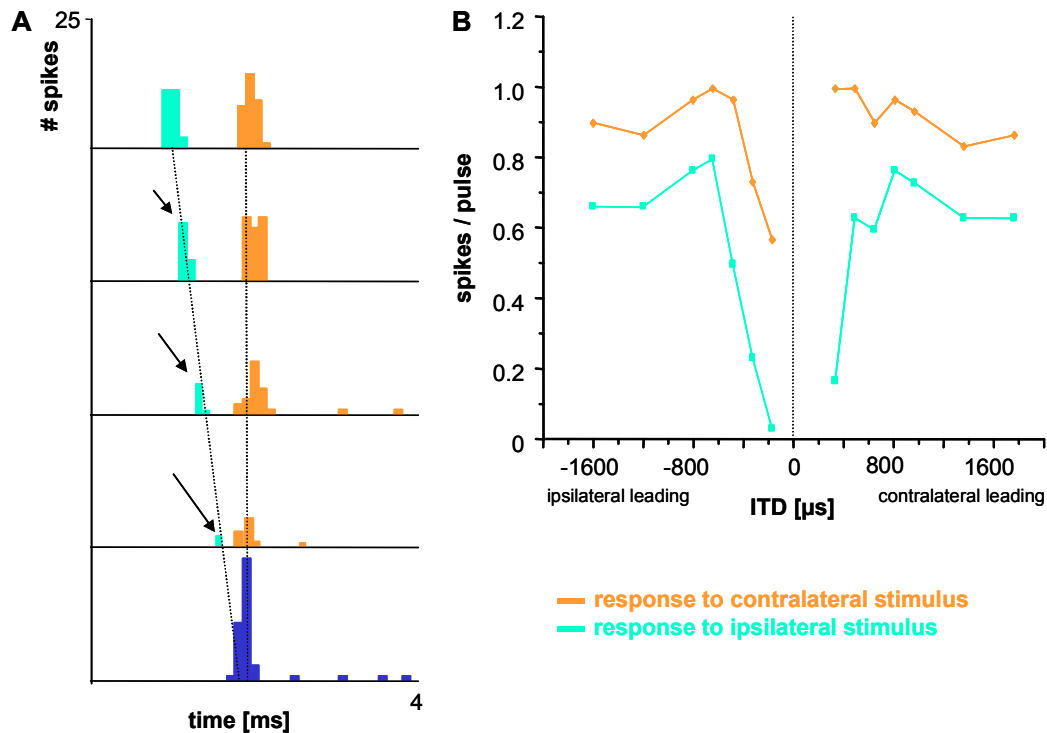
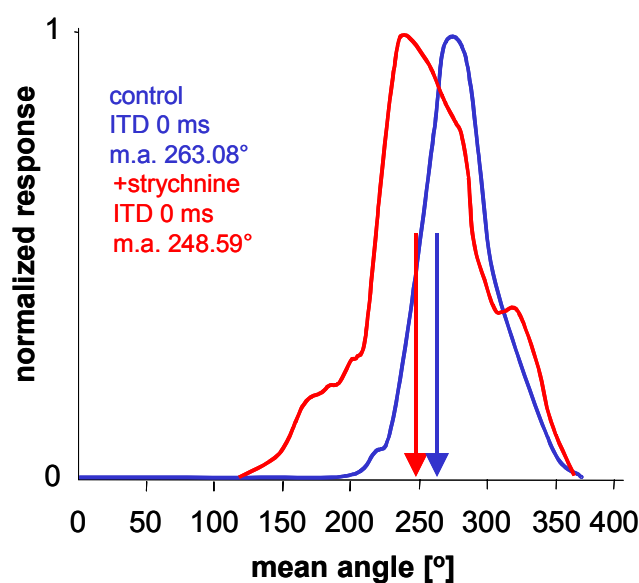


Figure 4.23

Response of a neuron to brief downward modulated sweeps (from 1500 Hz to 500 Hz in 5 ms). **A** PSTHs showing the ipsilateral (light green) and contralateral (orange) evoked responses (as apparent from the relative timing of the responses – the ipsilateral stimulus was varied, the contralateral was fixed in time). As the distance between ipsi – and contralateral stimulus got smaller (the ITD the ipsilateral stimulus was leading decreased), the ipsilaterally evoked response diminished although it still preceded the contralateral evoked response. **B** Quantification of the response to frequency modulated sweeps (for details see text).

stimulus. When the ipsilateral stimulus was delayed in time the neurons displayed a facilitated response indicating a coincidence of excitatory potentials elicited by both sides. Figure 4.23 B quantifies the response to the frequency modulated sweeps. Ipsilaterally evoked spikes were suppressed when the ipsilateral stimulus was still leading ($< 600 \mu\text{s}$). In contrast, when the contralateral stimulus was leading, the response to the contralateral stimulus was not affected. The contralaterally evoked response was only affected in a small range of ITDs (contralateral lagging), most likely due to a mild ipsilaterally evoked inhibition lagging ipsilateral excitation. Note that from $-100 \mu\text{s}$ to $+300 \mu\text{s}$ the responses could not be assigned as elicited from either the ipsilateral or contralateral ear.

Additional evidence for preceding contralateral inhibition comes from phase shifts that were observed in one neuron, when the phase-locked response was compared for control condition and in the presence of strychnine. Blockade of inhibition evoked a response earlier in the cycle of the tone, which again is only compatible with an “earlier”

**Figure 4.24**

Application of strychnine, hence blockade of inhibition leads to a shift in the mean angle of the response. The stimulus evoked response is elicited earlier in phase.

evoked excitation. The shift of the mean angle of the response (see arrows in Fig. 4.24) was statistically significant (Watson-Williams test, $p < 0.01$).

The cyclic shape of ITD functions seems to be preset by coincidence of binaural excitatory input. However, the crucial shift of the slope into the relevant range is achieved by precisely timed glycinergic inhibition.

4.1.10 ITD sensitivity to high frequencies

It is known that MSO neurons are sensitive to ITDs in the envelope of high frequency carriers as well. In only high frequency hearing animals like bats this observation is discussed as epiphenomenon generated by the E/E circuitry in the MSO (Grothe and Park 1998). There is some evidence that the same sensitivity is found in high frequency neurons of low frequency hearing animals (Batra et al. 1997ab, Yin and Chan 1990). Therefore, additionally high frequency binaurally excited neurons ($N=10$, four most likely and six potentially in the MSO) were tested for their ITD sensitivity with stimuli with high frequency carriers. As stimuli to present static ITDs, SAM tones with modulation frequencies to which the neuron synchronized to, and band-passed noise with high center frequencies, were used. In the population of E/E neurons, 77 % of the cells (7/9) showed flat ITD functions (see Fig. 4.25 A, B) in the range of ITDs the gerbil can detect. Three of the E/E neurons were tested in a broader time-scale (± 5 ms; Fig. 4.25 B). Only two neurons changed their spikerate clearly over the range of ITDs tested (see Fig. 4.26 A (most likely MSO), B (potentially MSO)) but still there is no significant

change within the physiological range. Moreover, the cyclic shape of the functions was not related to the envelope frequency used.

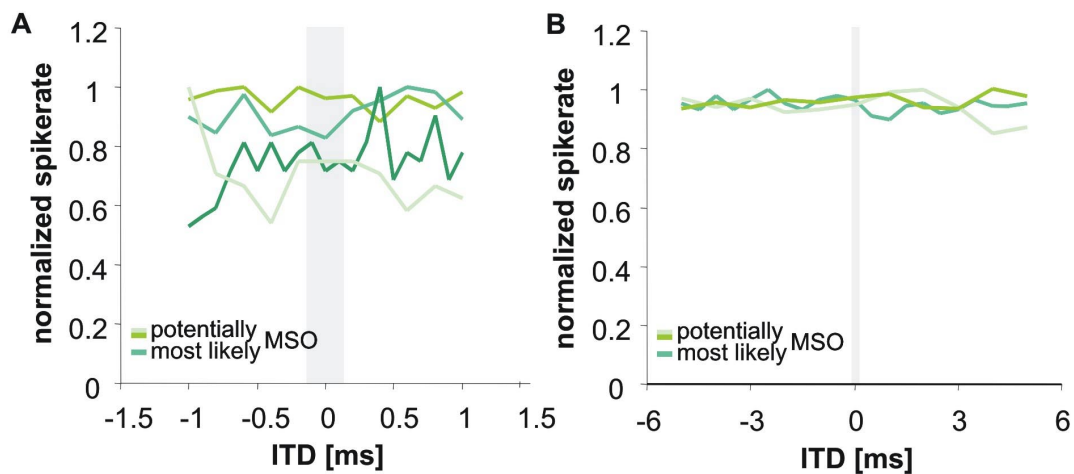


Figure 4.25

Responses of high frequency E/E neurons to interaural time differences (ITD). **A** ITD sensitivity to the envelopes of SAM stimuli in 5 neurons. None of the neurons showed sensitivity to ITDs within the physiological range (indicated by the shaded area). **B** Three neurons were tested with a larger time scale to cover all interaural time disparities occurring in a full SAM cycle. ITD functions are flat and did not exhibit a significant sensitivity within the physiological range.

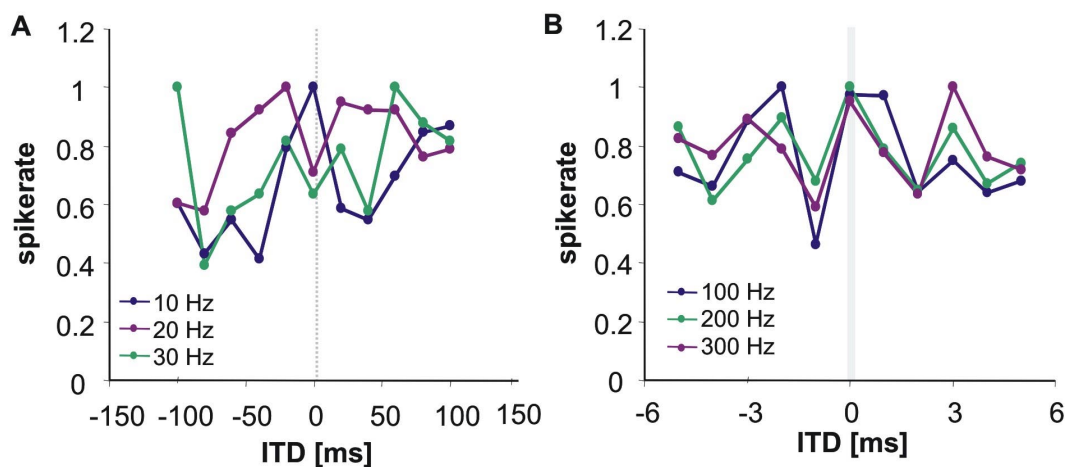


Figure 4.26

A, B Two high frequency MSO neurons displaying some cyclic regularities in their ITD functions.

4.1.11 Responses to SAM

High BF neurons were tested on their filter characteristics to SAM stimulation. Both neuronal filter properties to monaural and binaural stimulation with SAM were investigated.

Out of the 33 high frequency (BF above 2 kHz) neurons in the MSO, 28 have been tested with binaural (IID=0) SAM stimuli (20 to 1000 Hz modulation frequency),

independent of their binaural properties. Four neurons were directly reconstructed as MSO neurons, 10 were most likely in the MSO and 14 were potentially in the MSO.

All high frequency neurons tested responded to SAM stimulation. The majority of these neurons (24/28) showed an ongoing synchronization to the stimulus envelope (thus to the modulation frequency) with a synchronization coefficient $SC > 0.3$ (and $p < 0.05$, Rayleigh test) at least at some modulation frequencies. Most of these neurons (88%) showed a sustained response to pure tone stimulation, only three neurons had ON responses. The remaining four neurons that did not synchronize their response to the SAM envelope (one with an ON-response, one with an OFF-response, one “chopper” and one showing a tonic response) responded to SAM in the same way as to pure tones independent of modulation frequency.

To compare the precision of phase-locking to SAM in MSO neurons in gerbils to other SOC recordings (e.g. gerbil superior paraolivary nucleus, see below and bat MSO, Grothe et al. 2001) the average VS for the 24 SAM phase-locking neurons was determined at a modulation frequency of 114 Hz (recall that the step size used is logarithmic). The averaged VS for 22 phase-locking neurons (two neurons did not respond to 114 Hz modulation frequency with a synchronized response) is 0.56 ± 0.20 .

The average maximal VS (highest VS the neuron displayed to any modulation frequency) was 0.7 ± 0.16 .

To evaluate the temporal filter characteristics of MSO neurons in response to SAM, the 50% cut-offs of the rate based MTFs and the modulation frequency at which the VS dropped below 0.3 (or became insignificant, see methods) was investigated.

4.1.11.1 Rate-based modulation transfer functions

For binaural stimulation more than half of the neurons with ongoing phase-locked response to SAM (15/24, 63%) showed rate based MTFs that never dropped below 50% maximal spikerate. These neurons were classified as all-pass. All of them responded with a sustained firing pattern when tested with pure tones. Four neurons (17%) showed band-pass filter in rate based MTFs, with an upper and lower cut-off, only responding to a certain range of modulation frequencies and two neurons (9%) showed band-reject filter characteristics (no response at some or in a certain range of modulation frequencies). Again, all neurons in these two groups were sustained responders. One remaining neuron with a sustained response showed low-pass characteristics in the MTF

derived from spike count and was categorized as low-pass. The remaining two neurons with an ongoing phase-locked response to SAM showed an ON response to pure tones. Both of them (and none of the sustained responders) showed high-pass filter characteristics in their rate based MTFs, thus they did not respond to low modulation rates.

The averaged upper 50% cut-off (calculated out of the population of neurons showing band-pass and low-pass characteristics) is 490 ± 196 Hz.

4.1.11.2 Vector-strength based modulation transfer functions

Additionally, filter cut-offs in VS based MTFs ($VS < 0.3$) were evaluated. More than half of the neurons (14/24, 58%) showed low-pass filter characteristics in VS based MTFs. The remaining neurons showed all-pass (4/24, 17%), band-pass (2/24, 8%), band-reject (1/24, 4%) or low-pass (1/24, 4%) filter characteristics (see Table 4.3). One neuron responded only at some modulation frequency (responding up to 1000 Hz) not showing a systematic cut-off. This neuron showed an ON discharge to pure tone stimulation. The other neuron responding with an ON response showed low-pass filter characteristics.

The averaged upper cut-off (again out of the neurons showing band-pass or low-pass filter characteristics) is 499 ± 277 Hz.

	<i>rate MTF</i> all MSO; most likely MSO; potentially MSO	<i>VS MTF</i> all MSO; most likely MSO; potentially MSO	<i>spikes per cycle MTF</i> all MSO; most likely MSO; potentially MSO
all-pass	15 (63%) 3 (100%); 5 (71%); 7 (51%)	4 (17%) 0 (0%); 3 (43%); 1 (7%)	0 (0%) 0 (0%); 0 (0%); 0 (0%)
low-pass	1 (4%) 0 (0%); 0 (0%); 1 (7%)	14 (59%) 3 (100%); 2 (29%); 9 (64%)	23 (96%) 3 (100%); 7 (100%); 13 (100%)
high-pass	2 (8%) 0 (0%); 0 (0%); 2 (14%)	2 (8%) 0 (0%); 0 (0%); 2 (14%)	0 (0%) 0 (0%); 0 (0%); 0 (0%)
band-pass	4 (17%) 0 (0%); 2 (29%); 2 (14%)	2 (8%) 0 (0%); 2 (29%); 0 (0%)	1 (4%) 0 (0%); 0 (0%); 1 (7%)
band-reject	2 (8%) 0 (0%); 0 (0%); 2 (14%)	2 ¹ (8%) 0 (0%); 0 (0%); 2 (14%)	0 (0%) 0 (0%); 0 (0%); 0 (0%)
Σ	24 3; 7; 14	24 3; 7; 14	24 3; 7; 14

Table 4.3

Filter properties of MSO neurons in response to binaural presentation of sinusoidally amplitude modulations

¹ one neuron showing no systematic filter cut-off is added to the band-reject category here.

VS, vector strength; MTF, modulation transfer function

Table 4.3 summarizes filter characteristics in rate and VS based MTFs (in addition filter characteristics in MTFs based on spikes per cycle are shown) for all three subpopulations of neurons. A typical example of a neuron's response (displaying all-pass filter characteristics in its rate MTFs and low-pass in its VS MTFs) to different SAM frequencies is shown in figure 4.27.

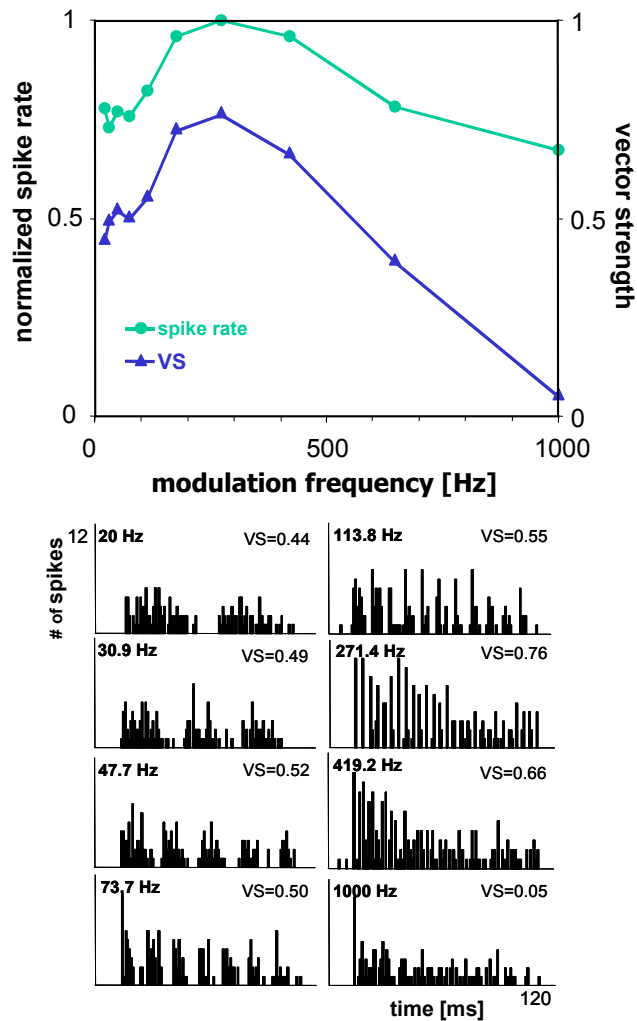


Figure 4.27

Typical example of a MSO neuron's response to SAM – neuron with a sustained response to pure tones, displaying low-pass filter characteristics in vector strength based and all-pass characteristics in rate based modulation transfer functions. *Bottom:* The PSTHs show that the neuron follows each cycle of the modulation up to ~ 700 Hz. Response to 10 stimulus presentations, bin width of the PSTHs is 1ms.

4.1.11.3 Monaural stimulation with SAM

Nine neurons (out of the population of SAM sensitive high frequency neurons) were tested with only contralateral and eight neurons with only ipsilateral SAM stimulation. Of these neurons all but two showed an ongoing phase-locked response to SAM. Table 4.4 combines filter properties for VS, spikerate and spikes/cycle for all three subpopulations of neurons. The filter characteristics in response to monaural stimulation of SAM almost reflect those obtained with binaural stimulation (compare to Table 4.3).

	<i>rate MTF</i> all MSO; most likely MSO; potentially MSO	<i>VS MTF</i> all MSO; most likely MSO; potentially MSO	<i>spikes per cycle MTF</i> all MSO; most likely MSO; potentially MSO
all-pass	8 (53%) 1 (50%); 5 (83%); 2 (29%)	1 (7%) 0 (0%); 1 (17%); 0 (0%)	0 (0%) 0 (0%); 0 (0%); 0 (0%)
low-pass	0 (0%) 0 (0%); 0 (0%); 0 (0%)	9 (60%) 0 (0%); 3 (50%); 6 (86%)	14 (93%) 2 (100%); 6 (100%); 6 (86%)
high-pass	1 (7%) 0 (0%); 0 (0%); 1 (14%)	2 (13%) 1 (50%); 1 (17%); 0 (0%)	0 (0%) 0 (0%); 0 (0%); 0 (0%)
band-pass	2 (13%) 0 (0%); 0 (0%); 2 (29%)	1 (7%) 0 (0%); 0 (0%); 1 (14%)	1 (7%) 0 (0%); 0 (0%); 1 (14%)
band-reject	4 (27%) 1 (50%); 1 (17%); 2 (29%)	2 ¹ (13%) 1 (50%); 1 (17%); 0 (0%)	0 (0%) 0 (0%); 0 (0%); 0 (0%)
Σ	15 2; 6; 7	15 2; 6; 7	15 2; 6; 7

Table 4.4

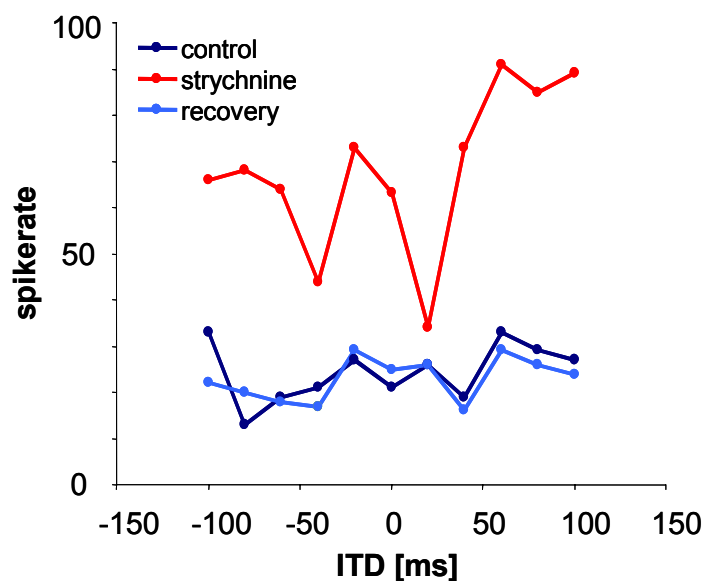
Filter properties of MSO neurons in response to monaural presentation of sinusoidally amplitude modulations

¹ two neurons showing no systematic filter cut-off are added to the band-reject category here.

VS, vector strength; MTF, modulation transfer function

4.1.12 Glycinergic inhibition and high frequency temporal processing

In three neurons (all of them most likely in the MSO) effects on SAM response properties of neurons were observed. In two neurons (responding synchronized to SAM envelopes) strychnine application changed the strength of phase-locking to the SAM envelope, e.g. at a frequency of 114 Hz VS dropped from 0.7 to 0.46. However, overall

**Figure 4.28**

ITD functions of a neuron in response to a 10 Hz SAM stimulus. Under control conditions ITD functions are flat, whereas application of strychnine increased activity and evoked a cyclic ITD sensitivity related to the stimulus envelope. However the sensitivity is unlikely to be of behavioral relevance.

filter properties in VS based MTFs never changed during strychnine application (thus “band-pass” neurons stayed “band-pass” etc.). Response rate in these neurons was not affected at all by strychnine application. An additional effect of strychnine is shown in figure 4.28. A high frequency E/E neuron (BF 2720 Hz, most likely in the MSO) showed flat ITD functions when stimulated with different delays of a 30 Hz modulation frequency SAM. Injection of strychnine, thereby blocking the glycinergic inhibition on this neuron, increased spikerate in some but not for all of the delays tested. The neuron now exhibited a cyclic ITD function related to the modulation frequency (30 Hz). Thus, glycinergic inhibition seems to be present in high frequency MSO neurons as well.

4.2 *The Superior Paraolivary Nucleus*

The superior paraolivary nucleus (SPN), even though big in size is sparsely investigated. Therefore, single cell recordings were obtained from SPN neurons to reveal general response patterns. The inputs onto SPN neurons suggest a role in temporal processing, hence ITD and IID sensitivity, as well as response to SAM were evaluated. The sample of neurons presented here was obtained in cooperation with Dr. Oliver Behrend.

4.2.1 *Reconstruction of recording sites*

Responses were recorded from 62 SPN neurons of which 22 were directly verified as SPN cells via marker injections at the recording site. The locations of the remaining neurons were stereotactically reconstructed as within the SPN, using marker injections at other recording sites. The recording sites were distributed across the entire dorsoventral and mediolateral extent of the nucleus. Figure 4.29 A depicts a recording site (marked with HRP and processed with standard protocols, see methods). The outline of the gerbil

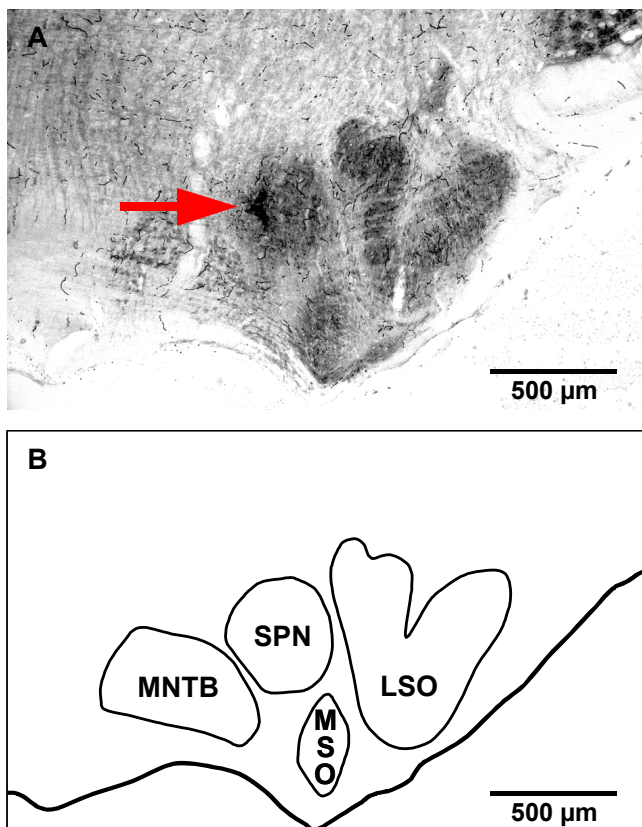


Figure 4.29

A Coronal section showing horseradish peroxidase injections through the multibarrel electrode into the SPN (arrow). The section is counterstained for cytochrome oxidase. **B** The principle SOC nuclei are indicated schematically.

SPN and its position in the SOC is depicted in Figure 4.29 B. The location of the remaining neurons was stereotactically reconstructed to be within the SPN using marker injections at other recording positions in the same animal (taken into account a confirmed accuracy of ± 80 for the mediolateral, ± 100 μm for the dorsoventral and rostrocaudal extension, see above).

4.2.2 Spontaneous activity

SPN neurons discharged spontaneously to different extents ranging from 0 spikes to 54 spikes. In the population of 62 cells, 21 (34%) responded with low spontaneous rates (< 1 spike/s). Out of the remaining neurons, 17 (27%) discharged moderately (1-10 spikes/s) and 24 (39%) with high spontaneous activity (> 10 spikes/s).

4.2.3 Tuning characteristics

More than 80 % of the neurons responded to pure tones (51/62). The rest of the neurons (11/62; 18%) were only driven by broadband stimuli; four by white noise and seven by stimulation with upwards modulated frequency sweeps. The physiological audiogram spanned a range from 700 Hz up to 37 kHz as shown in figure 4.30. Low best

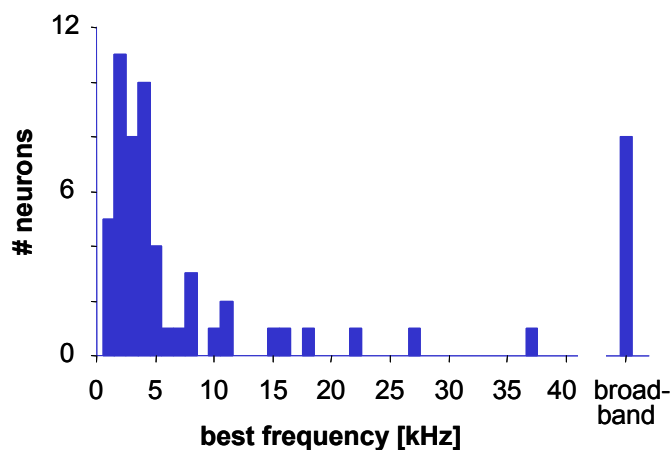


Figure 4.30

Distribution of best frequencies (BF) found in the gerbil SPN. Some neurons did not respond to pure tones but only to broadband stimulation with noise or frequency modulated sweeps

frequencies were over represented, 68% of the neurons showed best frequencies below 6 kHz. Thresholds varied from 2-52 dB SPL. Frequency tuning curves showed the typical v-shape with a steeper slope at the high frequency end. $Q_{10\text{dB}}$ -values ranged from 1.0 to 16.8 with an average of 3 (SD 2.9). Narrow tuning (indicated by high $Q_{10\text{dB}}$ -values) was only observed in neurons with BF above 4 kHz. The response behavior at increasing

amplitudes was examined in 49 neurons. At an IID = 0 (irrespective of the neuronal properties of the cell), 42 neurons (86%) displayed monotonic RLFs; only 14% (7/49) were non-monotonic.

4.2.4 Response pattern

Of the cells that responded to pure tones, 59% (30/51) showed sustained discharge patterns when tested at their BF, 20 dB a. T.. 15 of these neurons showed smooth PST histograms without strong onset effects or pauses (Fig. 4.31 A), whereas 9 neurons

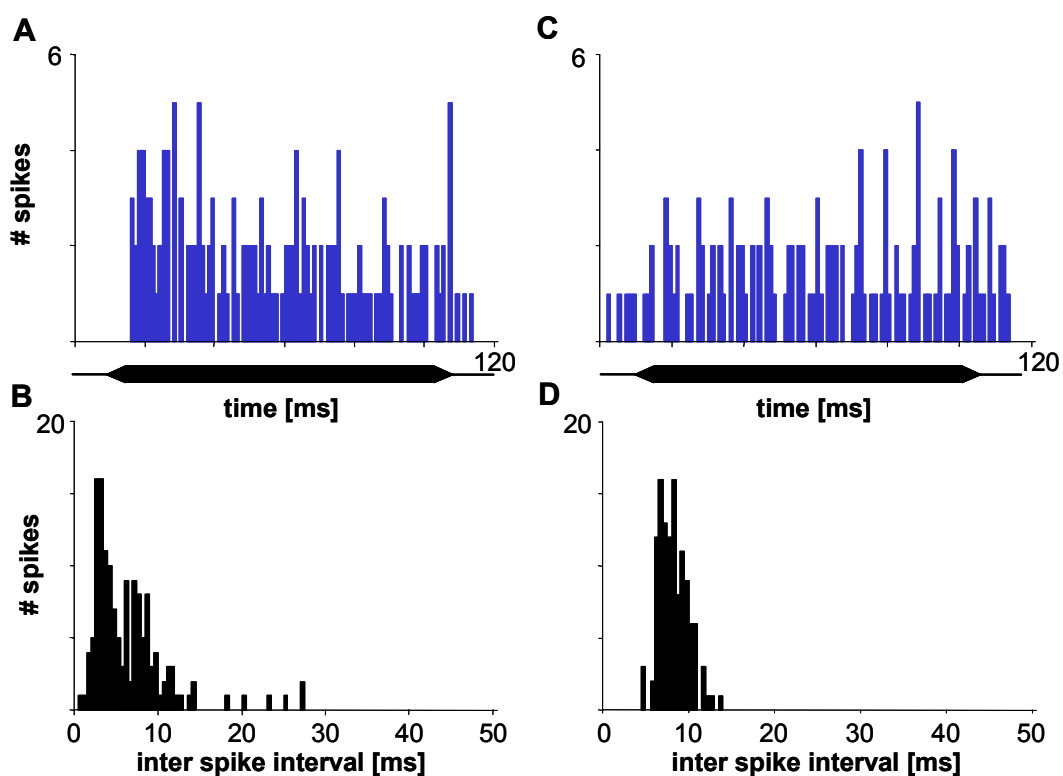


Figure 4.31

Discharge patterns of SPN neurons with sustained responses. **A** PST Histogram of a neuron with a sustained discharge throughout the entire stimulus duration (stimulus duration is indicated by the horizontal black bar, bin width 1 ms, PSTH from 10 repetitions). **B** Inter spike interval (ISI) histogram for the neuron shown in A (bin width 0.5 ms). **C/D** PST Histogram / ISI Histogram for a neuron with sustained response displays a tendency to “chopping” (regular discharges are not related to the stimulus frequency).

displayed primary-like discharge patterns. This subset of 24 cells exhibited no regularity in the inter-spike interval histogram (Fig. 4.31 B). Of the remaining 6 sustained neurons, four exhibited a regular inter spike interval that was not correlated to the stimulus frequency (“chopping”; Fig. 4.31 C, D). One cell showed a pause after a strong onset but

otherwise no regularity. Likewise, only one of the 30 sustained responders phase-locked to pure tones, although 6 of the sustained neurons had BFs below 2 kHz.

Phasic discharge patterns in response to pure tones were found in 21 neurons (41% of the 51 neurons which responded to pure tones), 18 showing a discharge related to the stimulus onset (Fig. 4.32 A), and three showing a discharge to the stimulus offset (Fig. 4.32 B). Figure 4.33 displays the distribution of discharge patterns of the 51 SPN neurons responding to pure tones.

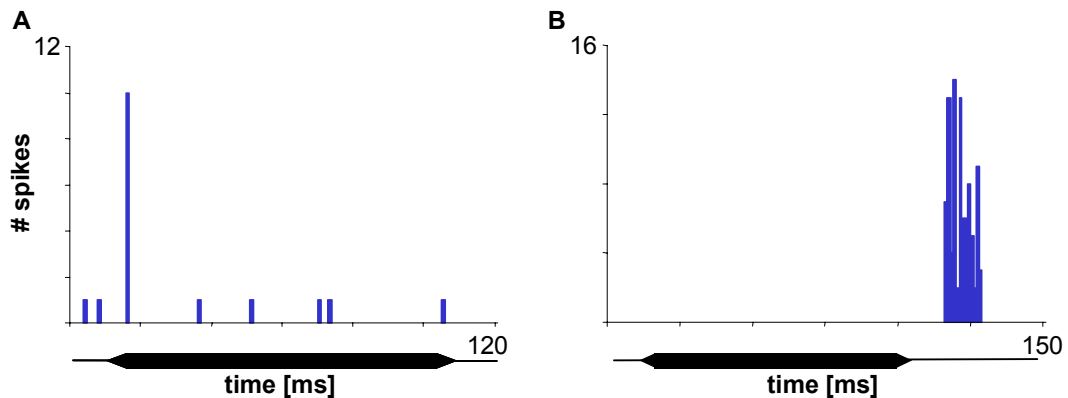


Figure 4.32

Response pattern of SPN neurons with phasic discharge. PST Histograms **A** of a neuron with a phasic ON discharge, and **B** of a neuron with a phasic OFF discharge, respectively. Bin width 1 ms. Histograms derived from 10 repetitions.

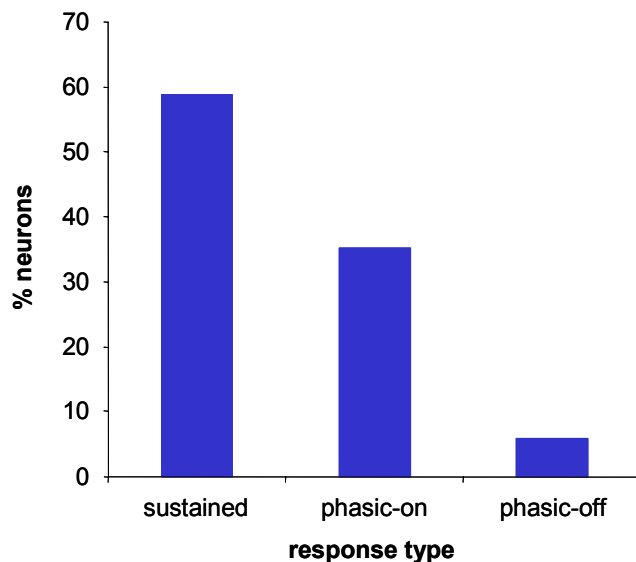


Figure 4.33

Distribution of discharge types in response to pure tones.

4.2.5 Response latency

The latency and the jitter of the neuronal response was analyzed in 48 neurons. Sustained and ON responders were characterized independently to reveal differences in accuracy of timing.

The sustained neurons (N=30) showed an average latency of 3.4 ± 1.7 ms (displaying latencies in the range from 0.6 to 7.8 ms). In 54 % of the neurons, latency got shorter with increasing amplitude of the sound with a trading ratio of 0.2 ms/dB. The remaining 46 % showed no systematic relation between latency and amplitude. The averaged jitter for the 30 sustained neurons was 933 ± 790 μ s, although only 13 % (4 neurons) out of this population showed very accurate responses with a “jitter” of less than 100 μ s.

Neurons with a phasic discharge to the stimulus onset (N=18) responded with an average latency of 5.1 ± 2.5 ms (in the range of 0.9 to 11.2 ms). Thus, neurons with an ON response showed longer latencies than the sustained responders with statistical significance (t-test, $p=0.008$). Latency got shorter with increasing amplitude in 62% of the ON responders (with a ratio of 0.11 ms/dB). The jitter in ON neurons was lower than in neurons with a sustained response. They displayed an average jitter of 588 ± 816 μ s (significance $p=0.08$, t-test). Furthermore 44 % (8/18) of the ON neurons responded with a jitter less than 100 μ s (Fig. 4.34).

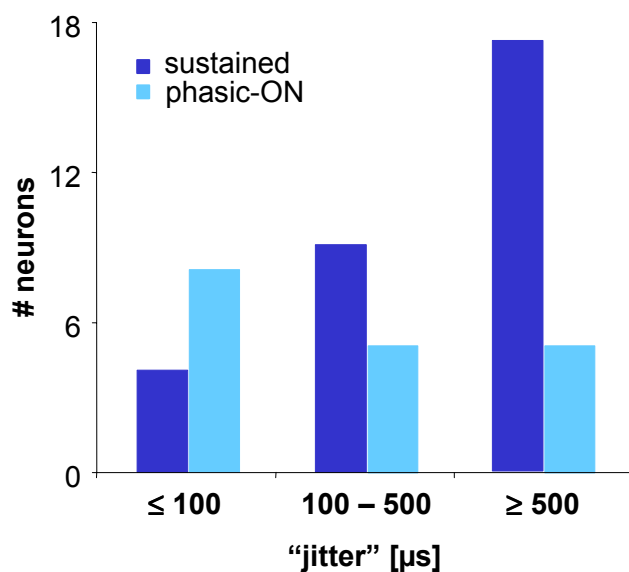


Figure 4.34

Comparison of the accuracy of the first spike of a tone evoked response (“jitter”). Values are displayed for neurons with phasic ON and sustained discharge patterns.

4.2.6 Binaural response characteristics

The binaural characteristics of 48 neurons were assessed. Neurons were again (see chapter 4.1.7) examined with a variety of paradigms to characterize their overall bilateral inputs. Out of the 48 cells tested, 25% were driven by the contralateral ear without any effect of ipsilateral stimulation (O/E) and 31% were characterized vice versa (E/O; Fig. 4.35). Thus, monaural neurons represented more than half of the recorded SPN neurons.

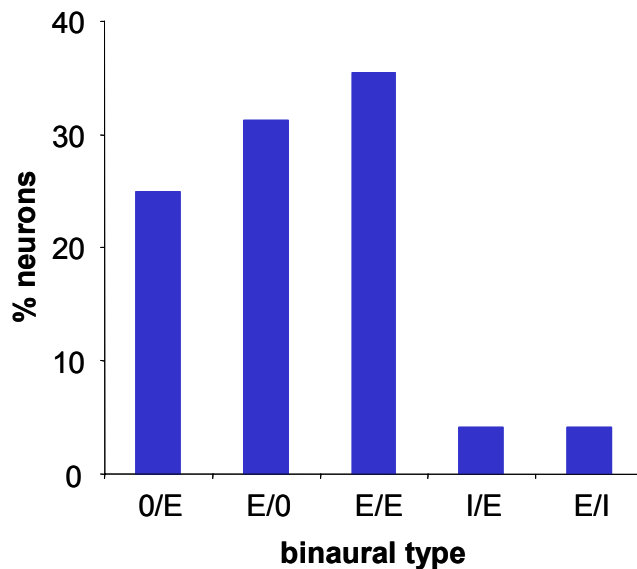


Figure 4.35

Distribution of overall binaural properties (E excitatory, I inhibitory, O no effect). The first letter indicates ipsilateral effects, and the second letter indicates contralateral effects.

The remaining neurons (44%) exhibited binaural interactions, mostly as binaural excitation or facilitation (E/E; 35%; 17/48). Only four neurons were characterized as being excited by stimuli at one ear and inhibited by stimuli at the other ear, each type (E/I and I/E) was found in two neurons. However, the IID sensitivity of these cells was weak and IID functions never dropped below 50% of the maximal discharge rate.

All but one of the E/E cells had monotonic RLFs for binaural stimulation at an IID of zero. Changing IIDs had only moderate effects on these cells. Four E/E neurons showed a monotonic increase in spikerate when the stimulus intensity was kept constant at either the ipsilateral or the contralateral ear (20 dB above the threshold for binaural stimulation) and systematically increased at the opposite ear (Fig. 4.36, upper left graph). This behavior was in line with their monotonic rate-level functions (Fig. 4.36, upper right graph) and indicates a strong facilitating effect of binaural stimulation. These cells showed no signs of inhibition. In nine out of the 17 E/E neurons, changing the stimulus intensity at one ear up to 30 dB above threshold (IID = +10 dB) did not have any effect

on the response to stimulus presentation at the opposite ear (Fig. 4.36, middle left graph). Four cells showed weak increases for more positive IIDs (Fig. 4.36, lower left graph).

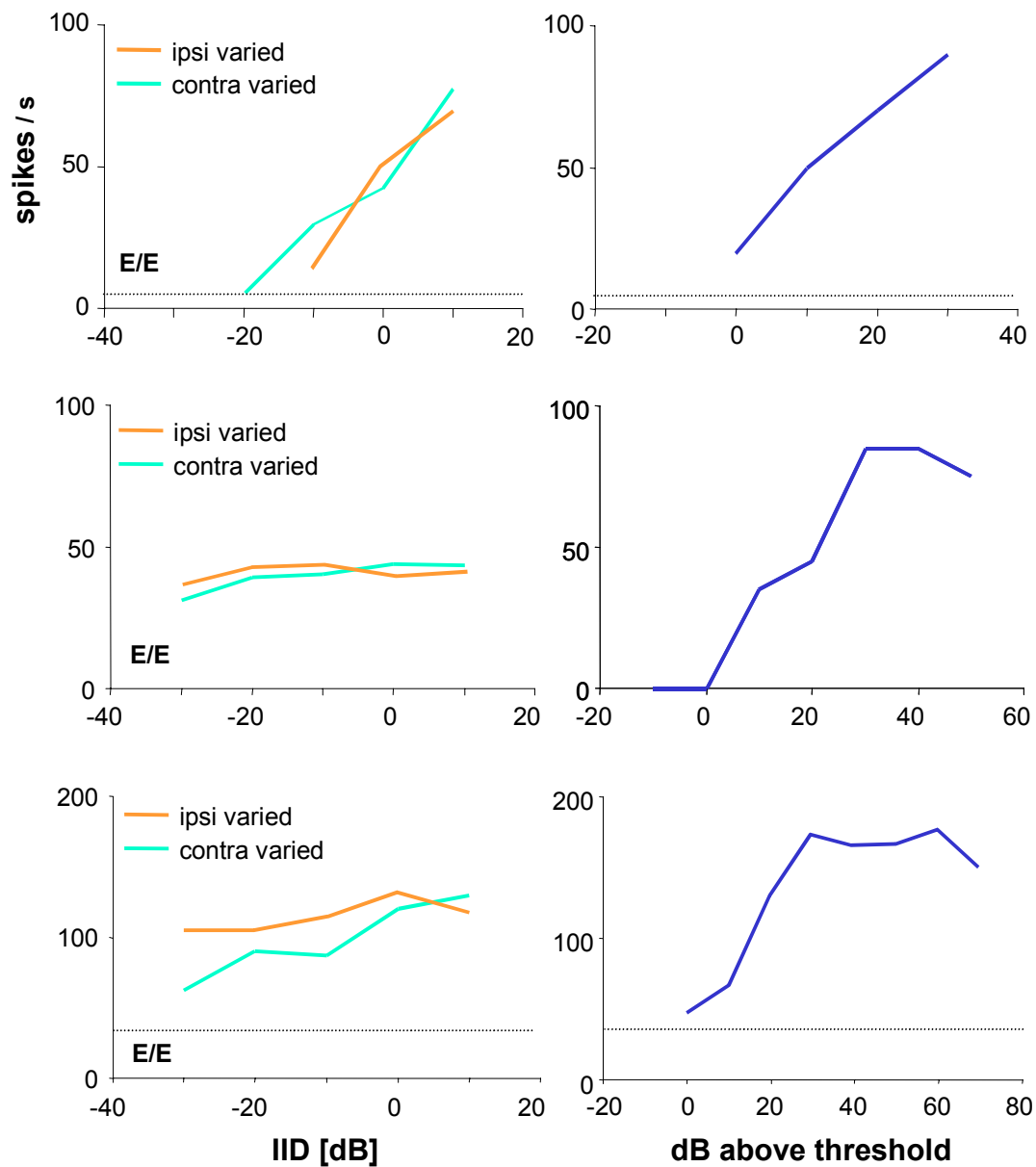


Figure 4.36

Response of three E/E neurons to different interaural intensity differences (IIDs; *left panels*) and the rate-level functions of the neurons with binaural stimulation at zero IID (*right panels*). For IID functions, the intensity at one ear was fixed at 20 dB above threshold for binaural stimulation and the intensity was varied at the other ear. Note that in the upper example spikerate is more than doubled at 0 IID compared to -20 dB (similar to monaural stimulation). The second neuron shows no effect of binaural stimulation although binaurally excitable. The lower example shows a summation effect with roughly the doubled rate for IID=0 compared to -30 dB (comparable to monaural stimulation). The dotted lines in the upper graphs and the middle graphs indicate the spontaneous activity.

Of the 17 E/E cells recorded, five had BFs below 2 kHz, hence, there might be some ITD sensitivity to ongoing pure tones in those neurons. Figure 4.37 A shows the ITD

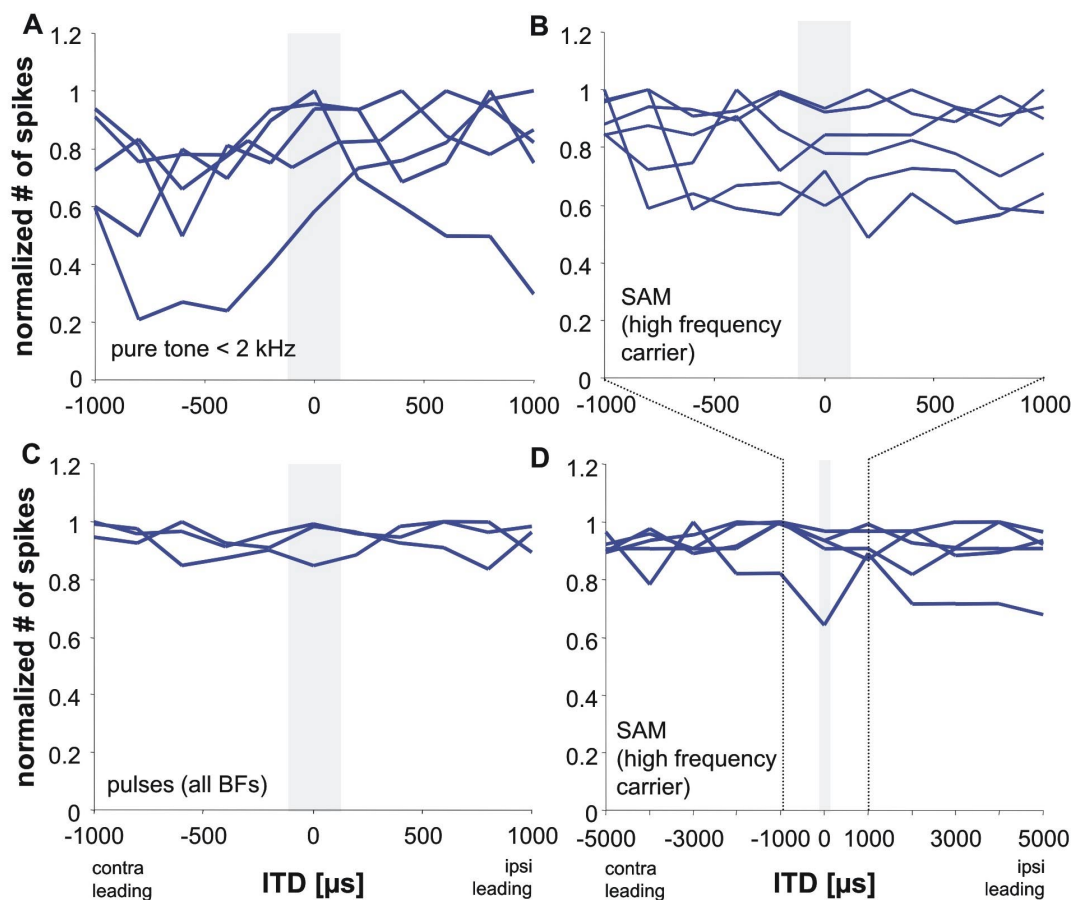


Figure 4.37

Response of E/E neurons to interaural time differences (ITD). **A** Response of five low frequency neurons (BF < 2 kHz). Only two neurons exhibited a weak sensitivity to ITDs within the physiological range (gray area). **B** ITD sensitivity to the envelopes of SAM stimuli of six high frequency neurons at the individual highest modulation frequency at which a robust phase-locked response was elicited (for details see text). No ITD sensitivity was observed, even when tested for five of the neurons over a larger range of ITDs to cover all interaural phase disparities of a full SAM cycle (**D**). **C** ITDs of short tone-pulses (5 ms) did not reveal any ITD sensitivity in three E/E neurons tested.

functions of these five neurons. Two of them showed some ITD sensitivity in the physiologically relevant range for the gerbil ($\pm 120 \mu\text{s}$; shaded blue areas in Fig. 4.37). However, this 20% change in spikerate across the relevant ITD range is rather insignificant when compared to the E/E neurons in the gerbil MSO (see chapter 4.1.8 and Spitzer and Semple, 1995). Moreover, one of these two neurons showed increasing spikerates for ipsilateral stimuli leading contralateral stimulation whereas the other neuron showed the opposite effect.

Neurons that did not phase-lock to SAM or pulses at an ITD of 0 ms never displayed phase-locked responses, regardless of the ITDs presented (not shown). Hence, phase-locking did not benefit from binaural time disparities. Accordingly, the only neuron in this sample that showed phase-locking to pure tones had a VS of approximately 0.5 for all ITDs tested. ITD sensitivity to the stimulus envelope was tested in six neurons using SAM stimuli at different modulation frequencies. Figure 4.37 B illustrates the SAM responses of these neurons at the highest modulation frequency that elicited a robust (>0.5 spikes/cycle) and significantly phase-locked response. No cyclic ITD sensitivity was apparent and only minimal changes in the discharge rate were observed within the relevant range of ITDs. In five of those neurons, ITD sensitivity was tested over a larger time scale, such that all interaural phase disparities of a complete SAM cycle were covered. Again, no ITD sensitivity was detected (Fig. 4.37 D; gray area indicates physiological range of ITDs). Three E/E neurons were additionally tested for ITD-sensitivity to trains of short tone pulses with steep rise-fall times (0.5 ms), but again no significant ITD sensitivity was observed (Fig. 4.37 C).

4.2.7 Responses to SAM

Depending on their discharge pattern to pure tones neurons, were analyzed in their response properties to SAM stimulation. All 39 neurons responded to SAM stimulation, but only 26 showed an ongoing synchronized response to the stimulus envelope with a significant VS > 0.3 ($p < 0.05$, Rayleigh test) to at least some frequencies. This was found in 95% of the sustained neurons (20/21) and 33% of the ON neurons (6/18). The remaining 13 neurons responded to SAM as to pure tones (10 ON responders, 2 OFF, 1 “chopper”), irrespective of the modulation frequency used (see table 4.4). For representative examples of the response to SAM (for sustained and ON responders) see figure 4.38.

To evaluate precision of phase-locking in those neurons the average VS at 114 Hz and the maximal VS (at the best frequency) was measured. Neurons phase-lock to 114 Hz with an averaged VS of 0.58 ± 0.19 and they maximally phase-lock with an average of 0.68 ± 0.15 . Interestingly, this was different for the two populations of sustained and ON responders (ON neurons: 0.78 ± 0.13 , sustainers: 0.67 ± 0.14). This observed difference was statistically significant ($p < 0.05$, Mann Whitney U test).

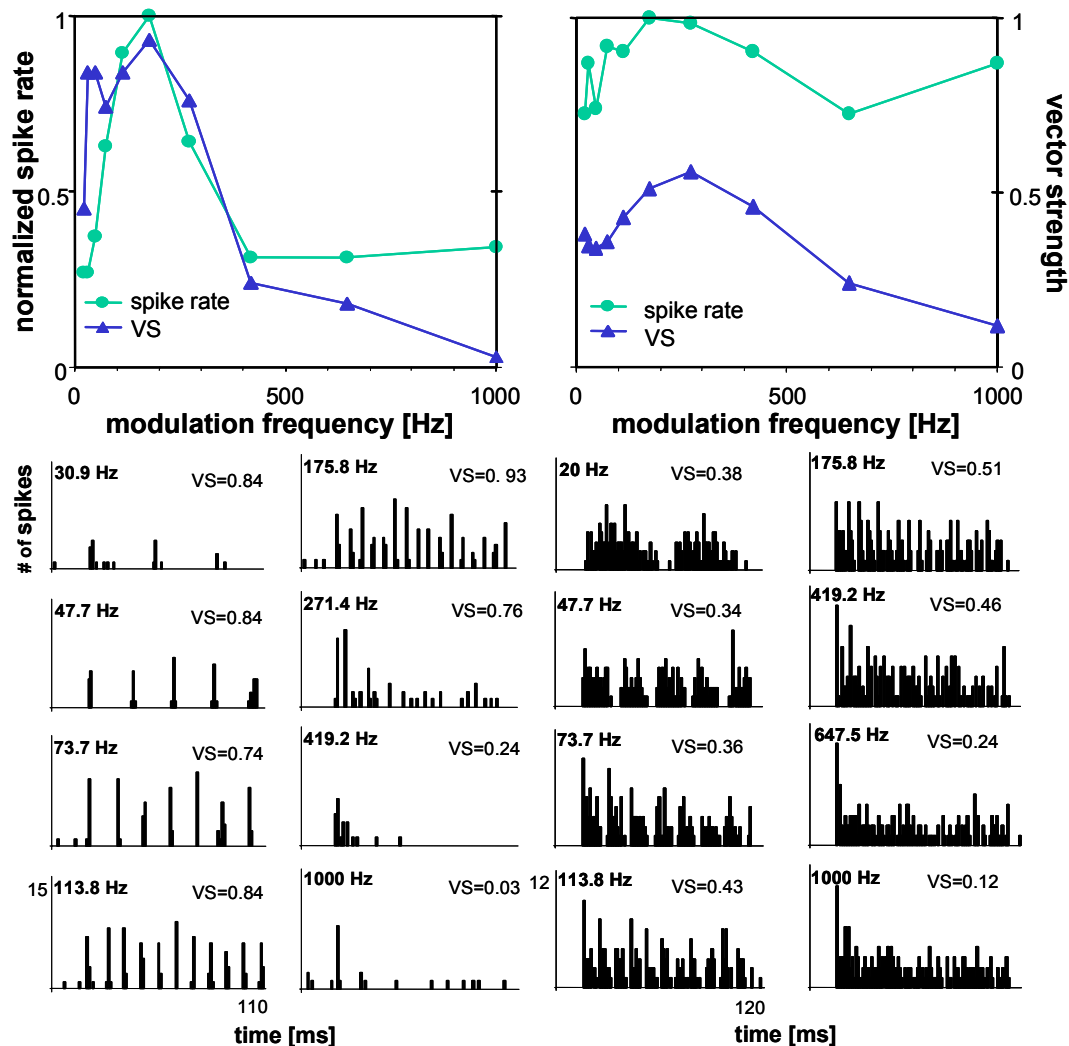


Figure 4.38

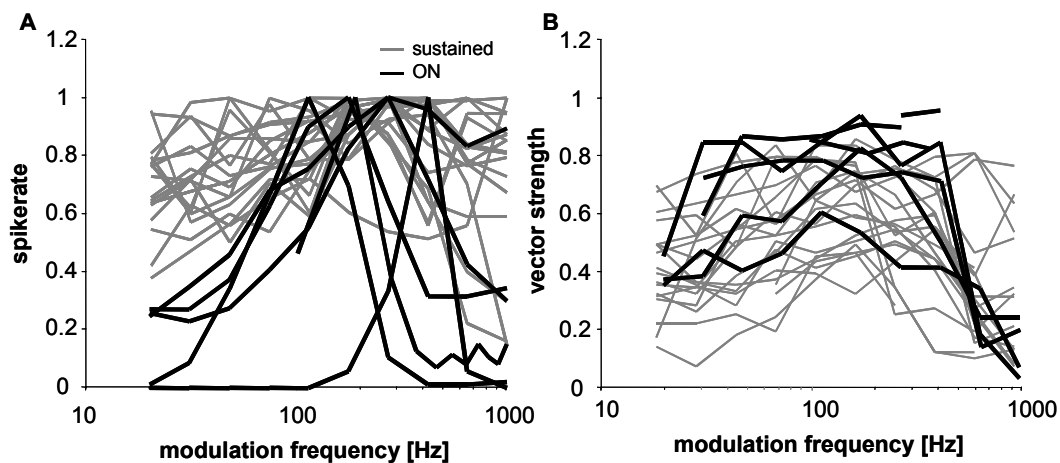
Response to SAM stimuli. *Left panels:* Neuron with a phasic ON response showing band-pass filter characteristics for rate based and low-pass filter characteristics for vector strength (VS) based MTFs. The PST histograms in the lower part of the figure show that the neuron's response followed each cycle of the SAM stimulus up to modulation frequencies of about 270 Hz. At higher modulation frequencies the neuron only responded to the first cycle. *Right panels:* Example of a neuron with sustained discharge showing all-pass filter characteristics in the rate based MTF and low-pass characteristics in the VS based MTF. PSTHs in the lower part indicate the phase-locking to the modulation envelope of the neuron up to about 419 Hz. The number in the left corner of the histograms indicates the modulation frequency, the VS values are shown in the right corner. The bin width of the PSTHs is 1 ms. Responses to 10 stimulus presentations are shown.

Moreover, temporal filter characteristics for all 26 neurons were tested using the same criteria as for SAM filter functions in the MSO (50% cut-offs for rate based MTFs and VS values below 0.3 or insignificant in VS based MTFs, Fig. 4.38 A, B). Flat rate based MTFs were only observed in sustained neurons (in 16 of the 20 sustained responders in this sample). The rate based MTFs never dropped below 50% of the total spike count (classified as “all-pass”). The remaining 4 neurons showed either low-pass (2/20), high-

	ON		Sustained	
	rate MTF	VS MTF	rate MTF	VS MTF
all-pass	-	-	16	5
low-pass	-	4	2	8
high-pass	1	-	1	3
band-pass	5	2	1	4
Σ	6	6	20	20

Table 4.5

Filter properties of SPN neurons in response to binaural presentation of sinusoidally amplitude modulations

**Figure 4.39**

Modulation transfer functions (MTFs) of all neurons with an ongoing response to SAM stimuli. MTFs of neurons with sustained responses to pure tones are shown in gray, MTFs of ON responders are shown in black. **A** Response rate based MTFs. **B** Vector strength (VS) based MTFs.

pass (1/20) or band-pass (1/20). ON neurons showed generally band-pass filter characteristics in rate based MTFs (5/6), only one neuron responded to high modulation frequencies exclusively (high-pass). The averaged upper cut-off of the low-pass and band-pass neurons was 477 ± 266 Hz

Additionally, phase-locking above $VS > 0.3$ was used as a criterion to reveal temporal filter properties. The sustained neurons showed either all-pass (5/20), low-pass (8/20), band-pass (4/20) or high-pass (3/20). In the population of six ON neurons, four exhibited low-pass and four band-pass. About one third of all neurons reflected the temporal pattern of the SAM stimulus up to 1000 Hz with some degree of phase-locking. It seems that filter characteristics in both rate based MTFs depend on the neuron's

discharge pattern to pure tones. ON neurons showed much narrower MTFs compared to sustained neurons.

4.2.8 Pharmacology

SPN neurons receive very strong glycinergic inputs. It is known that stainings of SPN neurons with antibodies against gephyrin, a protein anchoring the glycine receptor in the postsynaptic membrane, show very intense staining (Behrend et al. 2002). To test the effects of the inhibitory input on SPN neurons, glycine (or its receptor antagonist strychnine) was applied iontophoretically to single neurons during the recording of acoustic responses. The neural discharges before, during and after application of glycine and/or strychnine in a total of 14 SPN cells were recorded. Both drugs significantly influenced discharge rates and, in some cases, the VS based MTFs and the ITD sensitivity of SPN neurons. Interestingly, discharge patterns in response to pure tones remained unchanged by pharmacological manipulation. In all tested cells, glycine significantly inhibited stimulus evoked responses. In three of them no response at all could be elicited during the drug application and for a short period after the application (Fig. 4.40).

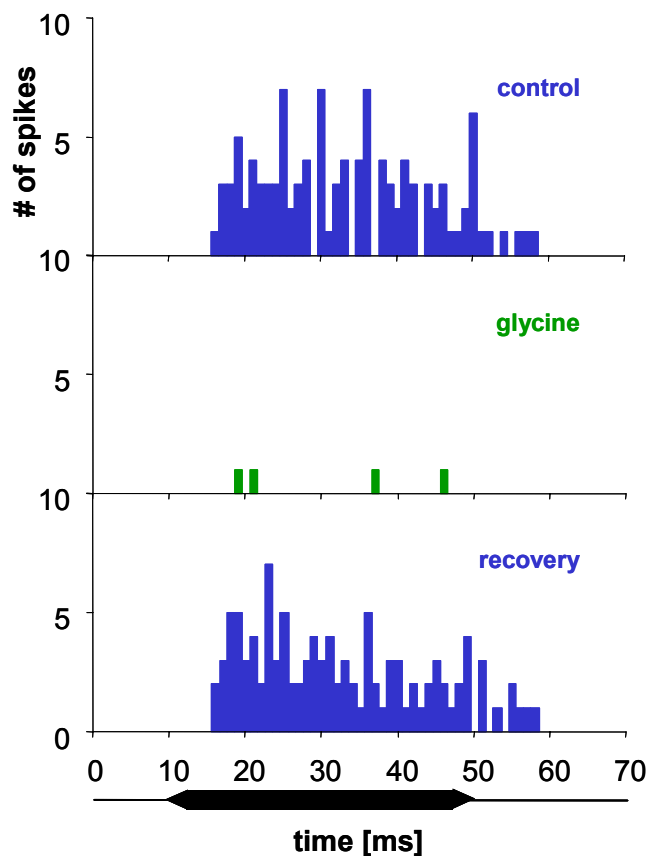


Figure 4.40

Application of glycine suppressed responses of SPN neurons to tones. *Upper panel:* PSTH from a neuron with a sustained response to binaural stimulation. *Middle panel:* The response could be blocked completely with glycine (after 10 s of iontophoretic application with 40 nA), and recovered fully after the application was stopped (*lower panel*). The bin width of the PSTHs is 1ms. Responses to 10 stimulus presentations are shown.

In seven neurons, effects of the glycine antagonist strychnine could be observed. In all cases, strychnine caused an increase in acoustically evoked responses (up to two times control). The effect of strychnine on the spontaneous discharge rate was found to be even stronger (average of 2.6 times control) and lasted several minutes after the application. In two cells (both sustained responders), the effect of strychnine on the discharge to SAM was tested. In both cases, phase-locking to low SAM frequencies was unchanged. However, the ability to phase-lock to modulation frequencies >400 Hz was significantly enhanced (Fig. 4.41), shifting the cut-off in the VS based MTF to >1000 Hz.

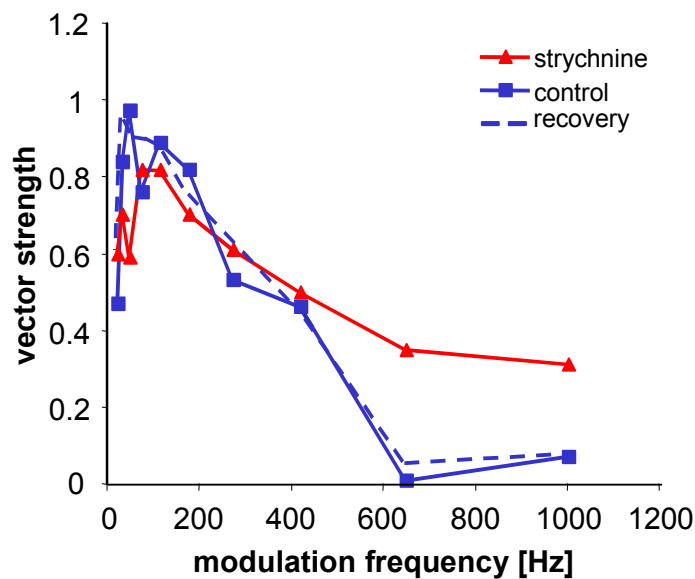


Figure 4.41

Effects of strychnine application on VS based MTFs. During application of strychnine (140nA), this neuron responded to higher modulation frequencies with phase-locked discharges when compared to the control and the recovered response.

Another effect of glycinergic inhibition on temporal processing is shown in figure 4.42. This E/E neuron was tested for sensitivity to ITDs in the envelope of SAM stimuli (tested at 75, 125 and 175 Hz modulation frequency; carrier frequency: 3.1 kHz). Note that the ITDs presented relate to the modulation frequency and are far beyond the physiological range. Under control conditions, the neuron showed no ITD-sensitivity in the spikerate (Fig. 4.42, upper left panel). However, the VS showed a cyclic function indicating good phase-locking when the binaural inputs were roughly in phase and low phase-locking when they were out of phase (upper right panel). Partial blocking of glycinergic inhibition via application of strychnine (middle panels) increased the spikerate but lowered the degree of phase-locking. However, the basic ITD sensitivity remained unchanged. Application of glycine, however, strongly inhibited the response rate and binaural excitation could only overcome the inhibitory effect when elicited in phase, hence, when excitatory inputs coincided (lower left panel). Although the ITD sensitivity created by experimentally induced inhibition in this neuron was far from being relevant

for sound localization, it indicates that inhibitory inputs might significantly alter and potentially sharpen the sensitivity of SPN neurons to temporal stimulus properties.

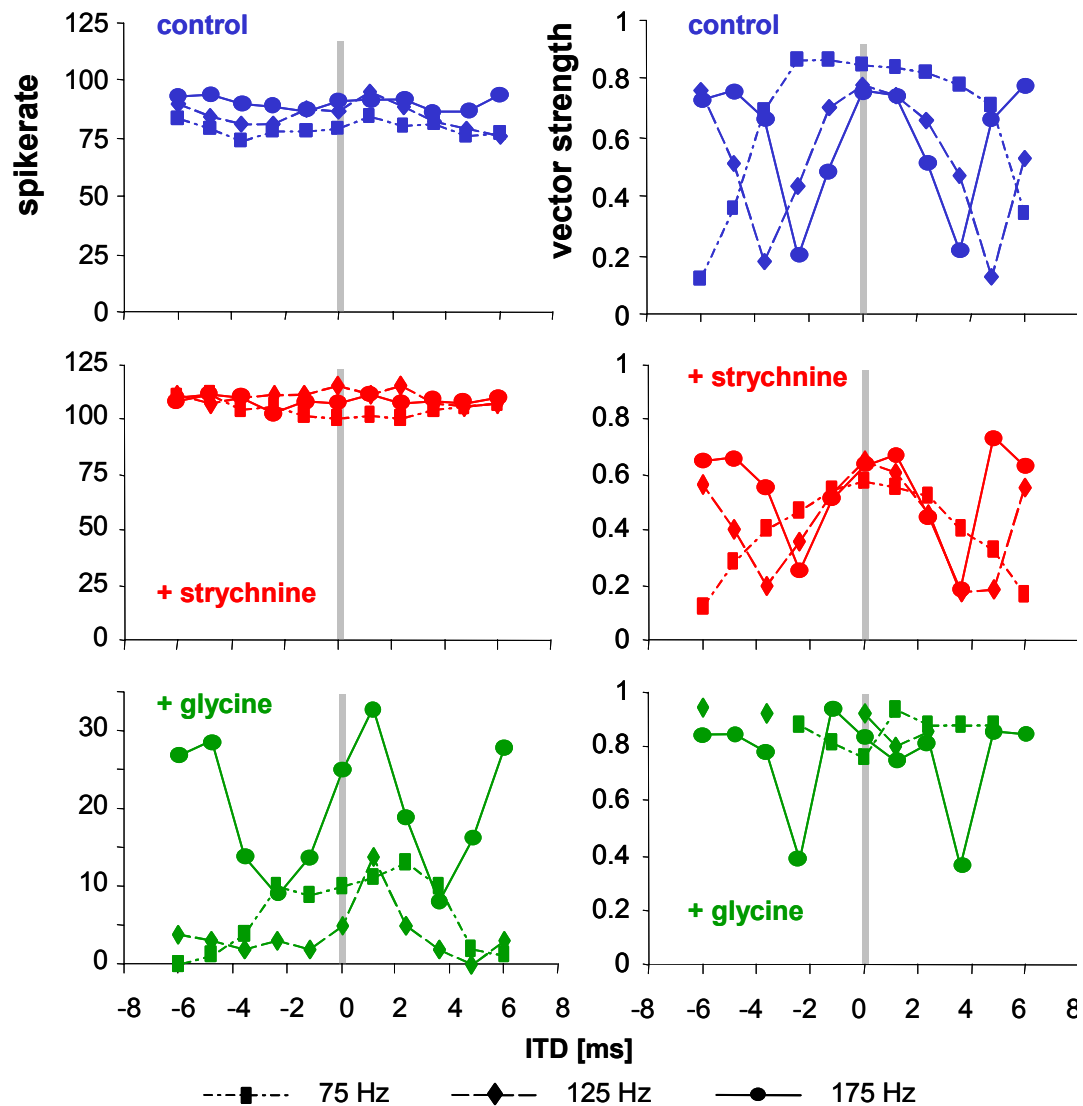


Figure 4.42

ITD functions of a neuron in response to SAM stimuli (75, 125, 175 Hz modulation frequency). *Left panels* show the spikerate based ITD functions. *Right panels* show VS based ITD functions. Only significant values are shown. Before drug application (upper panels) only the phase-locking but not the spikerate varied as a function of ITD. Iontophoretic application of strychnine (100 nA; middle panels) did not change the overall ITD sensitivity but decreased the maximum VS. Application of glycine (40 nA; lower panels) highly suppressed activity but evoked a rate based cyclic ITD sensitivity and increased the maximum VS. Note that the ITD sensitivity is related to the cyclic nature of the stimulus envelope, however, it is unlikely to be of behavioral relevance. ITDs within the physiological range are indicated by the gray area.

4.3 Comparison of neuronal properties in MSO and SPN

The main inputs to the SPN (binaural excitation and contralaterally driven inhibition) resemble on first sight those of the major MSO inputs. Table 4.6 combines most important response features of SPN and MSO neurons. SPN and MSO neurons were similar in response characteristics like, binaurality and response patterns. However, some differences were observed. Even though frequency tuning in MSO and SPN neurons is comparable, MSO neurons are even more biased to low frequency processing. More than half of the neurons in the MSO are tuned to frequencies below 2 kHz, whereas in the SPN it is less than a third. This is also reflected in the ability of neurons to phase-lock to pure tones. Whilst in the MSO 96 % (22/25) of all low frequency ($BF \leq 1.3$ kHz) sustained responders phase-lock to the stimulus, only one neuron (out of 11) in the SPN is doing so. SPN as well as MSO neurons (with slightly more neurons in the MSO) showed phase-locking to SAM envelopes with comparable synchronization abilities. In both nuclei, neurons mainly showed low-pass filter properties in VS based MTFs (cut-off around 500 Hz) and all-pass characteristics in rate based MTFs.

An important difference between MSO and SPN is their respective role in sound localization. SPN neurons exhibit flat discharge functions in response to ITDs in pure tones and high frequency envelopes. In contrast, the role of the MSO in low frequency sound localization is clear-cut. All of the binaurally innervated low frequency neurons showed ITD sensitivity to pure tones or broadband stimuli, confirming the role of the MSO in low frequency sound localization.

Iontophoretical application of neuroactive drugs affected discharge rates of MSO and SPN neurons in the same way. Injection of glycine at the recording site reduced or abolished the neuronal response. Strychnine increased spikerates of stimulus-evoked responses, as well as spontaneous activity. Moreover, the glycine antagonist reduced phase-locking abilities of MSO and SPN neurons to SAM stimulation. The effect seemed to be stronger in SPN neurons, blocking of inhibition even changed filter characteristics in VS based MTFs, indicating an important role of inhibition in temporal processing at least in this nucleus. However, blocking glycinergic inhibition in the MSO had a strong impact on low-frequency ITD-sensitive neurons.

		MSO	SPN
General response characteristics			
response to pure tones		97 %	82 %
BF distribution	range	500 Hz – 30 kHz	700 Hz – 37 kHz
	below 2 kHz	53 %	25 %
threshold at BF		- 10 to 73 dB SPL	2 to 52 dB SPL
Q ₁₀ dB		0.4 – 10.1	1.0 – 16.8
monotonic RLF		88 %	86 %
response pattern	sustained	78 % ¹	59 % ¹
	ON	22 %	41%
latency		5.5 ± 4.8 ms	4.1 ± 2.2 ms
latency shift		85% (trading ratio: 0.2 ms/dB)	57% (trading ratio: 0.17 ms/dB)
“jitter”		633 ± 840 μs	800 ± 802 μs
binaural properties	E/0	17 %	31 %
	0/E	26 %	25 %
	E/E	57%	36 %
	E/I	-	4 %
	I/E	-	4 %
ITD sensitivity		“peak-type”	none
Response to SAM tone (for frequencies below 1.3 kHz only)			
response to SAM	ongoing	86 %	62 %
	same as pure tone	14 %	38 %
VS	at 114 Hz	0.56 ± 0.20	0.50 ± 0.20
	maximal	0.70 ± 0.16	0.66 ± 0.11
modulation transfer functions	VS-based	mainly low-pass (58 %) (upper cut-off: 499 ± 277 Hz)	mainly low-pass (43 %) (upper cut-off: 493 ± 205 Hz)
	rate-based	mainly all-pass (63 %) (upper cut-off: 490 ± 196 Hz)	mainly all-pass (67 %) (upper cut-off: 450 ± 301 Hz)
ITD-SAM		flat or irregular ITD functions (no significant spikerate change within the physiological range)	flat ITD functions (no significant spikerate change within the physiological range)
Pharmacology			
glycine		inhibiting stimulus evoked responses	inhibiting stimulus evoked responses
strychnine	general	increase of spikerate increase of spontaneous activity	increase of spikerate increase of spontaneous activity
	temporal processing	affects ITD coding affects SAM coding, no changes in overall filter characteristics	potency of altering sensitivity to temporal stimulus patterns, i.e. changes in SAM filter properties

¹22 of 34 (65 %) low frequency MSO neurons phase-lock to pure tones, but only 1 out of 11 in the SPN.

Table 4.6 Comparison of basic response properties in MSO and SPN neurons

5.1 *The Medial Superior Olive*

In the present study, the role of MSO neurons in the processing of high and low frequency temporal cues was investigated. A big proportion of binaural excited MSO neurons displayed low best frequencies - these neurons are involved in ITD encoding. It is generally assumed that ITDs are represented in the brain in form of a space map, as in birds. This finding was generalized and assigned to the mammalian system. However, the findings in this study show that the representation of ITDs in mammals is significantly different from that found in birds and does not form a systematic map. Moreover, the findings in the present study showed that temporally precise inhibitory input to the MSO, which has been attracted far less attention than the excitation, is crucial to adjust the slope of ITD functions into the physiologically relevant range.

Additionally, MSO neurons with high best frequencies were tested with temporally structured sounds (SAM) in the second part of this study. Gerbil MSO neurons showed filter properties in response to SAM comparable to those found in only high frequency hearing animals, like bats. Therefore it is very likely that the MSO is involved in the processing of temporal cues in general.

5.1.1 *Localization of low frequency sounds*

5.1.1.1 *Representation of auditory space*

One of the major observations in the present study is that most binaural low frequency neurons in the MSO exhibit ITD sensitivity with maximal discharge outside or at the border of the physiological range. This finding challenges the idea of a topographical representation of azimuthal space. It seems that not the maxima of single neurons code for a particular position in azimuthal space, but that measuring the spike output of populations of neurons allows localizing sound sources in the horizontal plane.

In the present study, all neurons discharged maximally when the contralateral stimulus was leading in time (corresponding to positions in the contralateral hemisfield). The spikerate of the ITD functions is decreasing towards ITDs corresponding to ipsilateral positions in space. Therefore, the spikerate of a population of neurons is low, when the sound source is in the ipsilateral hemisfield, whereas the response of the same population

of neurons is maximal, when the sound source is in the contralateral hemisfield. In the relevant range of ITDs small changes in ITD result in maximal change in spikerate and can account for the spatial acuity of localization observed in mammals.

MSO neurons in the present study discharged maximally at a constant interaural phase difference, thereby adjusting the maximal slope into the relevant range independent of frequency. Previously, it was generally assumed that response maxima of ITD functions are independent of the frequency tuning characteristics of the neurons. McAlpine and colleagues (2001) presented a large sample of auditory midbrain neurons in the guinea pig showing similar distribution of ITD functions as in the gerbil MSO. They found maxima of ITD functions mainly when the contralateral stimulus was leading and additionally observed the same relation between BF and best ITD (including maximal response at a constant IPD). Not only is a maximal proportion of the slope of ITD functions in the physiological range, but the slope of the functions is steepest around zero ITD. This means that around the midline, the smallest changes in ITD provoke the biggest changes in spikerate. This could be correlated to psychophysical experiments on the spatial acuity of human listeners. Spatial resolution is most accurate directly in front of a listener, thus at zero ITD (Haftner and DeMaio 1975).

5.1.1.2 *Comparison to other ITD studies*

The observation that MSO neurons function as coincidence detectors (Goldberg and Brown 1968, Spitzer and Semple 1995, Yin and Chan 1990) and that the input onto these coincidence detector neurons is encoding the temporal structure of the low frequency input (Joris et al. 1994ab) led the authors of most MSO studies to assume that the Jeffress model is realized in the mammalian MSO. However, these data could also be interpreted as being consistent with the findings on ITD coding in the guinea pig midbrain (McAlpine et al. 2001) and the gerbil MSO (this study). In almost all of these studies, ITD neurons showed best ITDs preferably when the contralateral stimulus was leading in time (corresponding to the contralateral hemisfield). Extracellular recordings of cat, dog, chinchilla and gerbil MSO neurons (Caird and Klinke 1983, Goldberg and Brown 1969 Langford 1984, Spitzer and Semple 1995) also showed most of the peaks of ITD functions near or outside the contralateral border of the physiological range. Crow et al. (1978) investigated the relationship of BF and favorable delay in the kangaroo rat

brainstem. They showed that the two are not interdependent and moreover, that maxima of ITD functions are distributed at ipsi- and contralateral delays. However, it is not clear if they used the BF of a neuron for their correlation and if all of those neurons show “peak-type” behavior in response to ITDs. Moreover, it is not assured that really all of their recordings are in the MSO or if they are from neighbouring brainstem nuclei. In another study in the kangaroo rat, dealing with ITD sensitivity in the midbrain (Stillman 1971) almost all neurons discharged maximally when the contralateral input was leading in time. Stillman already observed that the slope is within a small temporal range around zero ITD. Most of the neurons in his sample discharged maximally at ITDs above 100 μ s. Assuming a physiological range of $\pm 80 \mu$ s for the kangaroo rat, maxima of most ITD functions are outside the relevant range of ITDs, as observed by McAlpine et al. (2001) in the guinea pig and in the present study in the gerbil.

Yin and Chan (1990) found, that most of the neurons discharge maximally at ITDs between zero and + 400 μ s ITD in their sample of cat MSO neurons. Consequently all the maxima of ITDs are in the physiological range of the cat. Given the fact that in the present study for the lowest BF recorded (500 Hz) best ITDs are around 400 μ s, thus outside the range of ITD the gerbil could detect. Considering the same situation in cats (or any animal with a larger inter-ear distance) an ITD maximum at 400 μ s would still be inside their physiological range even though the slope is maximally in the physiological relevant range. In animals with larger inter-ear distances and consequently larger physiologically relevant ranges, maxima of ITD functions could fall into the relevant range even at low BFs, if the slope is adjusted into the relevant range. These observations suggest that the findings in earlier studies could also be explained by the observations in the gerbil MSO and the guinea pig midbrain (McAlpine et al. 2001).

5.1.1.3 *Models of the representation of auditory space*

Contrary to earlier MSO studies, Fitzpatrick et al. (1997) addressed the idea that the maxima of a population of neurons determine the accurate position of a sound source. The discrepancy between precision of human listeners to locate a sound source (Mills 1958) and broad spatial tuning of auditory neurons inspired a model on the number of neurons needed to explain the behavioral observed acuity. The authors showed that 40 SOC neurons are sufficient to detect a change of 147 μ s. Because tuning to ITDs gets sharper in the ascending pathway efficiency of the population code increases, meaning

that less neurons are necessary to create similar accuracy or that with the same number of neurons higher accuracy can be achieved (e.g. for 40 neurons in the thalamus: 16 μ s detectable ITD). However, the model by Fitzpatrick et al. (1997) is depending on the maxima of the ITD function. A recent model initiated by Skottun (Skottun 1998, Skottun et al. 2001) is based on the slope of ITD functions and showed that already single neurons could accomplish high accuracy of ITD discrimination. Their finding suggests that the highly accurate sound localization of human observers is consistent with the resolution of single cells and that it is not necessary to combine the activity of many neurons. However, the integration of multiple stimulus parameters forces the need for more than one neuron.

5.1.1.4 *Encoding of ITDs in the avian system*

In the avian system all three assumptions of the Jeffress model are realized. They are best investigated in chickens and barn owls. Anatomical and physiological studies (Ramon y Cajal 1907, Rubel and Parks 1975, Overholt 1992) showed that the input pattern and the neuronal response to ITDs in chickens is in line with the Jeffress model. Axons collaterals from the contralateral NM act as delay lines leading to a mapping of space along the mediolateral axis as shown in anatomical studies (Parks and Rubel 1975, Young and Rubel 1983, Young and Rubel 1986). The dendrites seem to be specialized for ITD encoding. A gradient of dendritic length is arranged along the tonotopic axis (high frequency neurons have short dendrites whereas low frequency neurons have longer dendrites, Smith and Rubel 1975) that may reflect adaptations for coincidence detection at different frequencies (AgmonSnir et al. 1998).

In the barn owl, a bird that localizes the position of prey at night, sound localization mechanisms and their anatomical counterparts are more complex. Compared to other animals, barn owls use ITDs only for localization of azimuthal position. The location of sound sources in the elevation is encoded with IIDs (for review see Klump 2000). The auditory nerve and neurons in the NM are able to phase-lock up to 8 kHz, the border frequency of the barn owl audiogram (Quine and Konishi 1974) thus to much higher frequencies than mammals (Koppl 1997, Sullivan and Konishi 1984). This allows the barn owl to localize sound sources with ITDs up to these high frequencies. ITD information is conducted to the midbrain and is there combined with intensity information on single units creating space selective neurons tuned to a limited area of

space. These neurons are arranged in a topographic way building a mapped representation of space (Knudsen and Konishi 1978).

In contrast to the chicken NL, somata in the barn owl are not arranged in a layer of one or few rows of neurons but in a two-dimensional array (Carr and Boudreau 1993). NL neurons are binaurally innervated, axons from the ipsilateral NM branch into the nucleus from dorsal, whereas the contralateral NM-projection enters the nucleus from the ventral side (Carr and Boudreau 1993). These collaterals branch again to innervate single neurons thus forming delay lines in the dorsoventral axis (Carr and Konishi 1988, Carr and Konishi 1990). This additional branching creates multiple ITD-maps along the mediolateral axis, anatomically approving the Jeffress model. Interestingly, neurons in barn owl NL neurons are not bipolar, the dendrites are originating from all over the soma, and the inputs from ipsi- and contralateral NM are not segregated (Carr and Boudreau 1993).

As in chickens, the firing pattern of NL neurons is dependent on the interaural timing of binaural inputs (Carr and Konishi 1990). Recording of neurophonics at the outgoing fibres of the coincidence detector neurons revealed a systematic representation of best ITD with dorsoventral recording depth (Sullivan and Konishi 1986).

It seems that birds and mammals use different encoding strategies to achieve ITD localization. The assumptions of the Jeffress model are consistent with anatomical and physiological findings in birds. However, the barn owl, the principal animal under investigation on ITD coding, could use ITDs for sound localization up to stimulus frequencies of 8 kHz due to neuronal phase-locking up to these frequencies. Electrophysiological studies in the barn owl predominantly investigated neurons with BFs above 2 kHz. It could be that neurons with low and high frequency BF use different strategies for ITD encoding. Therefore, Wagner and colleagues (2000) addressed the question, if low-frequency neurons in the owl show similar response properties as low frequency neurons in the guinea pig (McAlpine et al. 2001). They found about 70% of neurons to peak within the physiologically relevant range of the owl and the slope of recorded ITD functions was not steepest around 0 ITD. Thus, they proposed that the same mechanism accounts for low and high frequency ITD coding in the NL. It seems that the encoding strategy for ITDs appears to be different in birds and mammals independent of frequency range.

5.1.2 *The role of inhibition in ITD coding*

5.1.2.1 *The mammalian system*

The observations in the present study not only showed that inhibition is involved in ITD processing, as it has been shown earlier (Grothe and Sanes 1994, Grothe 1994, Grothe and Park 1998), but that the temporal precise interaction of glycinergic inhibition and excitation shapes ITD functions. The present study showed that inhibition is responsible for shifting the slopes of ITD functions into the physiological range around zero ITD.

Different kinds of inhibition could be assumed to create the observed effects. One possibility is an overall tonic inhibition, without any temporal pattern. This possibility can be excluded, because this study showed that the inhibition must be asymmetric - it acts stronger for negative ITDs than for positive ITDs. Secondly, inhibition could be ITD sensitive in itself. Because glycinergic inputs to the MSO are ITD insensitive (both, inhibition from the LNTB and the MNTB are conducted via monaural pathways) this option is also very unlikely.

In order to explain the asymmetric effect of the inhibitory input, it is crucial that the inhibition occurs in specific phase relation to the excitation, that is, it is precisely phase-locked to the stimulus. And, in fact, the pathway that conducts the inhibition to the MSO is known to preserve timing of the stimulus. In the auditory nerve the neuronal response reflects the waveform of the stimulus (Palmer and Russell 1986). Interestingly in AVCN neurons phase-locking is even enhanced compared to the auditory nerve (in spherical bushy and globular cells, Joris et al. 1994a) by convergence of inputs. Globular bushy cells of the AVCN project to MNTB. In the AVCN-MNTB synapse, the calyx of Held, one of the largest synapses in the nervous system, excitatory potentials are known to have very rapid rise and fall times (Banks and Smith 1992). Therefore action potential threshold is reached very quickly and action potentials occur very reliable and with low temporal jitter, both features that promote phase-locking. Another adaptation for precise temporal transmission are low threshold potassium channels that have shown to be present in the MSO and MNTB (Banks and Smith 1992, Smith 1995, Kapfer unpublished observation). Indeed, in a model of gerbil MSO neurons low threshold potassium channels increased the temporal precision of model neurons (Svirskis et al. 2002).

Neurons in the MNTB, that project to the MSO, respond highly synchronized (SC values > 0.7) to the stimulus (Kopp-Scheinflug C. et al. 2002, Paolini et al. 2001, Smith et al. 1991, Smith et al. 1998, Wu and Kelly 1993) at least up to 1 kHz. Thus, all these features of neurons that are involved in conducting the inhibition to the MSO suggest an adaptation for high precision temporal processing.

Another question is how excitatory and inhibitory inputs onto single MSO neurons have to interact to create the observed ITD sensitivity. One could assume different combinations of inhibition and excitation, either ipsilaterally driven inhibition following the excitation, contralateral inhibition that precedes contralateral excitation or a combination of both. The most favorable explanation for the observed influence of the inhibition is a contralateral inhibition leading the contralateral excitation (as it will be shown below). Figure 5.1 depicts the effect of contralateral inhibition leading the

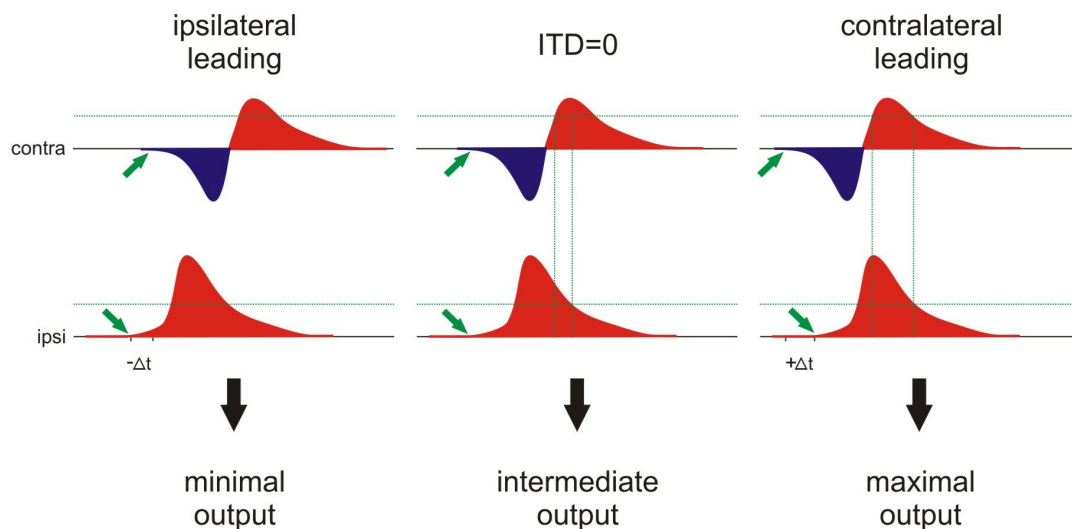


Figure 5.1

Interaction of contralateral inhibition (blue) leading the contralateral excitation (red) and contralateral inhibition (red) could create the physiologically observed ITD sensitivity (for details see text). Green arrows depict the onset of contralateral and ipsilateral potentials. Dotted green line indicates the spike threshold.

contralateral excitation. At an ITD of zero the inhibitory component of the contralateral input is reducing the window of possible coincidence of the two excitatory components, thus the neuron is responding with moderate spikerate (Fig. 5.1 B). However, for positive ITDs (contralateral stimulus is leading) the range of coincidence will be broadened creating maximal neuronal output, thereby generating the maximum of the ITD function (Fig. 5.1 C). Conversely, when the ipsilateral stimulus is leading in time the ipsilateral excitation and contralateral inhibition are coinciding, therefore, the output of the neuron

is minimal (Fig. 5.1 A). All possible ITDs ranging between those exemplified here create grading spikerates, again determined by the interaction of excitation from the ipsilateral side and inhibition and excitation from the contralateral side.

Indeed, it has been shown in the present study that there is inhibition that precedes the contralateral excitation by experiments with short frequency modulated pulses and by comparing phase angles of responses in control situations and during the application of strychnine. Also in the bat MSO (Grothe 1994, Grothe et al. 1997) contralateral inhibition leading excitation is a common phenomenon. Additionally, contralateral inhibition to the MSO has shown to be stronger than the ipsilateral one in gerbils and bats (Grothe and Sanes 1994, Grothe and Park 1998). Moreover, Moushegian et al. (1964, 1967) and Rupert et al. (1966) also observed that the contralateral input is consisting of inhibition that is leading the excitation.

The structures involved in transmitting inhibitory potentials make it likely that contralateral inhibition leads the contralateral excitation. The main projection to the MNTB is from globular bushy cells in the AVCN via large diameter fibres enhancing the conductance time (Schwartz 1992, Tolbert and Morest 1978, Yin 2001). Additionally, the calyx of Held, because of its fast receptor kinetics (Taschenberger and von Gersdorff 2000, von Gersdorff and Borst 2002) is adapted to minimize transmission delays at the synapse.

The shift of ITD tuning curves observed in the gerbil MSO was directly modeled by Torsten Marquardt (Brand et al. 2002) assuming a contralateral inhibition, leading the excitation from either side by 200 μ s, using a modified Hodgkin-Huxley model (Rothman et al. 1993) based on physiological findings in the AVCN (Oertel 1983). The non-linearity of membrane properties seen in AVCN neurons is alike to those observed in the MSO (Smith et al. 2000, Kapfer unpublished observation). In Marquardt's model, an additional voltage-dependent low-threshold potassium channel achieves a particular sensitivity to the relative timing of its spike inputs. Compared to earlier applications of the same model (Brughera et al. 1996, see below) excitatory and inhibitory time constants were considered short ($\tau = 0.1$ ms). The model could exactly simulate the effect of inhibition observed in physiological recordings. This indicates that an accurately timed synchronized contralateral inhibition preceding contralateral excitation (such as it potentially could be conveyed from the contralateral ear via the MNTB) can account for the neuronal response observed.

Even though the existence of inhibitory inputs to MSO neurons was known, earlier modelling studies could not satisfactorily explain the role of those inhibitory inputs in ITD coding. A model proposed by Colburn et al. (1990) including only excitatory inputs generated output patterns that are consistent with the patterns recorded in dogs (Goldberg and Brown 1969b) and cats (Yin and Chan 1990). The model implies a simple coincidence detection of binaural excitatory inputs to create ITD sensitivity, a mechanism unquestioned for creating ITD functions. In the view of the authors the findings suggest that inhibition is not necessary to describe the physiologically observed results. However, the present study showed that inhibition is not directly involved in creating the cyclic shape (which is physiologically obtained even after blocking of inhibition in the gerbil) but that it shifts the slope of ITD functions into the physiological range.

The first model implementing bilateral inhibition (Brughera et al. 1996) used large time constants for the inhibition (4 ms), much larger than those assumed in the model in Brand et al. (2002) in which timing of inhibitory inputs is known to be crucial for shaping ITD functions. Brughera and colleagues concluded that firing rate and synchronization are not dependent on inhibition facing the same constrictions as Colburn et al. (1990).

Simulations of the ITD shift created by timed contralateral inhibition (see above) led to the assumption that fast time constants (faster than that observed in the rat MSO, Smith et al. 2000) are crucial for creating ITD sensitivity observed in the gerbil. Preliminary studies on the inhibitory time constant in gerbil MSO slices (Kapfer personal communication) revealed that the time constant of inhibitory postsynaptic currents displays values around 0.5 ms (measured at 32°C) in 17 days old gerbils (adult like) in the range of the inhibitory time constant used to model the ITD sensitivity (Brand et al. 2002) observed in this study.

The temporal adjustment of this fast time constant, however, might be related to the experience dependent elimination of glycinergic synapses on gerbil MSO neurons (Kapfer et al. 2002). During the first days after hearing onset (postnatal day 10) the inputs are refined to the somata. Manipulations of binaural perceptions (by ablating one cochlea) revealed that the elimination of inhibitory synapses on the dendrite is activity dependent and requires binaural input.

Furthermore, stainings in gerbils that are reared in an environment where ITD cues are masked by omnidirectional white noise showed that the distribution of glycinergic synapses is significantly different to the one observed in normal animals (Kapfer et al.

2002). Moreover, electrophysiological recordings in those noise-reared gerbils revealed that sensitivity to ITDs is similar to that obtained during blockade of glycinergic inhibition (Seidl and Grothe unpublished observations).

In electron microscopic studies of cat (Clark 1969) and chinchilla (Perkins 1973) presynaptic terminals with flat vesicles (indicating inhibitory synapses) are similarly distributed as in the gerbil. All three species of animals hear well in the low frequency range and possess good low frequency sound localization abilities (Heffner and Heffner 1988, Heffner et al. 1994b, Heffner and Heffner 1985). As already discussed above, MSO neurons in these species are involved in the coincidence detection of timing cues (Langford 1984, Yin and Chan 1990).

Kapfer et al. (2002), moreover, showed that the confinement of inputs is not observed in predominantly high frequency hearing animals that are unlikely to use ITDs for sound localization (like rat, opossum and bats). The observed refinement of inhibitory synapses could minimize temporal summation of single synapses thereby sharpening the kinetics of inhibition.

5.1.2.2 *The avian system*

Inhibition has also shown to be involved in avian ITD coding. NL neurons receive massive inhibitory input, about one third of the synapses on single neurons use γ -aminobutyric acid (GABA) as a neurotransmitter (Carr and Boudreau 1993, Lachica et al. 1994, Carr et al. 1989). GABA inputs derive independently from either a population of interneurons around NL or from the superior olivary nucleus, driven indirectly by auditory stimulation (Bartheld et al. 1989). Because NL recordings turned out to be as difficult as those in the MSO, evidence about the involvement of inhibition in ITD coding in bird is rare. Recordings in NL of anesthetized barn owls addressed the question of how inhibition is involved in intensity stability of ITD functions (Pena et al. 1996). The authors assumed that inhibition acts as “gain control” at loud amplitudes to reduce the probability of monaural coincidence detection. Bruckner and Hyson (1998) proposed a similar mechanism after the observation that *in vitro* inhibition had different impacts on ITD coding depending on the applied GABA concentrations (consequently, on the strength of inhibition). Funabiki and al. (1998) also recorded *in vitro* from NL in chicken. They found that GABAergic inhibition improved the temporal discrimination of binaural inputs by decreasing the amplitude of excitatory potentials. They hypothesized that the

two distinct inhibitory inputs to the NL serve different tasks. In their view, inhibitory interneurons narrow windows for coincidence detection, thereby sharpening temporal acuity; projections from the superior olivary nucleus have a role in gain control.

Fujita and Konishi (1991) have assessed the role of inhibition in ITD coding in the NL indirectly. They injected the GABA_A antagonist bicuculline in the NL and recorded from neurons in the midbrain. Injections of the antagonist led to flattening of ITD curves, an observation that is in line with the proposed “gain control” mechanisms (Bruckner and Hyson 1998, Pena et al. 1996).

Interestingly, GABA application in the NL depolarised neurons upon stimulation, but has nonetheless an inhibitory effect. Studies in NL and NM (Funabiki et al. 1998, Hyson et al. 1995, Monsivais et al. 2000, Monsivais and Rubel 2001) showed that the chloride reversal potential (because of high concentration of chloride in the cell) was at more positive values than the resting potential, thus activation of the GABA receptor leads to an ion efflux and consequentially to a depolarisation of the membrane. The resulting change in membrane potential activated low threshold potassium channels. Hyperpolarisation of the membrane by potassium and chloride efflux led to a breakdown of membrane potential and thus to a drop of input resistance. Thus, it is more difficult to reach spiking threshold. The observed shunting inhibition is adequate to explain the observed effects of gain control in the avian system.

Thus, inhibition is involved in encoding of ITDs in birds as well as mammals. In birds the inhibition acts as gain control at high intensities. However, in mammals the inhibition already acts at the level of the coincidence detector neuron itself and shifts the maximum of the ITD function in a way that the slope is within the physiological range.

5.1.3 High frequency temporal processing

5.1.3.1 Temporal processing in non-spatial context

Recordings in low frequency hearing mammals dominate the picture of the function of the MSO in mammals. For decades the MSO was only discussed in the context of sound localization with the conclusion that only low frequency hearing mammals are possessing an MSO (Masterton and Diamond 1967, Masterton et al. 1975). This view was apparently supported by anatomical brainstem studies failed to describe the MSO in

small high frequency hearing animals (Harrison and Irving 1966, Irving and Harrison 1967).

However, the fact that the MSO in bats is not arranged in layers of neurons (that give the nucleus the characteristic shape in low frequency hearing animals) complicated the characterization of the nucleus. Schweizer (1981) was only the first one to reveal that bats do not only possess a MSO, but that the nucleus is well developed.

Subsequently, electrophysiological studies in various species of bats revealed that MSO neurons are involved in temporal processing (Grothe 1994, Grothe et al. 1997, Grothe et al. 2001). A role in the processing of low frequency spatial cues can be excluded as function of the MSO in these high frequency animals. However, the nucleus is discussed in the context of other temporal processing. As it was shown in bats (Grothe 1994, Grothe et al. 1997, Grothe et al. 2001), neurons encode the temporal structure of SAM stimuli by responding phase-locked to the stimulus envelope, but only up to modulation frequencies around 100 to 300 Hz.

There are functional considerations for this low-pass filtering of temporally structured sounds in bats. Bats rely almost only on echolocation cues for hunting. Analyzing the amplitude fluctuations of an echo perceived from a moving insect could be useful for identification of the prey. Moreover, it has been shown in the free-tailed bat (Grothe et al. 1997) that filter characteristics of SAM stimuli are influenced by stimulus location. An integration of the information of the stimulus pattern and the source position could be used to gain information additional information about the acoustical environment.

The observation that MSO neurons in low frequency hearing animals are able to encode ITDs, whereas MSO neurons in high frequency hearing animals, like bats, are involved in processing of temporal cues in the context of sound recognition may suggest the view that the nucleus is completing different tasks in different animals, depending on their hearing range. However, low frequency hearing animals like cats (Joris 1996), rabbits (Kuwada and Batra 1999) and gerbils (this study) also showed temporal filtering in high frequency MSO neurons. Compared to bats, filter cut-offs for synchronization to an SAM envelope in the MSO of low frequency hearing animals are high, but only few neurons phase-lock to higher modulation frequencies (> 700 Hz). Phase-locking decreased at higher modulation frequencies with filter cut-offs around 500 to 600 Hz. It seems that the MSO in low frequency hearing animals is involved in temporal processing in a non-spatial context as well. The processing of coincident binaural excitatory input

combined with inhibitory interaction is a general principle in the MSO. Encoding of ITDs is only one possibility to use that circuitry in low frequency hearing mammals, but is not ruling out the possibility of temporal processing of other, non-spatial, cues in these animals.

Investigations on the hearing system of early mammals showed that the MSO in those animals must have had another function than ITD processing. The first mammals in evolution presumably only heard high frequencies above 4 to 5 kHz (Fleischer 1978, Rosowski et al. 1999), hence, ITDs were sufficient cues for sound localization. The recent opossum, a mammal resembling auditory status of early mammals, possesses a MSO (Kapfer et al. 2002) and is hearing poorly below 6 kHz (Frost and Masterton 1994), even though hearing performance at higher frequencies is well-developed. Thus, the MSO in an evolutionary sense was consequently involved in other kind of processing than ITD encoding. Only the development of low frequency hearing in mammals made an ITD encoding structure necessary. In mammals that only hear high frequency (like recent bats) and are in no need to localize low frequency sounds, the MSO is involved in processing of other temporal qualities.

5.1.3.2 *Spatial Processing of high frequency cues*

ITD processing of ongoing tones requires the encoding of the temporal structure of a sound. Most mammals, including bats naturally only hear in the high frequency range far above 2 kHz. At those frequencies neurons do not phase-lock to the pure tone frequency (Galambos and Davis 1943, Rose et al. 1967). Nevertheless, neurons in the free-tailed bat MSO phase-locked to low modulation frequencies of SAM (Grothe and Park 1998, see above) and additionally, bat MSO neurons showed cyclically shaped functions in response to ITDs in SAM envelopes. Moreover, an interaction of excitation and inhibition was shown to create the observed ITD sensitivity (Grothe and Park 1998). This ITD sensitivity was discussed as epiphenomenal, because the physiological range of relevant ITDs is small in bats (because of the small inter-ear distance) and there is no significant change of spikerate in the physiological range. Recordings of high frequency neurons in cat MSO (Joris 1996, Yin and Chan 1990) and rabbit SOC (Batra et al. 1997a) revealed that ITD functions obtained with delays in SAM envelopes showed the same cyclic shape as those in the bat MSO. However, the inter-ear distance in those animals is

larger and the information in those ITD-SAM functions could be used for sound localization.

The high frequency neurons tested with ITDs in SAM in this study were either flat or did not show any systematic sensitivity to ITDs. It could be that the mechanism creating low frequency ITD sensitivity in the gerbil is not capable of SAM-ITD coding. There are no behavioral studies that prove that gerbils in fact use envelope information for ITD coding, as it has been shown for other mammals (Henning 1974, McFadden and Pasanen 1976). However, the modulation frequency of SAM used in cats and rabbits were higher than those used in the present study. Maybe there is ITD sensitivity to SAM in higher modulation frequencies than tested in this study.

5.1.4 *General response characteristics*

In the present study, neurons in the MSO showed BFs that cover most of the frequencies in the gerbil's audiogram (Ryan 1976). Moreover, neurons in the gerbil MSO are biased to best frequencies below 2 kHz, coherent with the ability of gerbils to localize low frequency sounds (Heffner and Heffner 1988, Ryan 1976). Guinan et al. (1972a) found an overrepresentation of low frequencies in the cat MSO - half of the neurons had BFs below 4 kHz. Goldberg and Brown (1969) recorded from SOC neurons of dog, which ranged in their BF between 1.5 kHz to 11.8 kHz. However, they only specified 16 neurons out of this population as MSO neurons, but it was not obvious how the frequency distribution of these neurons was. Yin and Chan (1990) investigated that most of the neurons in the cat MSO display low BFs (below 3 kHz). This sample may be biased towards low frequency BFs because the authors already aimed for the low frequency region in the MSO.

In rat and bat MSO only high frequency neurons have been recorded (rat: 2.2 kHz to 6.6 kHz, Inbody and Feng 1981, bat: in the range from 10 to 115 kHz, depending on the species used, Covey et al. 1991, Grothe 1994, Grothe et al. 1997, Grothe et al. 2001). Since in rats hearing in the low frequency range below 2 kHz is poor (Heffner et al. 1994a) and bats do not hear those low frequencies at all (Neuweiler 2000), the BF range of neurons in the MSO correlates with their audiogram fairly good.

The principle of tonotopy can be found throughout the ascending auditory pathway and has been shown for the MSO as well. Guinan et al. (1972b) and Goldberg and

Brown (1969) showed tonotopy in the MSO of cat or dog, respectively. Also in different species of bats (Covey et al. 1991, Harnischfeger et al. 1985) this tonotopy was confirmed.

However, in the present study evidence for tonotopy only comes from the anatomical position of neurons, whose position was marked. The reconstruction of all neurons did not lead to a topographical arrangement of BF, most likely due to a lack of sufficient accuracy.

There are some further speculations why it is difficult to reveal a tonotopic organisation with recordings of single units. Yin and Chan (1990) mentioned the possibility that action potentials in MSO neurons are generated not directly at the soma, but afar on the axon. Hence, action potentials are easier to record at that axonal position than at the soma because at the soma the back propagating action potentials are much smaller. This is consistent with the observation in this study: that in many cases pharmacological manipulations had no effect (suggesting axonal recordings) and many recording positions were reconstructed to be lateral to the somatic region in the dendritic area.

The revelation of tonotopy is additionally complicated by the finding that axons of MSO neurons project dorsally, perpendicular to the rostrocaudal plane (Kiss and Majorossy 1983, Kapfer personal communication). One could assume that the ordered arrangement of somata gets lost in the projecting axons. If indeed the action potential is generated on the axon, the actual recording position is not reflecting the position of the respective soma in a tonotopic map. In both, the studies in cats (Guinan et al. 1972b) and dogs (Goldberg and Brown 1968), metal electrodes were used and results were based, to a big proportion, on field potentials that are independent of spike generation at the soma or the axon. This is consistent with studies in the barn owl NL (Carr and Konishi 1990). The authors revealed that recordings of field potentials follow a tonotopic order in the dorsoventral dimension, whereas intracellular recordings of NL neurons did not confirm this observation of tonotopy. Moreover, there may be the possibility that not all of the recordings were obtained from neurons but from fibres originating in the AVCN projecting to MSO and other brainstem nuclei. Obviously, integration of those “neurons” would camouflage an existing tonotopy.

In the present study, more than 50% of the neurons were classified as binaural getting excitatory input from both ears (E/E neurons). In the low frequency proportion of those

cells a relatively higher amount of neurons (69 %) displayed binaural excitatory interactions. The remaining neurons only responded to stimulation from either the ipsi- or the contralateral ear. In an *in vitro* study in gerbil MSO 74 % of the neurons only responded with an action potential when ipsi- and contralateral inputs were stimulated (Grothe 1994), coherent with the present *in vivo* findings. .

As already mentioned, in some studies investigating response properties in the SOC, it is difficult to figure out which proportion of neurons is contributing to a response characteristics. Moreover, it was not clear if a particular population of neurons was recorded in the MSO or not. In those studies directly addressing neuronal properties in the MSO, findings on binaurality are consistent with observations in the gerbil (59 % E/E in the cat, Yin and Chan 1990, 50 % of low BF neurons in the kangaroo rat and rat, Inbody and Feng 1981, Moushegian et al. 1975, 60 % in the dog, Goldberg and Brown 1968). MSO neurons in bats show binaural excitatory interactions as well. Depending on the bat species under investigation different proportions of E/E interactions have been shown. In *Molossus ater* (Harnischfeger et al. 1985) and *Tadarida brasiliensis* (Grothe et al. 1997) about 50 % of the neurons were binaurally driven. However in *Eptesicus fuscus* (Grothe et al. 2001) and *Pteronotus parnellii* (Covey and Casseday 1991, Grothe 1994) ipsilateral inputs are reduced (21% in *E. fuscus* and about 10% in *P. parnellii* respectively). An exception is the chinchilla (Langford 1984) where more than 81 % of the neurons are E/E in the MSO.

Moreover, in dog (Goldberg and Brown 1969) and cat (Guinan et al. 1972ab) only few (dog) or none (cat) neurons showed overall inhibitory interactions from either the ipsi- or contralateral side in line with the finding that of no overall inhibitory effect of either ear was found in the gerbil MSO in the present study. However, studies in other rodents showed a somewhat different distribution. In the kangaroo rat (Moushegian et al. 1975) and in the albino rat (Inbody and Feng 1981) about half of the neurons showed inhibitory inputs (E/I or I/E). Inhibitory input from one side can be found in different species of bat as well (about 35% in *M. ater*, Harnischfeger et al. 1985, 30% in *T. brasiliensis*, Grothe et al. 1997, 20% in *E. fuscus*, Grothe et al. 2001 and 5 % in *P. parnellii*, Covey and Casseday 1991, Grothe 1994).

Hence, the distribution of monaural and binaural excitatory neurons is comparable to those in other low frequency hearing mammals.

Most of the neurons in this study showed sustained response pattern (78%) when tested with pure tones at BF. This finding is in line with the observations in other low

frequency hearing animals (Goldberg and Brown, 1968, Guinan et al. 1972ab. Yin and Chan 1990). However, studies in bats (Covey et al. 1991, Grothe 1994, Grothe et al. 1997, Grothe et al. 2001, Harnischfeger et al. 1985) revealed mostly phasic responses of MSO neurons.

Encoding and transmission of the temporal structure of pure tones is necessary for ITD processing of ongoing sounds, therefore, the vector strength of the response was also quantified for MSO neurons. All but two neurons with BFs below 1.3 kHz in the present study phase-locked to the stimulus frequency with a vector strength above 0.3. As in the gerbil, almost all low BF neurons in the cat (Yin and Chan 1990) phase-locked with high correlation values (0.8-1) to pure tone stimulation. Spitzer and Semple (1995) and Goldberg and Brown (1968) mentioned phase-locking units in and in the vicinity of the MSO but did not quantify strength of phase-locking.

General response characteristics are fairly similar across the different mammalian species. The observed pattern of phase-locking to low frequencies and overall binaural excitatory input are in line with sound localization with ITDs in low frequency hearing mammals.

5.1.5 *Reconstruction of recording sites*

Already the fact that only MSO neurons that could directly be correlated to a marked position revealed a tonotopic arrangement, indicates that the stereotactic measurements are not accurate and reproducible enough to assure that neurons particularly at the borders of the nucleus are in fact MSO neurons. However, some physiological characteristics of the recorded MSO neurons already indicate that most recordings are likely to be in the MSO.

Binaural excitation and “peak type” ITD sensitivity are neuronal properties that are apparently MSO like characteristics. The population of neurons from this study displaying those characteristics comprised more than 50%. However, the other half of the neurons was monaural. Even though that is a finding coherent with that in cats and dogs (Goldberg and Brown 1968 and Yin and Chan 1990 found 40% of monaurally innervated neurons) one has to be careful with the classification of those neurons..

There are different possibilities from which population of neurons, recordings could have been obtained if they were not from MSO neurons. One possibility is that recordings are obtained from axons of AVCN neurons that project binaurally to the

lateral lemniscus and the midbrain (Cant and Hyson 1992, Kil et al. 1995). AVCN neurons show strong onsets in their sustained response (“primary-like”) and phase-locking for low frequencies. However, 15 out of the 25 monaural units from this study did not display primary-like response patterns, but either an ON response (two neurons) or tonic responses (13 neurons). Eight of the remaining ten neurons showed phase-locking at BF. Indeed, five of those neurons were manipulated by application of glycine or strychnine, which makes it very unlikely, that their recordings were obtained from axons. However, for the remaining three phase-locking neurons and two neurons that showed primary like response patterns, the possibility that they are not MSO neurons, could not be excluded.

Moreover, monaural neurons could also belong to a population of olivo-cochlear neurons that are located medial to the somatic region of MSO principal cells (Aschoff et al. 1988a). These neurons are monaurally driven (usually by the contralateral ear, for review see (Smith and Spirou 2001), hence they are most likely O/E. However, only five of the O/E neurons are located on the medial side of the nucleus. Three of those neurons showed sustained, and two neurons showed phase-locked response to pure tones. Because olivo-cochlear neurons are not known to phase-lock (Brown 1989) to the phase of a stimulus, at least the two phase-locking neurons are not out of this population.

Thirdly, the MSO not only contains principal cells that form the characteristic somatic band, but there are also MSO marginal cells. These neurons are located in the dendritic region of principal cells and are monaural (Kiss and Majorossy 1983a, Schwartz 1977). Some of the recordings could have been obtained from this population of neurons, which are not physiologically investigated so far.

It could not be ruled out that some of the neurons are not originating in the MSO, however, the observed response patterns (as described above) makes it very likely that most of the neurons are in fact located in the MSO.

5.1.6 *Technical challenges of recording from single MSO neurons*

In the literature studies on single MSO neurons are underrepresented compared to other studies on auditory brainstem nuclei, because recordings in the MSO turned out to be difficult. One obvious reason for recording difficulties is the anatomical structure of the MSO. In low frequency specialists, there is only a small parasagittal plane of neurons (e.g. Kapfer et al. 2002), which lessens the probability to hit a single neuron.

Another difficulty is the location of the MSO in the brain. Approaching the MSO through the midbrain from dorsal to ventral leads to a penetration depth of already around 7500 to 8500 μm in the gerbil, making it difficult to hit the small MSO cell band.

Therefore, Yin and Chan (1990) penetrated from the ventral side of the skull to shorten the penetration depth. This approach is almost impossible in the gerbil, because the huge bullae would interfere with the electrode path. Moreover, the “ventral” approach requires profound surgery, hence, it demands a deeper anesthesia which is particularly difficult in small animals.

Inbody and Feng (1981) solved the problem of long distances by removing the whole cerebellum so that the brainstem is visible below the fourth ventricle and penetration tracks are shorter. This approach is highly invasive and again requires deep anesthesia.

Therefore, Spitzer and Semple (1995) developed a technique to penetrate into the MSO through the *Foramen magnum* at the caudal end of the skull. The *Foramen magnum* is a natural opening in the skull, only overlaid by some muscles and connective tissue. This approach has also been used in the present study. It reduces the recording depth to about 5000 μm and surgery is less invasive compared to the “ventral” approach and the removal of the cerebellum.

Not only long distances to the site of recording complicate MSO experiments, furthermore, extracellular single cell recordings in the MSO have proven to be extremely challenging (Caird and Klinke 1983, Goldberg and Brown 1968, Guinan et al. 1972ab, Spitzer and Semple 1995, Goldberg et al. 1963). Yin and Chan (1990) mentioned 75 penetrations that transversed the MSO and only 22 (29%) were successful to record at least from one single cell. Electron microscopic pictures of the MSO reveal a large amount of non-neuronal tissue, (particularly densely packed glia cells Kapfer personal communication). Therefore, neurons are electrically well isolated, which complicates the detection and recording from those neurons.

Recordings are further complicated by massive field potentials (so called “neurophonics”) that were observed with low impedance metal electrodes as well as with medium impedance glass electrodes. Those field potentials have been detected in the gerbil MSO as well (Spitzer and Semple 1995, this study). They originate from the convergence of many AVCN fibres carrying phase-locked input. This is of advantage when confirming the stereotactic measurements, but the potentials could be so large that they mask single cell activity. With higher impedance electrodes (up to 40 $\text{M}\Omega$) field potentials were not recorded, but the high impedance of the electrodes made it more

difficult to encounter single cells. As already mentioned, Yin and Chan (1990) speculated about a different position of spike generation, far more outside on the axon than in other neurons. The action potential would be largely diminished after back propagation to the soma, a fact that would additionally complicate recordings.

5.2 *The Superior Paraolivary Nucleus*

The SPN is a prominent SOC structure that rivals the size of the three so-called principal nuclei of the SOC, namely LSO, MSO and MNTB. In this study, the investigation addressed the potential relation of the gerbil SPN to either sound localization or temporal processing. The two basic findings were: Firstly, almost half of the SPN neurons showed signs of binaural interactions, although IID and ITD functions of binaural SPN neurons turned out to be shallow and ambiguous. Binaural processing as it occurs in MSO or LSO neurons can, therefore, be excluded as a function of SPN. However, binaural interactions might modulate SPN responses to complex sounds.

Secondly, SPN neurons respond to pure tones with a variety of discharge patterns dominated by sustained and phasic ON discharges. Overall, the temporal acuity of cells with ON responses turned out to be superior compared to sustained responders and ON responders showed sharper filter characteristics for SAM stimuli. Cells with sustained responses to pure tones showed weaker temporal acuity although some neurons showed some phase-locking to SAM stimuli presented with high modulation frequencies. These cells might provide a more diffuse inhibition to their targets, more likely to be of a modulatory nature than involved in precise temporal processing. Hence, SPN consist of at least two distinct groups of neurons, a finding that is in line with the different sources of excitatory inputs. Iontophoretic application of glycine or its antagonist strychnine indicated a major role of inhibitory inputs in creating responses of SPN neurons. This result is supported by the massive occurrence of gephyrin and glycine-receptors on SPN cell membranes which is in line with earlier findings of strong glycinergic and GABAergic inputs to guinea-pig SPN neurons (Helfert et al. 1992).

5.2.1 *Temporal processing*

Because SPN neurons receive substantial inputs from ventral cochlear nucleus (VCN) octopus and multipolar/stellate cells as well as inhibitory projections from the MNTB

(Friauf and Ostwald 1988), one hypothesis tested was if those neurons are involved in processing of temporal aspects of sound. Octopus cells, for instance, have a very low input resistance (Golding et al. 1999, Oertel et al. 2000) and very short time constants (Gardner et al. 1999), resulting in sharp onset responses with only one spike per pure tone stimulation (Golding et al. 1995). In the octopus cell region, onset neurons are able to accurately phase-lock to the cyclic envelope of SAM stimuli at rates of roughly up to 800 Hz (Rhode et al. 1983ab, Rhode and Greenberg 1994). A significant proportion of SPN cells shows an ON response that resembles PVCN octopus cell inputs in respect to the low jitter, when the rather long stimulus rise-fall time (5ms) used in the present study is taken into account. Additionally, the ability of this group of SPN cells to phase-lock to SAM stimuli is in line with octopus cell inputs (Rhode and Greenberg 1994).

PVCN inputs from multipolar/stellate cells would also be well suited for precise temporal processing (Ferragamo et al. 1998, Gardner et al. 1999). For PVCN multipolar cells, regular chopping responses to pure tones and SAM stimuli are reported in several mammals, including gerbils (Ferragamo et al. 1998, Frisina et al. 1990). However, only few neurons were classified as “chopper” and, compared to VCN neurons, they showed a rather weak regularity in their inter-spike interval.

An inhibitory input that indicates precise temporal processing in SPN neurons derives from glycinergic MNTB principal cells (Kuwabara et al. 1991, Sommer et al. 1993), matched by a strong presence of gephyrine and glycine-receptors on the cell membranes of gerbil SPN cells. MNTB cells receive their input from VCN bushy cells that accurately follow the temporal structure of sounds (Joris et al. 1994a) and convey this information via the calyx of Held onto MNTB cells (Brew and Forsythe 1995, Taschenberger and von Gersdorff 2000). As a consequence, MNTB cells also reliably convey the temporal structure of their inputs (Gardner et al. 1999, Smith et al. 1998). Indeed, glycinergic inhibition deriving from MNTB has been shown to participate in precise temporal filtering in bat MSO neurons. Combined with well timed excitatory inputs it creates precise ON or OFF responses and participates in the creation of precise filter properties for the temporal structure of sounds, including SAM (Grothe 1994, Grothe et al. 1997, Grothe et al. 2001). Similarly, OFF responders in the medial region of the rabbit SOC show very precise filter properties for SAM stimuli (Kuwada and Batra 1999). Moreover, in the rabbit and the bat SOC, these neurons show the highest vector strength in response to SAM stimuli (Kuwada and Batra 1999, Grothe et al. 2001). However, within

the present sample of SPN neurons only three units showed OFF discharges and these neurons did not phase-lock to SAM stimuli at all.

Interestingly, this is in sharp contrast to a remarkably uniform population of neurons recently described in the rat SPN. There, almost all neurons exhibited monaurally evoked OFF responses with sharp low-pass filtering (Kulesza et al. 2002). Moreover, in the gerbil SPN the blockade of glycinergic inhibition did not change the response properties to pure tones as described for bat MSO cells (Grothe 1994). Nevertheless, glycinergic inhibition seems to play a role in temporal processing. On the one hand an increased selectivity of coincident inputs was observed, when glycine was present, on the other hand, blocking glycinergic inhibition allowed some cells to respond to much higher modulation frequencies with a phase-locked response.

Differences between this and other studies concerning, e.g., the homogeneity of cell types or the abundant existence of OFF cells in the rat SPN might be due to different recording electrodes or anesthesia. The possibility that a specific population of cells with higher temporal precision has been missed can not be excluded. However, using identical recording procedures and often within the same electrode penetrations, neurons from neurons in neighboring structures (e.g. MSO) were recorded and those display an extreme temporal resolution in the microsecond range (compare findings in the MSO in the present study) and phase-locking OFF neurons outside the SPN. Also, the uniformity in the rat described by Kulesza and colleagues (2002) somewhat contradicts the anatomical diversity of SPN neurons and the fact that different CN cell populations project to SPN neurons (Schofield 1991, Schofield and Cant 1992, Schofield 1995, Schofield and Cant 1999). For instance, pure onset cells in the rat CN were described to project to the SPN (Friauf and Ostwald 1988). Moreover, Finlayson and Adam (1997) have demonstrated a variety of responses in the rat SPN, most commonly sustained (primary-like) and ON type, i.e., a pattern of cell types much like the gerbil SPN. Again, the fact that no OFF discharges at all were observed in Finlayson's study on rats gives rise to speculation as to what extent the selection of recording electrodes biases the neuron types recorded. Still, species-specific variation in the physiology of the SPN could be expected between the rat and the gerbil (Saldana and Berrebi 2000). For instance, the presence of cholinergic cells indicates that the gerbil SPN is part of the olivocochlear system. However, in rats no such cells are described (Aschoff et al. 1988, Osen et al. 1984, Vetter and Mugnaini 1990, Vetter et al. 1991, Vetter and Mugnaini 1992, Vetter et al. 1993, White and Warr 1983). A high potential for species-specific evolution of the

SPN is emphasized by findings in another mammal such as the mustached bat, *Pteronotus parnellii*. Here, the SPN might be partially merged with the MSO (Vater 1995).

Therefore, species-specific differences in the general function of the SPN and in the combination of subsets of response properties might well reflect evolutionary adaptations. This is not surprising since the medial region of the SOC has been shown to be, together with the ventral region of the lateral lemniscus, the region of the ascending auditory system that displays the highest variability among mammals (Covey and Casseday 1995; Grothe 2000). So far one can only speculate whether, e.g., the adaptation to hear low frequencies as it occurred in several desert rodents (Rosowski et al. 1999) elicited a different function of SPN in gerbils compared to the SPN of rats.

5.2.2 *Binaural processing*

About 40% of SPN cells are influenced by binaural inputs, most of them by binaural excitation. Traditionally, E/E neurons are associated with ITD detection as demonstrated for MSO neurons (Goldberg and Brown 1969, Spitzer and Semple 1995, Yin and Chan 1990, this study). Since Finlayson and Adam (1997) predominantly observed E/E neurons in the rat SPN, the speculation about binaural processing and, in particular, sound localization in the SPN of the gerbil seems appropriate. One might think that IID coding in the LSO and ITD coding in the MSO should be sufficient and additional binaural processing not necessary. However, it has been shown that, although starting in the LSO, IID sensitivity of many IC neurons is modified by inputs from the dorsal nucleus of the lateral lemniscus (Li and Kelly 1992) and a *de novo* IID sensitivity is created in other IC neurons (Park and Pollak 1994). Similarly, ITD functions of many IC neurons do not simply reflect single MSO inputs (McAlpine et al. 1998), ITD tuning gets sharper in the ascending auditory system (Fitzpatrick et al. 1997), and there is sensitivity to dynamic stimuli not seen in the MSO (Spitzer and Semple 1993). Hence, it seems feasible to assume that binaural cells other than those of MSO and LSO might considerably contribute to binaural characteristics of IC neurons.

The gerbil has evolved good low frequency hearing to match the requirements of the desert biotope and therefore has to use ITDs of low frequency sounds. The biased distribution of BFs in the gerbil SPN indeed emphasizes the relevance of low frequency hearing in this animal. Spitzer and Semple (1995) recorded four ITD-sensitive low frequency neurons anatomically confirmed to be in the SPN of the gerbil, and Batra and

colleagues (1997a) described ITD sensitive cells in the medial portion of the SOC that might well include SPN. Yet, the sample of 16 low frequency neurons included only 1 unit that exhibited phase-locking to pure tones, and none of the binaural cells exhibited a significant ITD-sensitivity. Addressing the differences in the present recordings, it is noteworthy that firstly, the entire partition of ITD sensitive SPN neurons in the sample of Spitzer and Semple is recorded at the lateral margin of the SPN, in close vicinity to LSO or MSO. Secondly, different electrode types were in use in the two studies.

5.2.3 *Tonotopy and cell subsets*

The SPN shares the tonotopic order of its principal input regions (Friauf 1992, Saldana and Berrebi 2000, Thompson and Thompson 1991), which is anatomically reflected by the flattened dendritic trees of SPN neurons, aligned to the rostral-caudal axis of the nucleus.

The monotonic rate-level functions and v-shaped tuning curves that were found to be typical for SPN neurons, largely resemble characteristics of their CN inputs. The distribution of best frequencies of SPN neurons in the gerbil is clearly biased to frequencies below 6 kHz. Since reconstruction of recording sites does not indicate any bias to a specific region within the SPN this bias seems to be real and spectral integration might therefore be ruled out as a major function of the gerbil SPN.

One might consider neurons with ON and sustained discharges as two different populations and the physiological results presented in this study support such an assumption. Subpopulations of SPN cells have been demonstrated to differ in either morphology, projections or input sources (Schofield 1991, Schofield and Cant 1992, Schofield 1995, Schofield and Cant 1999). In particular, olivocochlear projections originate within a subset of cells that was considered to form a distinct population among the SPN neurons. Typical SPN responses (ON) displayed short adaptation time constants and a non-significant overall trend to long time constants was apparent in the recovery from adaptation (Finlayson and Adam 1997). This characteristic might match the olivocochlear projections of the SPN and give rise to a quick feedback adjustment of auditory processing at lower levels when new stimulus configurations are detected.

- Adams, J.C. Technical considerations on the use of horseradish peroxidase as a neuronal marker. *Neurosci* 2, 141-145, 1977.
- AgmonSnir, H., Carr, C.E., and Rinzel, J. The role of dendrites in auditory coincidence detection. *Nature* 393: 268-272, 1998.
- Aschoff, A., Muller M., and Ott, H. Origin of the cochlea efferents in some gerbil species. *Exp Brain Res* 71: 252-261, 1988a.
- Banks, M. I. and Smith, P. H. Intracellular recordings from neurobiotin-labeled cells in brain slices of the rat medial nucleus of the trapezoid body. *J Neurosci* 12: 2819-2837, 1992.
- Bartheld, C.S., Code, R.A., and Rubel, E.W. GABAergic Neurons in Brainstem Auditory Nuclei of the Chick: Distribution, Morphology, and Connectivity. *J Comp Neurol* 287: 470-483, 1989.
- Batra, R., Kuwada, S., and Fitzpatrick, D.C. Sensitivity to interaural temporal disparities of low- and high- frequency neurons in the superior olivary complex. i. heterogeneity of responses. *J Neurophys* 78: 1222-1236, 1997a.
- Batra, R., Kuwada, S., and Fitzpatrick, D.C. Sensitivity to interaural temporal disparities of low- and high- frequency neurons in the superior olivary complex. ii. coincidence detection. *J Neurophys* 78: 1237-1247, 1997b.
- Batschelet, E. Circular statistics in Biology. London, Academic Press. 1991.
- Beckius, G.E., Batra, R., and Oliver, D.L. Axons from anteroventral cochlear nucleus that terminate in medial superior olive of cat: Observations related to delay lines. *J Neurosci* 19: 3146-3161, 1999.
- Behrend O, Brand A, Kapfer C and Grothe B, Auditory response properties in the superior paraolivary nucleus of the gerbil *J Neurophysiol* 87: 2915-2929, 2002
- Blauert, J. Räumliches Hören. Stuttgart, Hirzel. 1983.
- Brand, A., Behrend, O., Marquardt, T., McAlpine, D., and Grothe, B. Precise inhibition is essential for microsecond interaural time difference coding. *Nature* 417: 543-547, 2002.
- Brew, H.M. and Forsythe, I.D. Two voltage-dependent K⁺ conductances with complementary functions in postsynaptic integration at a central auditory synapse. *J Neurosci* 15: 8011-8022, 1995.

- Brown, M.C. Morphology and response properties of single olivocochlear fibers in guinea pig. *Hear Res* 40: 93-109, 1989.
- Bruckner, S. and Hyson, R.L. Effect of GABA on the processing of interaural time differences in nucleus laminaris neurons in the chick. *Eur J Neurosci* 10: 3438-3450, 1998.
- Brughera, A.R., Stutman, E.R., Carney, L.H., and Colburn, H.S. A Model with Excitation and Inhibition for Cells in the Medial Superior Olive. *Audit Neurosci* 2: 219-233, 1996.
- Caird, D. and Klinke, R. Processing of binaural stimuli by cat superior olivary complex neurons. *Exp Brain Res* 52: 385-399, 1983.
- Calford, M.B., Moore, D.R., and Hutchings, M.E. Central and peripheral contributions to coding of acoustic space by neurons in inferior colliculus of cat. *J Neurophys* 55: 587-603, 1986.
- Cant, N.B. Projections to the lateral and medial superior olivary nuclei from the spherical and globular bushy cells of the anteroventral cochlear nucleus. In Altschuler, R. A., Bobbin, R. P., Clopton, B. M., and Hoffman, D. W. eds. *Neurobiology of hearing: The central auditory system*. New York, Raven Press, pp. 99-119, 1991.
- Cant, N.B. and Hyson, R.L. Projections from the lateral nucleus of the trapezoid body to the medial superior olivary nucleus in the gerbil. *Hear Res* 58: 26-34, 1992.
- Carr, C.E. and Boudreau, R.E. Organization of the nucleus magnocellularis and the nucleus laminaris in the barn owl: encoding and measuring interaural time differences. *J Comp Neurol* 334: 337-355, 1993.
- Carr, C.E. and Code, R.A. The Central Auditory System of Reptiles and Birds. In Dooling, R. J., Fay, R. R., and Popper, A. N. eds. *Comparative Hearing: Birds and Reptiles*. New York, Springer, pp. 197-248, 2000.
- Carr, C.E., Fujita, I., and Konishi, M. Distribution of GABAergic neurons and terminals in the auditory system of the barn owl. *J Comp Neurol* 286: 190-207, 1989.
- Carr, C.E. and Konishi, M. Axonal delay lines for time measurement in the owl's brainstem. *PNAS* 85: 8311-8315, 1988.
- Carr, C.E. and Konishi, M. A circuit for detection of interaural time differences in the brain stem of the barn owl. *J Neurosci* 10: 3227-3246, 1990.
- Clark, G.M. Vesicle shape versus type of synapse in the nerve endings of the cat medial superior olive. *Brain Res* 15: 548-551, 1969.

- Clark, G.M. and Dunlop, C.W. Field potentials in the cat medial superior olivary nucleus. *Exp Neurol* 20: 31-42, 1968.
- Colburn, H.S., Han, Y.A., and Culotta, C.P. Coincidence model of MSO responses. *Hear Res* 49: 335-346, 1990.
- Covey, E. and Casseday, J.H. The monaural nuclei of the lateral lemniscus in an echolocating bat: parallel pathways for analyzing temporal features of sound. *J Neurosci* 11: 3456-3470, 1991.
- Covey, E. and Casseday, J.H. The lower brainstem auditory pathway. In Popper, A. N. and Fay, R. R. eds. *Hearing by bats*. New York, Springer-Verlag, pp. 235-295, 1995.
- Covey, E., Vater, M., and Casseday, J.H. Binaural properties of single units in the superior olivary complex of the mustached bat. *J Neurophys* 66: 1080-1094, 1991.
- Crow, G., Rupert, A.L., and Moushegian, G. Phase locking in monaural and binaural medullary neurons: implications for binaural phenomena. *J Acoust Soc Am* 64: 493-501, 1978.
- Fedderson, W.E., Sandel, T.T., Teas, D.C., and Jeffress, L.A. Localization of high frequency tones. *J Acoust Soc Am* 29:988-991, 1957.
- Ferragamo, M.J., Golding, N.L., and Oertel, D. Synaptic inputs to stellate cells in the ventral cochlear nucleus. *J Neurophys* 79: 51-63, 1998.
- Finlayson, P.G. and Adam, T.J. Excitatory and inhibitory response adaptation in the superior olive complex affects binaural acoustic processing. *Hear Res* 103: 1-18, 1997.
- Fitzpatrick, D.C., Batra, R., Stanford T.R., and Kuwada, S. A neuronal population code for sound localization. *Nature* 388: 871-874, 1997.
- Fitzpatrick, D.C., Kuwada, S., and Batra, R. Neural sensitivity to interaural time differences: beyond the Jeffress model. *J Neurosci* 20: 1605-1615, 2000.
- Fitzpatrick, D.C., Kuwada, S., and Batra, R. Transformations in processing interaural time differences between the superior olivary complex and inferior colliculus: beyond the Jeffress model. *Hear Res* 168: 79-89, 2002.
- Fleischer, G. Evolutionary Principles of the Mammalian Middle Ear. *Advances in Anatomy, Embryology and Cell Biology* 55: 7-60, 1978.
- Friauf, E. Tonal Order in the Adult and Developing Auditory System of the Rat as shown by c-fos Immunocytochemistry. *Eur J Neurosci* 4: 798-812, 1992.

- Friauf, E. and Ostwald, J. Divergent projections of physiologically characterized rat ventral cochlear nucleus neurons as shown by intra-axonal injection of horseradish peroxidase. *Exp Brain Res* 73: 263-284, 1988.
- Frisina, R.D., Smith, R.L., and Chamberlain, S.C. Encoding of amplitude modulation in the gerbil cochlear nucleus: I. A hierarchy of enhancement. *Hear Res* 44: 99-122, 1990.
- Frost, S.B. and Masterton, R.B. Hearing in primitive mammals: *Monodelphis domestica* and *Marmosa elegans*. *Hear Res* 76: 67-72, 1994.
- Fujita, I. and Konishi, M. The role of GABAergic inhibition in processing of interaural time difference in the owl's auditory system. *J Neurosci* 11: 722-739, 1991.
- Funabiki, K., Koyano, K., and Ohmori, H. The role of GABAergic inputs for coincidence detection in the neurones of nucleus laminaris of the chick. *J Physiol Lond* 508: 851-869, 1998.
- Galambos, R. and Davis, H. The response of single auditory-nerve fibres to acoustic stimulation. *J Neurophys* 6: 39-57, 1943.
- Galambos, R., Schwartzkopff, J., and Rupert, A. Microelectrode study of superior olivary nuclei. *Am J Physiol* 197: 527-536, 1959.
- Gardner, S.M., Trussell, L.O., and Oertel, D. Time course and permeation of synaptic AMPA receptors in cochlear nuclear neurons correlate with input. *J Neurosci* 19: 8721-8729, 1999.
- Goldberg, J.M. and Brown, P.B. Functional organization of the dog superior olivary complex: an anatomical and electrophysiological study. *J Neurophys* 31: 639-656, 1968.
- Goldberg, J.M. and Brown, P.B. Response of binaural neurons of dog superior olivary complex to dichotic tonal stimuli: some physiological mechanisms of sound localization. *J Neurophys* 32: 613-636, 1969.
- Golding, N.L., Ferragamo, M.J., and Oertel, D. Role of intrinsic conductances underlying responses to transients in octopus cells of the cochlear nucleus. *J Neurosci* 19: 2897-2905, 1999.
- Golding, N.L., Robertson, D., and Oertel, D. Recordings from slices indicate that octopus cells of the cochlear nucleus detect coincident firing of auditory nerve fibers with temporal precision. *J Neurosci* 15: 3138-3153, 1995.
- Grothe, B. Interaction of excitation and inhibition in processing of pure tone and amplitude-modulated stimuli in the medial superior olive of the mustached bat. *J Neurophys* 71: 706-721, 1994.

-
- Grothe, B. The evolution of temporal processing in the medial superior olive, an auditory brainstem structure. *Prog Neurobiol* 61: 581-610, 2000.
- Grothe, B., Covey, E., and Casseday, J.H. The medial superior olive in the big brown bat: neuronal response to pure tones, amplitude modulations, and pulse trains. *J Neurophys* 86: 2219-2230, 2001.
- Grothe, B. and Neuweiler, G. The function of the medial superior olive in small mammals: temporal receptive fields in auditory analysis. *J Comp Physiol A* 186: 413-423, 2000.
- Grothe, B. and Park, T.J. Sensitivity to interaural time differences in the medial superior olive of a small mammal, the Mexican free-tailed bat. *J Neurosci* 18: 6608-6622, 1998.
- Grothe, B., Park, T.J., and Schuller, G. Medial superior olive in the free-tailed bat: response to pure tones and amplitude-modulated tones. *J Neurophys* 77: 1553-1565, 1997.
- Grothe, B. and Sanes, D.H. Bilateral inhibition by glycinergic afferents in the medial superior olive. *J Neurophys* 69: 1192-1196, 1993.
- Grothe, B. and Sanes, D.H. Synaptic inhibition influences the temporal coding properties of medial superior olivary neurons: an in vitro study. *J Neurosci* 14: 1701-1709, 1994.
- Grothe, B., Schweizer, H., Pollak, G.D., Schuller, G., and Rosemann, C. Anatomy and projection patterns of the superior olivary complex in the Mexican free-tailed bat, *Tadarida brasiliensis mexicana*. *J Comp Neurol* 343: 630-646, 1994.
- Grothe, B., Vater, M., Casseday, J.H., and Covey, E. Monaural interaction of excitation and inhibition in the medial superior olive of the mustached bat: an adaptation for biosonar. *PNAS* 89: 5108-5112, 1992.
- Guinan, J.J.Jr., Guinan, S.S., and Norris, B.E. Single Auditory Units in the Superior Olivary Complex I: Responses to Sounds and Classifications Based on Physiological Properties. *Intern J Neurosci* 4: 101-120, 1972a.
- Guinan, J.J.Jr., Norris, B.E., and Guinan, S.S. Single Auditory Units in the Superior Olivary Complex II: Locations of Unit Categories and Tonotopic Organization. *Intern J Neurosci* 4: 147-166, 1972b.
- Hafer, E.R. and DeMaio J. Difference threshold for interaural delay. *J Acoust Soc Am* 57: 181-187, 1975.

- Harnischfeger, G., Neuweiler, G., and Schlegel, P. Interaural time and intensity coding in superior olivary complex and inferior colliculus of the echolocating bat *Molossus ater*. *J Neurophys* 53: 89-109, 1985.
- Harrison, J.M. and Feldman, M.L. Anatomical aspects of the cochlear nucleus and superior olivary complex. *Contrib Sens Physiol* 4: 95-142, 1970.
- Harrison, J.M. and Irving, R. Visual and nonvisual auditory systems in mammals. Anatomical evidence indicates two kinds of auditory pathways and suggests two kinds of hearing in mammals. *Science* 154: 738-743, 1966.
- Harrison, J.M. and Warr, W.B. A Study of the Cochlear Nuclei and Ascending Auditory Pathways of the Medulla. *J Comp Neurol* 119: 341-380, 1962.
- Harvey, D.C. and Caspary, D.M. A simple technique for constructing 'piggy-back' multibarrel microelectrodes. *Electroencephalogr Clin Neurophys* 48: 249-251, 1980.
- Heffner, H.E., Heffner, R.S., Contos, C., and Ott, T. Audiogram of the hooded Norway rat. *Hear Res* 62: 247, 1994a.
- Heffner, R.S. and Heffner, H.E. Hearing range of the domestic cat. *Hear Res* 19: 85-88, 1985.
- Heffner, R.S. and Heffner, H.E. Sound localization and use of binaural cues by the gerbil (*Meriones unguiculatus*). *Behav Neurosci* 102: 422-428, 1988.
- Heffner, R.S. and Heffner, H.E. Evolution of sound localization in mammals. In Webster, D. B., Fay, R. R., and Popper, A. N. eds. The evolutionary biology of hearing. New York, Springer, pp. 691-714, 1992.
- Heffner, R.S., Heffner, H. E., Kearns, D., Vogel, J., and Koay, G. Sound localization in chinchillas. I: Left/right discriminations. *Hear Res* 80: 247-257, 1994b.
- Helfert, R.H., Bonneau, J.M., Wenthold, R.J., and Altschuler, R.A. GABA and glycine immunoreactivity in the guinea pig superior olivary complex [published erratum appears in *Brain Res* 1990 Feb 12;509(1):180]. *Brain Res* 501: 269-286, 1989.
- Helfert, R.H., Juiz, J.M., Bledsoe, S.C., Bonneau, J.M., Wenthold, R.J., and Altschuler, R.A. Patterns of glutamate, glycine, and GABA immunolabeling in four synaptic terminal classes in the lateral superior olive of the guinea pig. *J Comp Neurol* 323: 305-325, 1992.
- Henning, G.B. Detectability of interaural delay in high frequency complex waveforms. *J Acoust Soc Am* 55: 84-90, 1974.
- Houtgast, T. and Aoki, S. Stimulus-onset dominance in the perception of binaural information. *Hear Res* 72: 29-36, 1994.

- Huffman, R.F., Argeles, P.C., and Covey, E. Processing of sinusoidally amplitude modulated signals in the nuclei of the lateral lemniscus of the big brown bat, *Eptesicus fuscus*. *Hear Res* 126: 181-200, 1998.
- Hyson, R.L., Reyes, A.D., and Rubel, E.W. A depolarizing inhibitory response to GABA in brainstem auditory neurons of the chick. *Brain Res* 677: 117-126, 1995.
- Inbody, S.B. and Feng, A.S. Binaural response characteristics of single neurons in the medial superior olivary nucleus of the albino rat. *Brain Res* 210: 361-366, 1981.
- Irving, R. and Harrison, J.M. The superior olivary complex and audition: a comparative study. *J Comp Neurol* 130: 77-86, 1967.
- Jeffress, L.A. A place theory of sound localization. *J Comp Physiol Psychol* 41: 35-39, 1948.
- Joris, P.X. Envelope coding in the lateral superior olive. ii. characteristic delays and comparison with responses in the medial superior olive. *J Neurophys* 76: 2137-2156, 1996.
- Joris, P.X., Carney, L.H., Smith, P.H., and Yin, T.C. Enhancement of neural synchronization in the anteroventral cochlear nucleus. I. Responses to tones at the characteristic frequency. *J Neurophys* 71: 1022-1036, 1994a.
- Joris, P.X., Smith, P.H., and Yin, T.C. Enhancement of neural synchronization in the anteroventral cochlear nucleus. II. Responses in the tuning curve tail. 71: 1037-1051, 1994b.
- Joris, P.X. and Yin, T.C. Envelope coding in the lateral superior olive. i. sensitivity to interaural time differences [published errata appear in *J Neurophysiol* 1995 may;73(5):following table of contents and 1995 jun;73(6):following table of contents]. *J Neurophys* 73: 1043-1062, 1995.
- Kapfer, C., Seidl, A.H., Schweizer, H., and Grothe, B. Experience-dependent refinement of inhibitory inputs to auditory coincidence-detector neurons. *Nat Neurosci* 5: 247-253, 2002.
- Kil, J., Kageyama, G.H., Semple, M.N., and Kitzes, L.M. Development of ventral cochlear nucleus projections to the superior olivary complex in gerbil. *J Comp Neurol* 353: 317-340, 1995.
- Kiss, A. and Majorossy, K. Neuron morphology and synaptic architecture in the medial superior olivary nucleus. Light- and electron microscope studies in the cat. *Exp Brain Res* 52: 315-327, 1983.
- Klump, G.M. Sound Localization in birds. In Dooling, R.J., Fay, R.R., and Popper, A.N. eds. *Comparative Hearing: Birds and Reptiles*. New York, Springer, pp. 249-307, 2000.

- Knudsen, E.I. and Konishi, M. Center-surround organization of auditory receptive fields in the owl. *Science* 202: 778-780, 1978.
- Kopp-Scheinflug C., Lippe, W.R., Dorrscheidt, G.J., and Rubsamen, R. The Medial Nucleus of the Trapezoid Body in the Gerbil Is More Than a Relay: Comparison of Pre- and Postsynaptic Activity. *JARO Online first* 2002.
- Koppl, C. Phase locking to high frequencies in the auditory nerve and cochlear nucleus magnocellularis of the barn owl, *Tyto alba*. *J Neurosci* 17: 3312-3321, 1997.
- Kudo, M., Nakamura, Y., Tokuno, H., and Kitao, Y. Auditory brainstem in the mole (*mogeta*): nuclear configurations and the projections to the inferior colliculus. *J Comp Neurol* 298: 400-412, 1990.
- Kulesza, R.J., Spirou, G.A., and Berrebi, A.S. Response Properties of Neurons in the Superior Paraolivary Nucleus of the Rat. Abstract Viewer, Association of Research in Otorhinolaryngology # 422. 2002.
- Kuwabara, N., DiCaprio, R.A., and Zook, J.M. Afferents to the medial nucleus of the trapezoid body and their collateral projections. *J Comp Neurol* 314: 684-706, 1991.
- Kuwabara, N. and Zook, J.M. Projections to the medial superior olive from the medial and lateral nuclei of the trapezoid body in rodents and bats. *J Comp Neurol* 324: 522-538, 1992.
- Kuwada, S. and Batra, R. Coding of sound envelopes by inhibitory rebound in neurons of the superior olivary complex in the unanesthetized rabbit. *J Neurosci* 19: 2273-2287, 1999.
- Lachica, E.A., Rubsamen, R., and Rubel, E.W. GABAergic terminals in nucleus magnocellularis and laminaris originate from the superior olivary nucleus. *J Comp Neurol* 348: 403-418, 1994.
- Langford, T.L. Responses elicited from medial superior olivary neurons by stimuli associated with binaural masking and unmasking. *Hear Res* 15: 39-50, 1984.
- Lay, D.M. Differential predation on gerbils (*Meriones*) by the little owl, *Athene-Brama*. *J Mammalogy* 55: 608-614, 1974.
- Li, L. and Kelly, J.B. Inhibitory influence of the dorsal nucleus of the lateral lemniscus on binaural responses in the rat's inferior colliculus. *J Neurosci* 12: 4530-4539, 1992.
- Litovsky, R.Y. and Yin, T.C. Physiological studies of the precedence effect in the inferior colliculus of the cat. I. Correlates of psychophysics. *J Neurophys* 80: 1285-1301, 1998.

- Loskota, W.J., Lomax, P., and Verity, M.A. A Stereotaxic Atlas of the Mongolian Gerbil Brain. Ann Arbor, Ann Arbor Science Publishers, 1974.
- Masterton, R.B. and Diamond, I.T. Medial superior olive and sound localization. *Science* 155: 1696-1697, 1967.
- Masterton, R.B., Thompson, G.C., Bechtold, J.K., and RoBards, M.J. Neuroanatomical basis of binaural phase-difference analysis for sound localization: a comparative study. *J Comp Physiol Psychol* 89: 379-386, 1975.
- May, B.J. Role of the dorsal cochlear nucleus in the sound localization behavior of cats. *Hear Res* 148: 74-87, 2000.
- McAlpine, D., Jiang, D., and Palmer, A.R. A neural code for low-frequency sound localization in mammals. *Nat Neurosci* 4: 396-401, 2001.
- McAlpine, D., Jiang, D., Shackleton, T.M., and Palmer, A.R. Convergent input from brainstem coincidence detectors onto delay-sensitive neurons in the inferior colliculus. *J Neurosci* 18: 6026-6039, 1998.
- McFadden, D. and Pasanen, E.G. Lateralization of high-frequencies based on interaural time differences. *J Acoust Soc Am* 59: 634-639, 1976.
- Mills, A.W. On the minimum audible angle. *J Acoust Soc Am* 30: 237-246, 1958.
- Moller, A.R. Coding of amplitude and frequency modulated sound in the cochlear nucleus of the rat. *Acta Physiol Scand* 86: 233-117, 1972.
- Moller, A.R. Responses of units in the cochlear nucleus to sinusoidally amplitude modulated tones. *Exp Neurol* 45: 104-117, 1976.
- Monsivais, P. and Rubel, E.W. Accommodation enhances depolarizing inhibition in central neurons. *J Neurosci* 21: 7823-7830, 2001.
- Monsivais, P., Yang, L., and Rubel, E.W. GABAergic inhibition in nucleus magnocellularis: implications for phase locking in the avian auditory brainstem. *J Neurosci* 20: 2954-2963, 2000.
- Moore, D.R. Auditory brainstem of the ferret: sources of projections to the inferior colliculus. *J Comp Neurol* 269: 342-354, 1988.
- Moushegian, G., Rupert, A., and Whitcomb, M.A. Medial superior-olivary-unit response patterns to monaural and binaural clicks. *J Acoust Soc Am* 36: 196-202, 1964.
- Moushegian, G., Rupert, A.L., and Gidda, J.S. Functional characteristics of superior olivary neurons to binaural stimuli. *J Neurophys* 38: 1037-1048, 1975.

- Moushegian, G., Rupert, A.L., and Langford, T.L. Stimulus coding by medial superior olivary neurons. *J Neurophys* 30, 1239-1261, 1967.
- Neuweiler, G. The biology of bats, Oxford, Oxford University Press, 2000.
- Nordeen, K.W., Killackey, H.P., and Kitzes, L.M. Ascending auditory projections to the inferior colliculus in the adult gerbil, *Meriones unguiculatus*. *J Comp Neurol* 214: 131-143, 1983.
- Oertel, D. Synaptic responses and electrical properties of cells in brain slices of the mouse anteroventral cochlear nucleus. *J Neurosci* 3: 2043-2053, 1983.
- Oertel, D., Bal, R., Gardner, S.M., Smith, P.H., and Joris, P.X. Detection of synchrony in the activity of auditory nerve fibers by octopus cells of the mammalian cochlear nucleus. *PNAS* 97: 11773-11779, 2000.
- Ollo, C. and Schwartz, I.R. The superior olivary complex in C57BL/6 mice. *Am J Anat* 155: 349-373, 1979.
- Osen, K.K. Cytoarchitecture of the cochlear nuclei in the cat. *J Comp Neurol* 136: 453-484, 1969.
- Osen, K.K., Mugnaini, E., Dahl, A.L., and Christiansen, A.H. Histochemical localization of acetylcholinesterase in the cochlear and superior olivary nuclei. A reappraisal with emphasis on the cochlear granule cell system. *Arch Ital Biol* 122: 169-212, 1984.
- Overholt, E., Rubel, E.W., and Hyson, R.L. A circuit for coding interaural time differences in the chick brainstem. *J Neurosci* 12: 1698-1708, 1992.
- Palmer, A.R. and Russell, I.J. Phase-locking in the cochlear nerve of the guinea-pig and its relation to the receptor potential of inner hair-cells. *Hear Res* 24: 1-15, 1986.
- Paolini, A.G., FitzGerald, J.V., Burkitt, A.N., and Clark, G.M. Temporal processing from the auditory nerve to the medial nucleus of the trapezoid body in the rat. *Hear Res* 159: 101-116, 2001.
- Park, T.J. and Pollak, G.D. Azimuthal receptive fields are shaped by gabaergic inhibition in the inferior colliculus of the mustache bat. *J Neurophys* 72: 1080-1102, 1994.
- Parks, T.N. and Rubel, E.W. Organization and development of brain stem auditory nuclei of the chicken: organization of projections from n. magnocellularis to n. laminaris. *J Comp Neurol* 164: 435-448, 1975.
- Pena, J.L., Viète, S., Albeck, Y., and Konishi, M. Tolerance to sound intensity of binaural coincidence detection in the nucleus laminaris of the owl. *J Neurosci* 16: 7046-7054, 1996.

- Perkins, R.E. An electron microscopic study of synaptic organization in the medial superior olive of normal and experimental chinchillas. *J Comp Neurol* 148: 387-415, 1973.
- Peyret, D., Geffard, M., and Aran, J.M. GABA immunoreactivity in the primary nuclei of the auditory central nervous system. *Hear Res* 23: 115-121, 1986.
- Quine, D. B. and Konishi, M. Absolute frequency discrimination in the barn owl. *J Comp Physiol A* 93: 347-360, 1974.
- Ramon y Cajal, S. *Histologie du systeme nerveux de l'homme et des vertebrates*. Paris, Maloine. 1907.
- Rayleigh, L.J.W.S.3.B.R. On the amplitude of sound waves. *Proceedings of the Royal Society* 26: 1877.
- Rayleigh, L.J.W.S.3.B.R. On our perception of sound direction. *Philos Mag* 13: 214-232, 1907.
- Rhode, W.S. and Greenberg, S. Physiology of the Cochlear Nuclei. In Popper, A.N. and Fay, R.R. eds. *The Mammalian Auditory Pathway: Neurophysiology*. New York, Springer, pp. 94-152, 1991.
- Rhode, W.S. and Greenberg, S. Encoding of amplitude modulation in the cochlear nucleus of the cat. *J Neurophys* 71: 1797-1825, 1994.
- Rhode, W.S., Oertel, D., and Smith, P.H. Physiological response properties of cells labeled intracellularly with horseradish peroxidase in cat ventral cochlear nucleus. *J Comp Neurol* 213: 448-463, 1983a.
- Rhode, W.S., Smith, P.H., and Oertel, D. Physiological response properties of cells labeled intracellularly with horseradish peroxidase in cat dorsal cochlear nucleus. *J Comp Neurol* 213: 426-447, 1983b.
- Rose, J.E., Brugge, J.F., Anderson, D.J., and Hind, J.E. Phase-locked response to low-frequency tones in single auditory nerve fibers of the squirrel monkey. *J Neurophys* 30: 769-793, 1967.
- Rose, J.E., Gross, N.B., Geisler, C.D., and Hind, J.E. Some neural mechanisms in the inferior colliculus of the cat which may be relevant to localization of a sound source. *J Neurophys* 29: 288-314, 1966.
- Rosowski, J.J. Hearing in transitional mammals. Predictions from the middle ear anatomy and hearing capabilities of extant mammals. In Webster, D.B., Fay, R.R., and Popper, A.N. eds. *The evolutionary biology of hearing*. New York, Springer-Verlag, pp. 615-632, 1992.

- Rosowski, J.J., Ravicz, M.E., Teoh, S.W., and Flandermeyer, D. Measurements of middle-ear function in the Mongolian gerbil, a specialized mammalian ear. *Audiology & Neuro-Otology* 4: 129-136, 1999.
- Rothman, J.S., Young, E.D., and Manis, P.B. Convergence of auditory nerve fibers onto bushy cells in the ventral cochlear nucleus: implications of a computational model. *J Neurophys* 70: 2562-2583, 1993.
- Rubel, E.W. and Parks, T.N. Organization and development of brain stem auditory nuclei of the chicken: tonotopic organization of n. magnocellularis and n. laminaris. *J Comp Neurol* 164: 411-433, 1975.
- Rupert, A., Moushegian, G., and Whitcomb, M.A. Superior-olivary response patterns to monaural and binaural clicks. *J Acoust Soc Am* 39: 1067-1076, 1966.
- Ryan, A. Hearing sensitivity of the mongolian gerbil, *Meriones unguiculatus*. *J Acoust Soc Am* 59: 1222-1226, 1976.
- Saint-Marie, R.L., Ostapoff, E.M., Morest, D.K., and Wenthold, R.J. Glycine-immunoreactive projection of the cat lateral superior olive: possible role in midbrain ear dominance. *J Comp Neurol* 279: 382-396, 1989.
- Saint Marie, R.L. and Baker, R.A. Neurotransmitter-specific uptake and retrograde transport of [3H]glycine from the inferior colliculus by ipsilateral projections of the superior olivary complex and nuclei of the lateral lemniscus. *Brain Res* 524: 244-253, 1990.
- Saldana, E. and Berrebi, A.S. Anisotropic organization of the rat superior paraolivary nucleus. *Anat Embryol* 202: 265-279, 2000.
- Schofield, B.R. Superior paraolivary nucleus in the pigmented guinea pig: separate classes of neurons project to the inferior colliculus and the cochlear nucleus. *J Comp Neurol* 312: 68-76, 1991.
- Schofield, B.R. Projections from the cochlear nucleus to the superior paraolivary nucleus in guinea pigs. *J Comp Neurol* 360: 135-149, 1995.
- Schofield, B.R. and Cant, N.B. Organization of the superior olivary complex in the guinea pig. I. cytoarchitecture, cytochrome oxidase histochemistry, and dendritic morphology. *J Comp Neurol* 314: 645-670, 1991.
- Schofield, B.R. and Cant, N.B. Organization of the superior olivary complex in the guinea pig: II. Patterns of projection from the periolivary nuclei to the inferior colliculus. *J Comp Neurol* 317: 438-455, 1992.

- Schofield, B.R. and Cant, N.B. Descending auditory pathways: Projections from the inferior colliculus contact superior olivary cells that project bilaterally to the cochlear nuclei. *J Comp Neurol* 409: 210-223, 1999.
- Schwartz, I.A. Dendritic arrangements in the cat medial superior olive. *Neuroscience* 2: 81-101, 1977.
- Schwartz, I.R. The superior olivary complex and lateral lemniscal nuclei. In Webster, D.B., Popper, A.N., and Fay, R.R. eds. *The Mammalian Auditory Pathway: Neuroanatomy*. New York, Springer pp. 117-167, 1992.
- Schweizer, H. The connections of the inferior colliculus and the organization of the brainstem auditory system in the greater horseshoe bat (*Rhinolophus ferrumequinum*). *J Comp Neurol* 201: 25-49, 1981.
- Shannon, R.V., Zeng, F.G., Kamath, V., Wygonski, J., and Ekelid, M. Speech recognition with primarily temporal cues. *Science* 270: 303-304, 1995.
- Skottun, B.C. Sound localization and neurons [letter; comment]. *Nature* 393: 531, 1998.
- Skottun, B.C., Shackleton, T.M., Arnott, R.H., and Palmer, A.R. The ability of inferior colliculus neurons to signal differences in interaural delay. *PNAS* 98: 14050-14054, 2001.
- Smith D.J. and Rubel, E.W. Organization and development of brain stem auditory nuclei of the chicken: dendritic gradients in nucleus laminaris. *J Comp Neurol* 186: 213-239, 1975.
- Smith, A.J., Owens, S., and Forsythe, I.D. Characterisation of inhibitory and excitatory postsynaptic currents of the rat medial superior olive. *J Physiol* 529: 681-698, 2000.
- Smith, P.H. Structural and functional differences distinguish principal from nonprincipal cells in the guinea pig MSO slice. *J Neurophys* 73: 1653-1667, 1995.
- Smith, P.H., Joris, P.X., Carney, L.H., and Yin, T.C. Projections of physiologically characterized globular bushy cell axons from the cochlear nucleus of the cat. *J Comp Neurol* 304: 387-407, 1991.
- Smith, P.H., Joris, P.X., and Yin, T.C. Projections of physiologically characterized spherical bushy cell axons from the cochlear nucleus of the cat: evidence for delay lines to the medial superior olive. *J Comp Neurol* 331: 245-260, 1993.
- Smith, P.H., Joris, P.X., and Yin, T.C. Anatomy and physiology of principal cells of the medial nucleus of the trapezoid body (MNTB) of the cat. *J Neurophys* 79: 3127-3142, 1998.

- Smith, P.H. and Rhode, W.S. Structural and functional properties distinguish two types of multipolar cells in the ventral cochlear nucleus. *J Comp Neurol* 282: 595-616, 1989.
- Smith, P.H. and Spirou, G.A. Cochlea to Cortex and Back. In Oertel, D., Fay, R.R., and Popper, A.N. eds. Integrative Functions in the Mammalian Auditory Pathway. New York, Springer, pp. 19-71, 2001.
- Sommer, I., Lingenhohl, K., and Friauf, E. Principal cells of the rat medial nucleus of the trapezoid body: an intracellular in vivo study of their physiology and morphology. *Exp Brain Res* 95: 223-239, 1993.
- Spirou, G.A., Rowland, K.C., and Berrebi, A.S. Ultrastructure of neurons and large synaptic terminals in the lateral nucleus of the trapezoid body of the cat. *J Comp Neurol* 398: 257-272, 1998.
- Spitzer, M.W. and Semple, M.N. Responses of inferior colliculus neurons to time-varying interaural phase disparity: effects of shifting the locus of virtual motion. *J Neurophys* 69: 1245-1263, 1993.
- Spitzer, M.W. and Semple, M.N. Neurons sensitive to interaural phase disparity in gerbil superior olive: diverse monaural and temporal response properties. *J Neurophys* 73: 1668-1690, 1995.
- Stillman R.D. Characteristic delay neurons in the inferior colliculus of the kangaroo rat. *Exp Neurol* 32: 432-440, 1971.
- Stotler, W.A. An experimental study of the cells and connections of the superior olivary complex of the cat. *J Comp Neurol* 98: 401-432, 1953.
- Sullivan, W.E. and Konishi, M. Segregation of stimulus phase and intensity coding in the cochlear nucleus of the barn owl. *J Neurosci* 4: 1787-1799, 1984.
- Sullivan, W.E. and Konishi, M. Neural map of interaural phase difference in the owl's brainstem. *PNAS* 83: 8400-8404, 1986.
- Svirskis G., Kotak, V. C., Sanes, D. H., and Rinzel, J. Enhancement of signal-to-noise ratio and phase locking for small inputs by a low threshold outward current in auditory neurons. *J Neurosci* 15: 1019-25, 2002.
- Taschenberger, H. and von Gersdorff, H. Fine-tuning an auditory synapse for speed and fidelity: developmental changes in presynaptic waveform, EPSC kinetics, and synaptic plasticity. *J Neurosci* 20: 9162-9173, 2000.
- Thompson, A.M. and Schofield, B.R. Afferent projections of the superior olivary complex. *Microsc Res Tech* 51: 330-354, 2000.

- Thompson, A.M. and Thompson, G.C. Projections from the posteroventral cochlear nucleus to the superior olivary complex in guinea pig: light and EM observations with the PHA-L method. *J Comp Neurol* 311: 495-508, 1991.
- Thompson, S. P. On the function of the two ears in the perception of space. *Philos Mag* 13: 406-416, 1882.
- Tolbert L.P. and Morest, D.K. Patterns of synaptic organization in the cochlear nuclei of the cat. *Neurosci Abs* 4(11). 1978.
- Vater, M. Single Unit Responses in Cochlear Nucleus of Horseshoe Bats to Sinusoidal Frequency and Amplitude Modulated Signals. *J Comp Physiol* 149: 369-388, 1982.
- Vater, M. Ultrastructural and immunocytochemical observations on the superior olivary complex of the mustached bat. *J Comp Neurol* 358: 155-180, 1995.
- Vetter, D.E., Adams, J.C., and Mugnaini, E. Chemically distinct rat olivocochlear neurons. *Synapse* 7: 21-43, 1991.
- Vetter, D.E. and Mugnaini, E. An evaluation of retrograde tracing methods for the identification of chemically distinct cochlear efferent neurons. *Arch Ital Biol* 128: 331-353, 1990.
- Vetter, D.E. and Mugnaini, E. Distribution and dendritic features of three groups of rat olivocochlear neurons. A study with two retrograde cholera toxin tracers. *Anat Embryol* 185: 1-16, 1992.
- Vetter, D.E., Saldana, E., and Mugnaini, E. Input from the inferior colliculus to medial olivocochlear neurons in the rat: a double label study with PHA-L and cholera toxin. *Hear Res* 70: 173-186, 1993.
- Viete, S., Pena, J.I., Konishi, M. Effects of interaural intensity differences on the processing of interaural time differences in the barn owl's nucleus laminaris. *J Neurosci* 17: 1815-1824, 1997.
- von Gersdorff, H. and Borst, J.G. Short-term plasticity at the calyx of held. *Nat Rev Neurosci* 3: 53-64, 2002.
- Wagner, H., Mazer, J.A., and von Campenhausen, M. Response properties of neurons in the core of the central nucleus of the inferior colliculus of the barn owl. *Eur J Neurosci* 15: 1343-1352, 2002.
- Wakeford, O.S. and Robinson D.E. Lateralization of tonal stimuli by cat. *J Acoust Soc Am* 55: 649-652, 1974.
- Warr, W.B. Fiber degeneration following lesions in the anterior ventral cochlear nucleus of the cat. *Exp Neurol* 14: 453-474, 1966.

- Webster, D.B. and Plassmann W. Parallel evolution of low-frequency sensitivity in old world and new world desert rodents. In Webster, D.B., Fay, R.R., and Popper, A.N. eds. *The evolutionary biology of hearing*. New York, Springer, pp. 633-636, 1992.
- Webster, D.B. and Webster, M. Auditory systems of Heteromyidae: functional morphology and evolution of the middle ear. *J Morphol* 146: 343-376, 1975.
- Wenthold, R.J., Huie, D., Altschuler, R.A., and Reeks, K.A. Glycine immunoreactivity localized in the cochlear nucleus and superior olivary complex. *Neuroscience* 22: 897-912, 1987.
- White, J.S. and Warr, W.B. The dual origins of the olivocochlear bundle in albino rats. *J Comp Neurol* 219: 203-214, 1983.
- Willard, F. and Martin, G.F. The auditory brainstem nuclei and some of their projections to the inferior colliculus in the North American opossum. *Neuroscience* 10: 1203-1232, 1983.
- Wu, S.H. and Kelly, J.B. Response of neurons in the lateral superior olive and medial nucleus of the trapezoid body to repetitive stimulation: intracellular and extracellular recordings from mouse brain slice. *Hear Res* 68: 189-201, 1993.
- Yang, L. and Pollak, G.D. Differential response properties to amplitude modulated signals in the dorsal nucleus of the lateral lemniscus of the mustache bat and the roles of gabaergic inhibition. *J Neurophys* 77: 324-340, 1997.
- Yapa, W.B. Social behaviour of the Mongolian gerbil *Meriones unguiculatus*, with special reference to acoustic communication. Dissertation LMU München, Germany, 1994.
- Yin, T.C. Neural mechanisms of encoding binaural localization cues. In Oertel, D., Fay, R R., and Popper, A N. eds. *Integrative functions in the mammalian auditory pathway*. New York, Springer, pp. 99-159, 2001.
- Yin, T.C. and Chan, J.C. Interaural time sensitivity in medial superior olive of cat. *J Neurophys* 64: 465-488, 1990.
- Yin, T.C. and Kuwada, S. Binaural interaction in low-frequency neurons in inferior colliculus of the cat. III. Effects of changing frequency. *J Neurophys* 50: 1020-1042, 1983.
- Young, E.D. and Rubel, E.W. Frequency-specific projections of individual neurons in chick brainstem auditory nuclei. *J Neurosci* 3: 1373-1378, 1983.

Young, E.D. and Rubel, E.W. Embryogenesis of arborization pattern and topography of individual axons in N. laminaris of the chicken brain stem. *J Comp Neurol* 245: 425-459, 1986.

Zook, J.M. and Casseday, J.H. Cytoarchitecture of auditory system in lower brainstem of the mustache bat, *Pteronotus parnellii*. *J Comp Neurol* 207: 1-13, 1982.

Zook, J.M. and DiCaprio, R.A. Intracellular labeling of afferents to the lateral superior olive in the bat, *Eptesicus fuscus*. *Hear Res* 34: 141-147, 1988.



List of Abbreviations

0/E	no overall input (ipsi) / excitatory (contra)
a.T.	above threshold
AVCN	anteroventral cochlear nucleus
BF	best frequency
CN	cochlear nucleus
CP	characteristic phase
DMPO	dorsomedial periolivary nucleus
DNLL	dorsal nucleus of the lateral lemniscus
E/E	excitatory (ipsi) / excitatory (contra)
E/I	excitatory (ipsi) / inhibitory (contra)
E/0	excitatory (ipsi) / no overall input (contra)
GABA	γ -amino-butyric acid
HRP	horseradish peroxidase
I/E	inhibitory (ipsi) / excitatory (contra)
IID	interaural intensity difference
IPD	interaural phase difference
ISI	inter-spike-intervall
ITD	interaural time difference
LNTB	lateral nucleus of the trapezoid body
LSO	lateral superior olive
MNTB	medial nucleus of the trapezoid body
MSO	medial superior olive
MTF	modulation transfer function
NL	Nucleus laminaris
NM	Nucleus magnocellularis
PSTH	Peri-Stimulus-Time Histogram
PVCN	posteroventral cochlear nucleus
RLF	Rate-Level Function
SAM	sinusoidally amplitude modulated
SOC	superior olivary complex
SPL	sound pressure level
SPN	superior paraolivary nucleus
VCN	ventral cochlear nucleus
VS	vector strength



Acknowledgements

First and foremost, I would like to thank PD Dr. Benedikt Grothe for the assignment of the interesting topic, for his support during experiments and data analysis and for helpful discussions particularly in the ending phase of this work.

Additionally, I want to thank Prof. Thomas Park for a pile of motivation during the critical period of the experiments and for lots of advice in all respects.

I thank Dr. Oliver Behrend for the interesting and instructive time when we recorded together.

Moreover, I would like to thank Prof. Gerhard Neuweiler and Dr. Mark Hübener for fruitful discussions during thesis committee meetings and at any other time point I asked for their advice.

Without the support of Christoph Kapfer, Iris Kehrer and Claudia Schulte the histology part of this thesis would have been much more difficult. Gerhard Breutel and especially Volker Staiger assured that technical problems, starting with the lack of alligator clips up to severe setup grounding problems, did not interfere too much with actual experiments.

Dr. Mark Hübener, Prof. Thomas Park, Dr. Thomas Mrsic-Flögel, Dr. Ursula Koch, Claudia Roth and Petra Kufner read at least parts of an earlier version of this work and their comments and suggestions provided valuable help.

A special thanks goes to all Bonhoeffer lab members and certainly to the Grothe lab - people who were prepared to give any support at any time, Armin Seidl, Christoph Kapfer, Marianne Braun and Dr. Ursula Koch.

I was lucky that Claudia Roth and Eva Hartfuß were around, not only because of their willingness to help in all situations but mainly for their empathy to all scientific and non-scientific problems.

Dr. Elisabeth Foeller, Markus Drexler and Rudi Marsch were wonderful discussion partners in all kinds of conversations. Above all I thank Markus and Rudi for all the “copying-scanning-faxing-mailing papers” sessions they performed for me.

I thank my Papa for supporting me all these years, especially during times of obvious “indecisiveness” towards my future.

Last but not least, I want to thank my “non-scientific“ social background that gave me the emotional stability I needed: Pezi, of course, but also Rupert, Marion, Lisa, Anja, Olaf, Flocky and Ulli.



Curriculum Vitae

09 May 1971	born in Gräfelfing, Germany
September 77 to July 81	elementary school, Volksschule Krailling
September 81 to June 90	grammar school, Gymnasium Starnberg
November 90 to November 92	studies in agricultural sciences, technical university Munich
December 92 to March 94	loan officer in Citibank Munich
May 94 to April 99	studies in biology, Ludwig-Maximilians-University Munich
April 99	diploma in biology (major subject: neurobiology, minor subjects: pharmacology, biochemistry, zoology) <u>diploma thesis:</u> “Sensitivität auditorischer Mittelhirnneurone auf interaurale Zeitdifferenzen“ (<i>Sensitivity of auditory midbrain neurons to interaural time differences</i>)
since May 99	graduate student in the laboratory of PD Dr. Benedikt Grothe, “Auditory Processing”, Max Planck Institute of Neurobiology, Martinsried, Germany